Title:
Population Consequences of Age-Dependent Maternal Effects in Rockfish (Sebastes spp.)

Author:
Lucero, Yasmin, University of California, Santa Cruz

Publication Date:
06-01-2007

Series:
Research Theses and Dissertations

Publication Info:
Research Theses and Dissertations, California Sea Grant College Program, UC San Diego

Permalink:
http://escholarship.org/uc/item/3jj1r53n

Additional Info:
Dissertation submitted by Yasmin Lucero in partial satisfaction of the requirements for the degree of Doctor of Philosophy in Ocean Sciences to the University of California, Santa Cruz.

Keywords:
rockfish, Sebastes spp., population simulation, biomass

Abstract:
I present a model of the early life history of a rockfish that includes an age-dependent maternal effect. The model is designed to accurately reflect the diverse uncertainties we have about early life history processes. The first portion of this thesis is devoted to an analytical treatment of the deterministic early life history model. I emphasize uncertainty about the functional form of density-dependent processes in the juvenile stage. The remainder of the thesis is devoted to demonstrating the properties of an agestructured population simulation with a productivity function that includes a maternal effect. I begin by examining a deterministic system, and then extend the analysis to a stochastic system. The simulation is used to calculate the time to recovery of an overfished rockfish population. I find that in the presence of an age-dependent maternal effect: (1) older populations are generally more productive than younger populations of the same biomass, (2) old fish provide a recovering population with buffering from environmental variability, (3) the size of the population impact of the effect depends significantly on the underlying life history pattern, and (4) managing an overfished population for age-structure has the largest positive impact when the rebuilding plan includes moderate harvest.

UNIVERSITY OF CALIFORNIA
SANTA CRUZ

POPULATION CONSEQUENCES OF AGE-DEPENDENT MATERNAL EFFECTS IN ROCKFISH (*SEBASTES SPP.*)

A dissertation submitted in partial satisfaction of the
requirements for the degree of

DOCTOR OF PHILOSOPHY

in

OCEAN SCIENCES

by

Yasmin Lucero

June 2007

The Dissertation of Yasmin Lucero
is approved:

Professor Marc S. Mangel, Chair

Professor Christopher A. Edwards

Dr. Alec D. MacCall

Lisa C. Sloan
Vice Provost and Dean of Graduate Studies

Table of Contents

List of Figures

List of Tables

Abstract

Population Consequences of Age-Dependent Maternal Effects in Rockfish

(*Sebastes spp.*)

by

Yasmin Lucero

I present a model of the early life history of a rockfish that includes an age-dependent maternal effect. The model is designed to accurately reflect the diverse uncertainties we have about early life history processes. The first portion of this thesis is devoted to an analytical treatment of the deterministic early life history model. I emphasize uncertainty about the functional form of density-dependent processes in the juvenile stage. The remainder of the thesis is devoted to demonstrating the properties of an age-structured population simulation with a productivity function that includes a maternal effect. I begin by examining a deterministic system, and then extend the analysis to a stochastic system. The simulation is used to calculate the time to recovery of an overfished rockfish population. I find that in the presence of an age-dependent maternal effect: (1) older populations are generally more productive than younger populations of the same biomass, (2) old fish provide a recovering population with buffering from environmental variability, (3) the size of the population impact of the effect depends significantly on the underlying life history pattern, and (4) managing an overfished population for age-structure has the largest positive impact when the rebuilding plan includes moderate harvest.

To J.M.,

for everything

Acknowledgments

I am grateful to my committee: Marc Mangel, Alec MacCall and Chris Edwards for all of their hard work. In particular, I would like to thank my advisor and teacher, Marc Mangel for showing me how to see things his way.

Many thanks to Phil Levin for setting me on this course and for many helpful discussions. Thanks to Herbie Lee for teaching me the fundamentals of probability and for answering all my questions. Thanks to Bruno Sansó for setting me on firm statistical footing, and to Andi Stephens for making sure that I learned R properly. Thanks to Chris Petersen for teaching me all I really needed to know about marine life histories. And, as always, acknowledgement is due to John G. T. Anderson for being my first teacher, and encouraging high standards, enforced from within.

Thanks and true gratitude are due to Cristie Boone, Leah Johnson, Kristen Honey, Kate Siegfried, Kate Cresswell, Andi Stephens, Christine Alfano, Lee Maranto, Jay Strader and Jason Melbourne for being on my team.

Thanks to Darren Johnson for giving permission to use his data to illustrate uncertainty about density-dependence. Thanks to Steve Ralston for sharing the settlement data. And thanks to Sue Sogard for sharing with me some insightful preliminary results of her follow-up research.

This work was supported by the NMFS/Sea Grant Population Dynamics Fellowship and the Center for Stock Assessment Research, a partnership between UC Santa Cruz and the NMFS-SWFSC Santa Cruz Lab.

Chapter 1

Introduction

1.1 Age-Based Differences

An important goal of contemporary fisheries science is to make Ecosystem Based Management operational. This congressionally mandated program is intended to improve fisheries management by placing it in the broader ecosystem context. A small subset of this large program is the goal to improve stock assessment estimates by addressing intra-population heterogeneity (Pikitch et al. 2004).

Traditional stock assessment models, like many process based models, work by scaling up the properties of an idealized "average" individual. However, ecology informs us of many ways in which fish populations are poorly represented by the idealized individual. Among other things, fisheries scientists are concerned with determining when stock assessment estimates can be improved by addressing deviations from the idealized average model.

One such area of intra-population heterogeneity is age-based differences. It is common in fishes for fecundity per unit-biomass to be age-dependent. Some examples of species with this characteristic are Atlantic cod (*Gadus morhua*, Marteinsdottir and Begg 2002), Northern mottled sculpin (*Cottus b. bairdi*, Ludwig and Lange 1975), North sea haddock (*Melanogrammus aegelfinus*, Hislop 1988), and Pacific sardine (*Sardinops sagax*, Plaza et al. 2002).

Stock assessment models often address this heterogeneity by using age-dependent fecundity parameters. An example of this approach is found in *Stock Synthesis 2 (SS2)*, a software package commonly used for stock assessments on the U.S. west coast (Methot 2005). This approach requires measurements of fecundity at age, which are not always available, especially for the oldest individuals. But, overall the solution implemented in *SS2* adequately addresses differences in fecundity with age.

Until recently, interest in age-based differences has focused on age-based fecundity (i.e., offspring quantity as a function of the mother's age—hereafter referred to as "maternal age"). But there is a new focus on offspring quality as a function of maternal age. In Figure 1.1 I show results from a laboratory study that found an effect of maternal age on larval quality in Black rockfish, *Sebastes melanops* (Berkeley et al. 2004a). They found that maternal age affects the larvae's rate of growth and ability to resist starvation. Specifically, larvae from older mothers grow faster (3–4 times as fast) and resist starvation better (more than twice as long) than larvae from younger mothers.

This phenomenon is an age-dependent maternal effect. A maternal effect is a

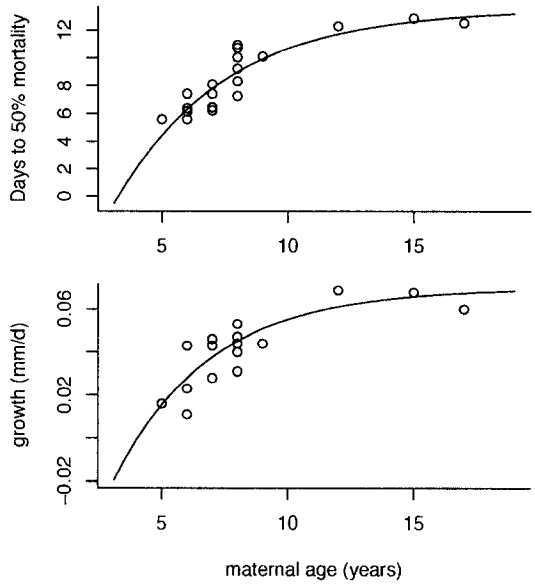

Figure 1.1: Larval growth and survival under starvation conditions for *S. melanops*. Figure redrawn from Berkeley et al. 2004a, data and regression coefficients taken from the paper. The upper panel regression equation is $T = -15.23 + 28.79(1 - e^{-0.23a})$, where $r^2 = 0.80$ and $p < 0.0001$. The lower panel regression equation is $G = -0.13 + 0.2(1 - e^{-0.26a})$, where $r^2 = 0.71$ and $p = 0.0006$.

trait that is inherited, but non-genetic (Lacey 1998). An age-dependent maternal effect occurs when the inheritance of the trait is determined by maternal age. Maternal effects are common in nature, but are usually driven by features of the maternal experience, such as the climate conditions experienced by the mother (Beckerman et al. 2002, Beckerman et al. 2006, Benton et al. 2001, Ginzburg 1998, Plaistow et al. 2006). An age-dependent maternal effect is unusual.

Follow-up research uncovered similar maternal effects in *Sebastes serranoides, mystinus* and *flavidus* (Sogard 2006, personal communication); this result, in combi-

nation with the overall similarity in reproductive physiology of rockfishes (Love et al. 2002), makes it likely that an age-dependent maternal effect is common in rockfish.

1.2 Scientific Response to the Maternal Effect

The idea that reproductive quality depends on age is new, so the result in Figure 1.1 has attracted considerable interest. Many species of rockfish (genus *Sebastes*) are harvested and several are overfished (PFMC 2006), resulting in dramatic changes in population age-structure (Harvey et al. 2006). As a consequence, the discovery of an age-dependent maternal effect has raised significant interest in learning whether population recovery can be accelerated by managing rockfish for age-structure (Palumbi 2004).

Several researchers have suggested that an age-dependent maternal effect renders rockfish especially well-suited to marine reserves. Individuals within a reserve experience lowered mortality and thus survive longer on average, leading to an older subpopulation within the reserve. Among others, Berkeley at al. (2004b) predict that this older subpopulation will have increased productivity due to the age-dependent maternal effect (Birkeland and Dayton 2004).

However, it can not be assumed that the observed effect will result in greater productivity for older populations. The age-dependent maternal effect has been measured only in the first several weeks of life, but productivity depends on the number of individuals who survive to reproductive age, about six years in Black rockfish. Larvae

must overcome many obstacles before they recruit to the reproductive population, as sketched in Figure 1.2.

O'Farrell and Botsford (2005 and 2006) sought to calculate the population consequences of an age-dependent maternal effect. They transformed the improved larval quality into units of effective fecundity, thereby reducing the problem of age-dependent larval quality to the problem of age-dependent fecundity which is familiar and well understood. They did this by constructing a statistic named lifetime egg production (LEP), modeled so that an individual's egg production increases with age. They calculated population-wide LEP as a function of population age-structure. They found that, based on the laboratory measurements shown in Figure 1.1, most of the young mothers with low larval success were not yet mature, or only recently mature. The net result was that the addition of an age-dependent maternal effect had an impact very much like a small shift in the maturity function.

Spencer et al. (2007) sought to to determine whether successful pacific ocean perch (*Sebastes alutus*) management requires considering maternal effects. They were concerned that the presence of a maternal effect in *S. alutus* could invalidate their calculations of sustainable harvest levels because they failed to take into account changes in productivity due to changes in population age-structure. They constructed a hypothetical maternal effect for *S. alutus*, based on the the results from Berkeley et al. (2004a), and used this to calculate F_{msy}, the fishing level that produces maximum sustainable yield. They found F_{msy} to be insensitive to the presence of maternal effects.

Both of these investigations found that maternal effects had only marginal

population consequences, suggesting that no management action is necessary. However, both studies assumed that increasing larval quality is equivalent to increasing fecundity. Neither study addressed the potential consequences of differential larval quality on the early life ecology of rockfish.

There are five kinds of process uncertainty that are obstacles to predicting the population consequences of an age-dependent maternal effect:

1. Persistence of the maternal effect
2. Magnitude of maternal effect advantage
3. Magnitude of early life survival rates
4. Functional form of density-dependence
5. Environmental variability

I develop these five uncertainties in the following section.

1.3 Rockfish Ecology

Rockfish are remarkable for their high speciosity and their potential for long lives. There are over fifty species along the west coast of North America (Love et al. 2002) and they have maximum ages ranging from about 10-200 years (Mangel et al. 2007). Like most marine animals, their early life history is composed of a pelagic larval stage followed by a benthic juvenile stage (Figure 1.2). This sequence is called a bipartite life history. In the case of rockfish, the pelagic stage is approximately six

months long, and the juvenile stage is from eighteen months to several years, depending on the species and how we define recruitment.

Larvae do not eat in the laboratory; by necessity laboratory studies are limited to several weeks, until the larvae die of starvation (personal communication, Berkeley 2006). The maternal effect has thus only been observed in the early larval stage, and there is no empirical evidence to support or refute an impact at later life stages.

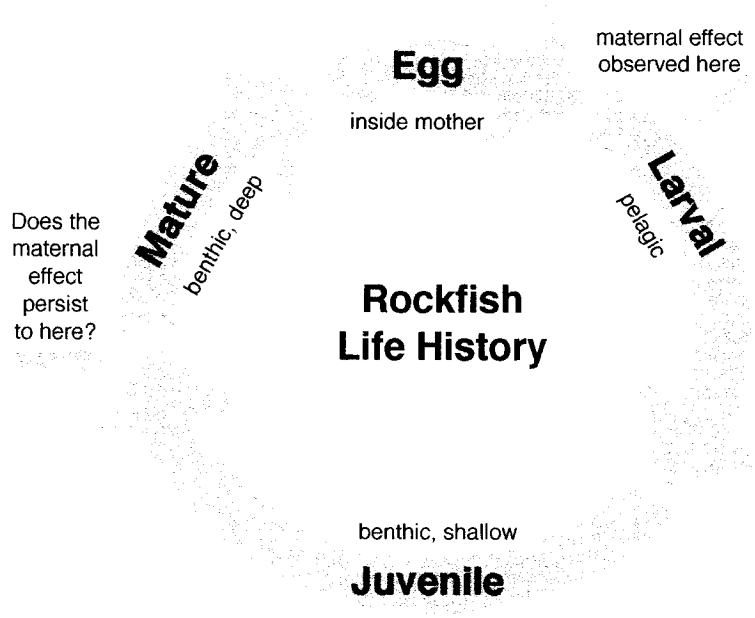

Figure 1.2: Schematic diagram of rockfish life history. Laboratory results reveal a strong maternal effect in the early larval stage. We want to know if this impacts how many fish survive to reproductive maturity.

However, there is an extensive literature about the latent effect of variation in larval growth in fishes with bipartite life histories (Shima and Findlay 2002, Pechenik 1998). Variation in larval growth often leads to variation in growth or size at settlement.

Variation in size and growth at settlement often leads to variation in juvenile survival, sometimes called the growth-mortality hypothesis (see Sogard (1997) for a review). Thus we have reason to expect that this early advantage may persist. In Figure 1.3, I present three hypotheses for the persistence of the maternal effect.

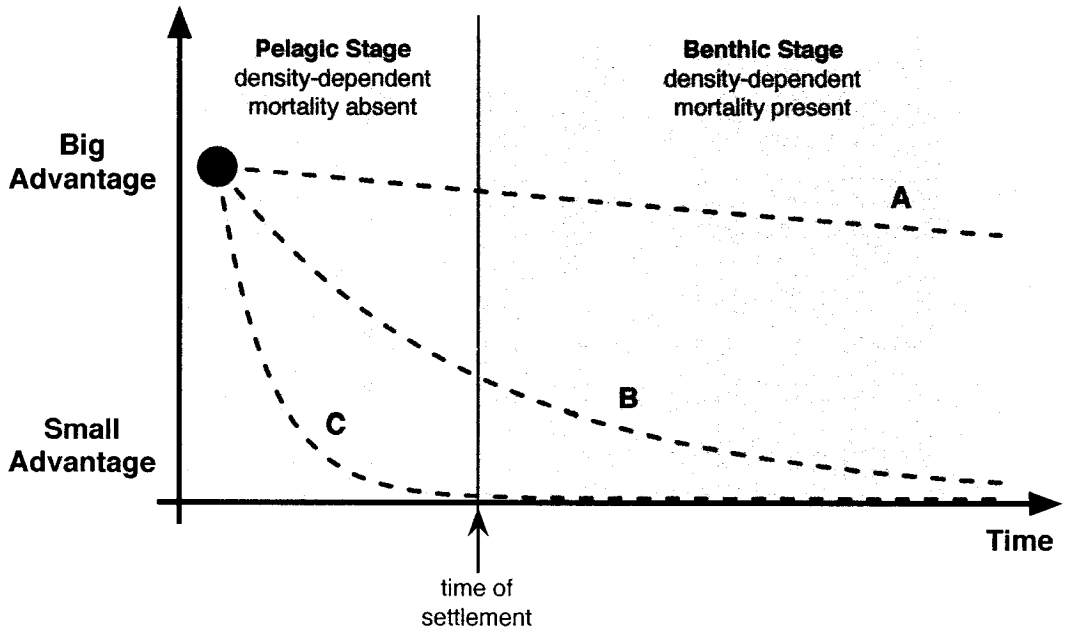

Figure 1.3: The x-axis is time in the early life history, the y-axis is the size of the advantage, due to a maternal effect, enjoyed by offspring from old mothers over offspring from young mothers. The red circle represents data that show the maternal effect confers a big advantage in the early pelagic stage. We do not know what follows: Does the advantage (A) persist? Does it (B) dissipate gradually? Or, does it (C) dissipate immediately? The dashed lines illustrate these hypothetical patterns. A major life history shift occurs at the time of settlement. The population consequences of the maternal effect depends on whether there is still a significant advantage at the time of settlement.

Notice that the y-axis in Figure 1.3 lacks numbers or units. We expect that the observed changes in resistance to starvation and growth rate are ecologically important.

But, we do not have a clear idea of how to translate those numbers into overall survival or mortality rates for the pelagic and benthic stages. And we do not know how the advantage in survival rate will evolve over time.

To understand how an age-dependent maternal effect could influence recruitment success, we must examine the ecological processes that contribute to recruitment. In Figure 1.4 I provide a stage-structured summary of the significant ecological factors in the early life history of a rockfish.

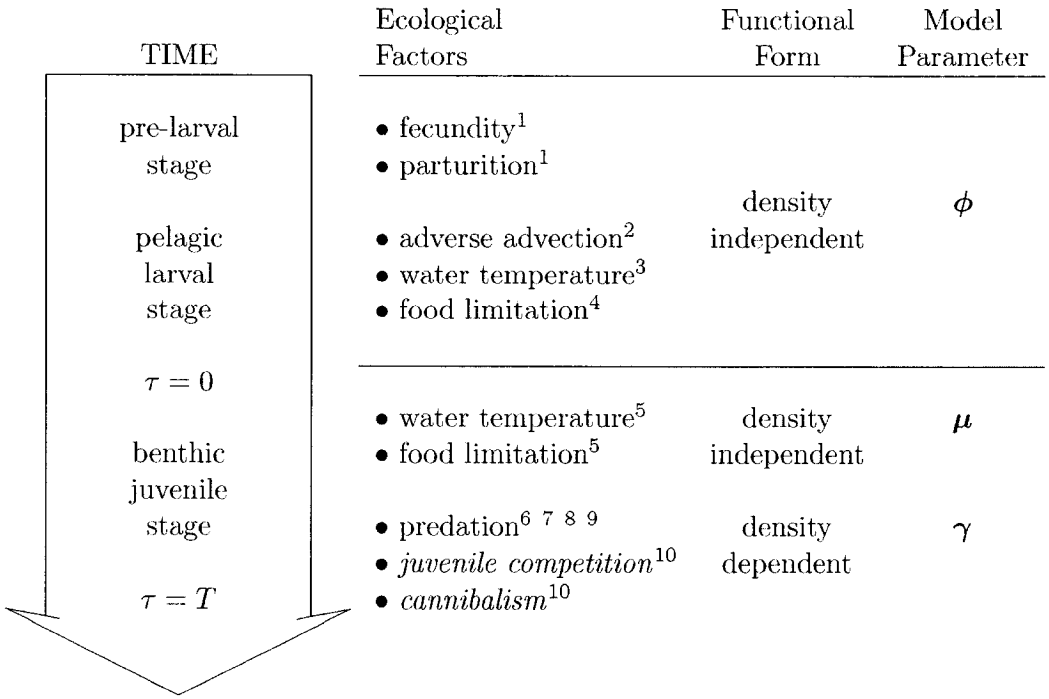

[1]Bobko and Berkeley 2004, [2]Ainley et al. 1993, [3]Ralston and Howard 1995, [4]Bjorkstedt et al. 2002, [5]Love et al. 1991, [6]Hobson et al. 2001, [7]Hixon and Jones 2005, [8]Johnson 2006a, [9]Adams and Howard 1996, [10]included as plausible, but speculative, mechanisms.

Figure 1.4: The model treats production in two steps, pre-settlement ($\tau < 0$) and post-settlement ($\tau > 0$). All pre-settlement processes are summarized by ϕ, the rate settlement. Post-settlement processes are separated into the density-independent rate of mortality, μ, and the density-dependent rate of mortality, γ.

The first stage presented in Figure 1.4 is the pre-larval stage. Rockfish are viviparous; unlike most fishes they do not release eggs and sperm (i.e., spawning) but rather they release larvae (i.e., parturition). Therefore, their reproductive investment occurs in two stages: pre- and post-fertilization. The fecundity rate measures the success of the pre-fertilization stage of egg development (i.e., vitellogenesis). The parturition rate measures the success of the post-fertilization stage of maternal feeding (i.e., matritrophy). Both the rate of fecundity and the rate of parturition are influenced by maternal condition and thus indirectly by the availability of food in the previous year. Older mothers are known to have both higher fecundity and parturition rates (Bobko and Berkeley 2004). All other things being equal, this alone would cause a positive correlation between the settlement rate (ϕ) and maternal age.

The next stage presented in Figure 1.4 is the pelagic larval stage. Once released, rockfish larvae are part of the diurnally migrating micronekton layer of the surface ocean. They are opportunistic feeders. When they are very small they rely on copepod nauplii and invertebrate eggs. As they grow larger they extend their diets to include copepodites, adult copepods, and euphausiids (Moser and Boehlert 1991). In addition to participating in the diurnal migration they school most intensely at shallow depths (Lenarz et al. 1991), these are both behaviors for avoiding surface predators (e.g., seabirds, marine mammals, larger pelagic fishes). However, they also diurnally migrate to maintain proximity to their prey.

Like many animals, the optimum temperature for growth shifts ontegenetically: smaller fish grow fastest at higher temperatures and as the fish grow their thermal

optimum declines (Lenarz at al. 1991, Boehlert and Yoklavich (1983) demonstrate this specifically for Black rockfish). Surface water temperature in the California Current varies generally with climate state (e.g., El nino years bring warmer surface oceans into central California). The depth of the thermocline is also a significant feature of the thermal environment of larvae.

Larvae control their depth to manage several competing needs. Larvae need to maximize their rate of food encounter; this is why they diurnally migrate and also why the highest larval densities are found near upwelling fronts (Bjorkstedt et al. 2002, Lenarz et al. 1991). Larvae need to avoid predators; this is why they exhibit strong schooling behavior in the surface ocean (Lenarz et al. 1991) and also an additional reason for diurnal migration. Larvae need to manage their body temperature to optimize growth; this is why they are observed at deeper depths as they growth larger (Sakuma et al. 1999). Finally, larvae need to avoid being transported away from nutrient rich fronts; this is why larvae generally avoid the shallow surface offshore currents caused by Ekman transport (Lenarz et al. 1991).

As larvae get larger they are found in a wider range of depths. Small larvae choose a depth that is favorable on average while larger larvae take advantage of their greater swimming strength to continuously relocate to the most favorable depth (Lenarz et al. 1991).

Eventually, succesful larvae undergo the physiological transition to become juveniles (flexion). These pelagic juveniles must move inshore to find suitable benthic habitat for settlement. The ability to swim to the appropriate depth is crucial for finding

onshore currents to carry them to suitable habitats.

Throughout the larval stage, larger body size provides a significant survival advantage. The positive correlation between growth rate and maternal age shown in Figure 1.1 should lead to a positive correlation between the settlement rate ϕ and maternal age. Additionally, the greater starvation resistance of larvae from older mothers (also shown in Figure 1.1) should improve their settlement rate by leaving them less dependent on finding food and better able to attend to their competing needs to avoid predators and manage their body temperature.

The final stage presented in Figure 1.4 is the benthic juvenile stage. If a rockfish survives to settle, it continues to face several of the same concerns of the pelagic environment: they need to maximize their food intake, manage their body temperature and avoid predators. In the pelagic stage these concerns were managed largely through vertical migration. But in the benthic stage they are managed primarily by finding shelter space. Juveniles in benthic habitat rely on shelter from habitat structure such as rocky crevices or kelp fronds (Love et al. 2002). Suitable shelter space is often limited, this creates competition for the optimal habitat (Johnson 2006b).

Additionally, the horizontal distribution of juveniles is far more concentrated in the benthic environment than in the pelagic environment. This high population density attracts density-cued predators, such as adult rockfish (Hobson et al. 2001, Adams and Howard 1996). The density-cued behavior of predators renders predation mortality a density-dependent process in the benthic stage.

Large body size continues to be a significant survival advantage in the ben-

thic stage. Larger juveniles can swim away from predators more quickly and compete more effectively for quality shelter space (Paradis et al. 1996). The latent effect of a an early life growth advantage can be an important determinant of juvenile mortality rates. This advantage does not only impact the privileged juveniles from older mothers. Large juveniles continue to attract density-cued predators, however, those predators preferentially target the easier to catch smaller juveniles. Thereby, the presence of these privileged juveniles serves to increase predation pressure on their smaller conspecifics. This raises the possibility that an age-dependent maternal effect may have negative as well as positive impacts on population productivity.

The time of transition from the pelagic to the benthic stage is ecologically significant. As shown in Figure 1.4, at the time of settlement there is a qualitative shift in the ecological processes from strictly density-independent processes to a combination of density-independent and density-dependent processes. Because of this, I model productivity in two stages: the pelagic stage before settlement and the benthic stage after settlement. Mortality in the pre-settlement stage is density-independent (Hixon and Webster 2002, Ralston and Howard 1995). Therefore, this is modeled with a simple proportionality constant. Mortality in the post-settlement stage is more complex, having both density-independent and density-dependent components. For this stage, I employ a stock-recruitment model with both density-independent mortality and density-dependent mortality.

The production model is reduced to these three important basic parameters: ϕ, the rate of settlement per-unit spawning stock biomass; μ, the density-independent

rate of per-capita mortality in the juvenile stage; and γ, the density-dependent rate of per-capita mortality in the juvenile stage.

There are no data to suggest what the values of these parameters should be in nature. Ignorance of these basic survival rates is a major source of uncertainty about population productivity—true even in the absence of maternal effects—and complicates our ability to assess the consequences of the maternal effects.

Finally, field studies indicate that predation is the significant source of density-dependent mortality, either by direct mortality or by interference competition (e.g., competition for shelter) (Hobson et al. 2001, Hixon and Jones 2005, Hixon and Webster 2002, Johnson 2006a). A recent study illustrated that the functional form of density-dependence is a function of predator density: Johnson (2006b) built nine cubic meter enclosures in kelp beds off the coast of central California. He controlled densities of juveniles and predators within the enclosures and monitored juvenile mortality for forty-eight hours. Figure 1.5a shows his result, along with the best fit linear models. It is not known which of these predator densities most resemble the experience of rockfish.

Five sources of process uncertainty prevent us from predicting the population consequences of an age-dependent maternal effect. These are:

1. Persistence of the maternal effect. How does the advantage evolve in time? Do juveniles from older mothers have a survival advantage over juveniles from younger mothers? Do recruits from older mothers have an advantage?

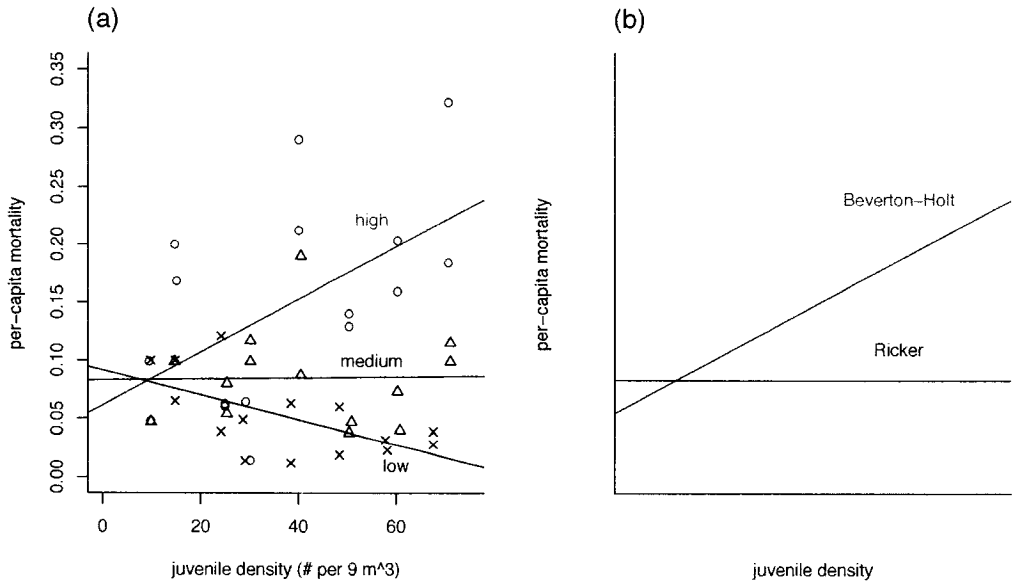

Figure 1.5: Panel (a) shows data from an enclosure study of juvenile rockfish (Johnson 2006b). The red circles are from an enclosure with a high density of predators (five predators), the blue triangles are from an enclosure with medium density of predators (three predators) and the green crosses are from an enclosure with a low density of predators (one predator). The lines are the best fit lines to data: for high predation (red line), $p = 0.03$, $R^2 = 0.297$, $F = 5.914$; for medium predation (blue line), $p = 0.94$, $R^2 = 0.0004$, $F = 0.005$; for low predation (green line), $p = 0.017$, $R^2 = 0.37$, $F = 7.566$. Panel (b) shows the Beverton-Holt and Ricker models.

2. Magnitude of maternal effect advantage. Do larvae from old mothers settle 50% more than larvae from young mothers, or 100% more? Do juveniles from older mothers have 20% lower mortality than juveniles from young mothers, or 60% lower mortality?

3. Magnitude of early life survival rates. How many settlers are there per mother? How many juveniles die each day after settlement? How many juvenile deaths are due to density-dependent processes?

4. Functional form of density-dependence. Does density-dependent mortality follow a Beverton-Holt pattern or a Ricker pattern? Or, some other pattern? (Munch et al. 2005a)

5. Environmental variability. Does the variability in food availability, water temperature, and current speed interact with other factors to change the consequences of the maternal effect?

I model these uncertainties, and examine how population changes depend on each of them. In this way, I identify the most influential uncertainties and find patterns that are robust to uncertainty.

1.4 Summary of Modeling Approach

I chose to address the substantial complexity and uncertainty of this system by adopting a multiple models or multiple hypothesis approach (Hilborn and Mangel 1997). In Figure 1.6 I show a schematic of the computational approach. At the core of the work is a population simulation that simulates the rebuilding of an overfished population. The simulation outputs the number of years required for a population to recover given the harvest rate during rebuilding, the populations productivity, and the presence and form of a maternal effect. I find that the time to recovery is a valuable population metric because it is a single measurement that reflects all of the inputs about which we are uncertain.

I developed a model of an age-dependent maternal effect with the flexibility

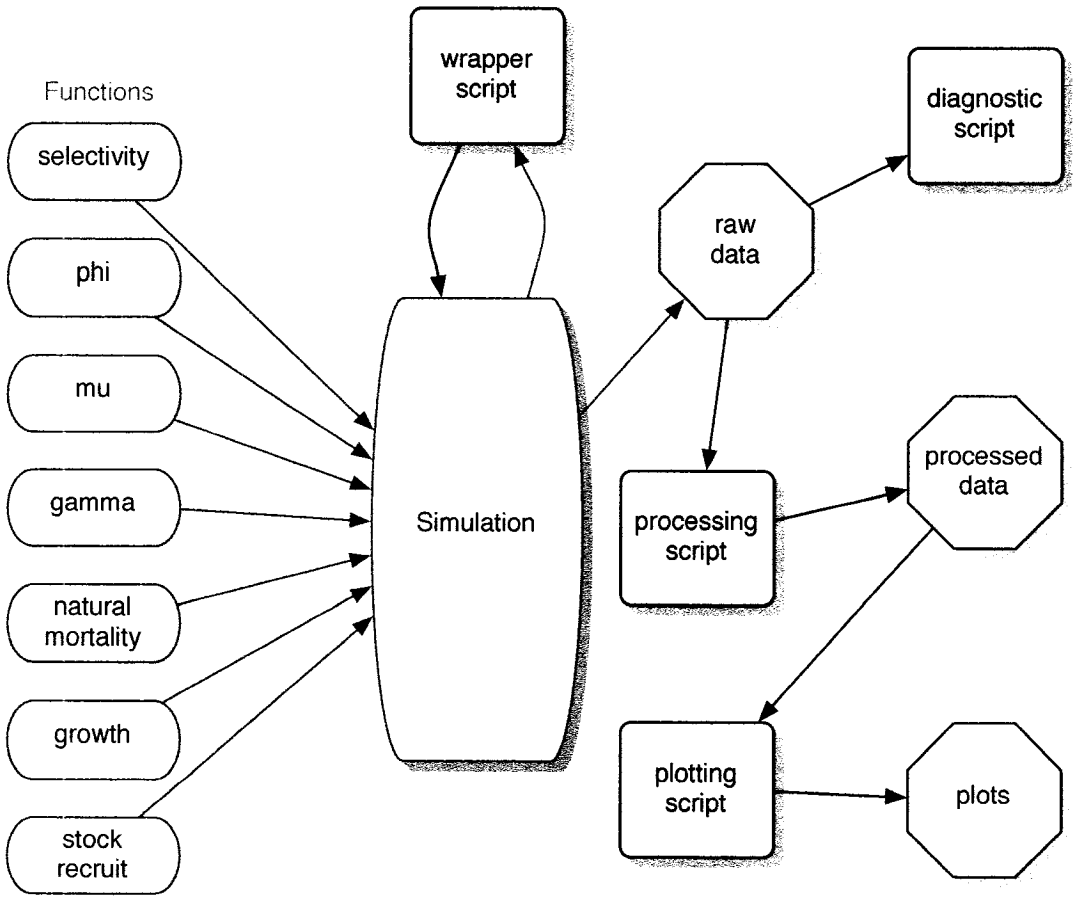

Figure 1.6: Illustration of the computational approach: Several subroutines support an *R* script with a population simulation. The simulation script is iterated by a wrapper script. All of the output of the simulation is stored, including several outputs of nominal interest. Diagnostic scripts are used to detect failures of the code to behave as expected. A processing script is used to sift out important outputs from the the raw output. Plotting scripts are used to visualize and summarize the results.

to accomodate the range of our uncertainty about the true population consequences of an age-dependent maternal effect in a rockfish population. I chose a range of input parameters designed to reflect our uncertainty and I calculated time to recovery for each set of inputs. This process results in a large simulated dataset.

The heart of the model is the productivity function that incoporates a maternal effect. In Chapter 2, I present the properties of three versions of the production function, each with a different assumption about the functional form of density-dependent mortality. In Chapter 3, I develop the mechanics of the population simulation based on the productivity function and I explain the model parameterization. Chapters 4 and 5 are devoted to analysis of the resulting simulated dataset.

A particular problem was posed by the solution of the production function. To model productivity with an age-dependent maternal effect, I developed a multi-variate stock-recruitment relationship. This allows us to assign different juvenile and larval mortality rates to the offspring of young and old mothers.

Traditionally, rockfish stock-recruitment is modeled with a Beverton-Holt model. Unfortunately, the multi-variate version of a Beverton-Holt stock-recruitment model is technically challenging to work with. The model is a matrix Ricatti equation of a form that lacks an analytical solution (Zwillinger 1992). The system can be solved numerically, however, the numerical solution also presents technical challenges. The multi-variate Beverton-Holt model exhibits a numerical property called stiffness. Stiff systems of differential equations cannot be solved by explicit algorithms such as the Runge-Kutte algorithm at the base of most numerical solvers. In Section B.3.6 I explain

the numerical algorithm I used in the simulation to find a solution to the multi-variate Beverton-Holt stock-recruit function.

Understanding the population consequences of age-dependent maternal effects is a small piece of the much larger program to implement Ecosystem Based Management (EBM). The challenges we face in understanding this one phenomenon are representative of the challenges facing EBM more broadly: incorporating new ecological knowledge usually raises numerous complexities and uncertainties. There are key process rates that have not been measured and may never be measured. Ecological processes are complex and difficult to describe precisely. And large variability is inherent to the system. Once crucial measurement needs can be identified, we can find robust patterns even without perfect ecological knowledge, and that good science can make possible good decisions in the face of tremendous uncertainty.

Chapter 2

Productivity with a Maternal Effect

To include a maternal effect in the model, I modify a stock-recruitment model so that there are multiple age-classes of mothers, each with its own offspring mortality rates. I then choose values for the mortality and settlement rates that emulate the age-dependent maternal effect. There are three parameters in the model whereby the maternal effect may impact productivity (see Figure 1.4). It may be that larvae from older mothers perform better in the pelagic stage, so that ϕ, the per-capita rate of settlement, is a function of maternal age. It may be that the maternal effect impacts post-settlement abilities such as cold tolerance and swimming speed (helpful to prevent being swept offshore), so that μ, the benthic rate of density-independent mortality, is a function of maternal age. Finally, the maternal effect may impact body size at the time of settlement and thereby impact the ability to avoid predators or compete for shelter; under these conditions γ, the benthic rate of density-dependent mortality, is a function of maternal age.

2.1 The Model

The traditional derivation of a stock-recruitment model begins with an ordinary differential equation describing per-capita mortality of juveniles. If $n(\tau)$ is numbers of juveniles at time τ, then the differential equation can be written

$$\frac{1}{n}\frac{dn}{d\tau} = -\mu - \Delta(n) \tag{2.1}$$

where μ is the rate of density-independent mortality and $\Delta(n)$ is the rate of density-dependent mortality. Stock-recruitment models differ in the form of $\Delta(n)$ (i.e., the functional form of density-dependence). The two most familiar stock-recruitment models are the Beverton-Holt model, where $\Delta(n) = \gamma n$, and the Ricker model, where $\Delta(n) = \gamma S$ (Haddon 2001). Here, γ is the per-capita rate of density-dependent mortality and S is the spawning stock biomass.

Most stock-assessments for rockfish use a Beverton-Holt model, but usually only find moderate to low goodness of fit (Munch et al. 2005, also see Dorn (2002) for several examples). The assumed form of density-dependence has potential to strongly influence the conclusions we draw. For this reason, I will consider a range of forms for density-dependent mortality.

If we compare the experimental result in Figure 1.5 to stock-recruitment models, we see that when predator density is high a Beverton-Holt model ($\Delta(n) = \gamma n$) provides a satisfying summary of the data. However, when predator density is lower a Ricker model ($\Delta(n) = \gamma S$) is a better fit. In the case of very low predator densi-

ties, per-capita mortality actually declines with juvenile density. This outcome occurs presumably because the predator experiences a capacity constraint and cannot further increase the predation pressure, even when juvenile density increases. There is no traditional stock-recruit model for the capacity constraint scenario. We could invent a new stock-recruitment relationship for this case, but this would require a behavioral model of predation that is beyond the scope of this work (Walters and Martell 2004). However, we can consider a limiting case of the capacity constraint, the model where there is no predation at all, and consequently no compensation ($\Delta(n) = 0$). For brevity, I will treat this as a special case of the Ricker model where $\gamma = 0$.

I assume that all three forms of density-dependence are relevant. We begin with the Ricker model because it is analytically tractable, and this analysis prepares us to understand the other two models. Next, we consider the no predation case, as a special case of the Ricker model. We then cover the Beverton-Holt model; the general Beverton-Holt model lacks an analytical solution, and so we build intuition by analyzing a special case of the Beverton-Holt model that can be solved analytically. Finally, we look at the numerical solution to the general Beverton-Holt model.

2.2 The Ricker Model

The traditional derivation of a Ricker model begins with Equation (2.1) where $\Delta(n) = \gamma S$. This differential equation is solved and evaluated at time T, the end of the juvenile period. The solution requires an initial condition, $n(0) = fS$, where f is

usually interpreted to be the fecundity rate. Finally, the equation is re-parameterized by $\alpha = fe^{-\mu T}$ and $\beta = \gamma T$. This yields the familiar Ricker stock-recruitment model (Quinn and Deriso 1999)

$$R = \alpha S e^{-\beta S} \tag{2.2}$$

To modify the Ricker model, I begin with a differential equation with multiple age-classes, where the juvenile mortality rates (μ and γ) depend on maternal age (a).

$$\frac{1}{n_a}\frac{dn_a}{d\tau} = -\mu_a - \sum_{k=1}^{a_{max}} \gamma_{ak} S_k \tag{2.3}$$

Here a_{max} is the maximum maternal age and k is the maternal age of the cohort. In vector form this is

$$\mathrm{diag}(\boldsymbol{n})^{-1}\frac{d\boldsymbol{n}}{d\tau} = -\boldsymbol{\mu} - \boldsymbol{\gamma}\boldsymbol{S} \tag{2.4}$$

where $\boldsymbol{n}$, $\boldsymbol{S}$ and $\boldsymbol{\mu}$ are vectors of length a_{max}, and $\boldsymbol{\gamma}$ is a matrix of dimension $a_{max} \times a_{max}$. This equation can be solved analytically with the initial condition

$$n_a(0) = \phi_a S_a \tag{2.5}$$

Here ϕ_a is the settlement rate (i.e., the number of juveniles to settle per unit of spawning stock biomass for juveniles with maternal age a). The solution to the multi-class Ricker model is

$$n_a(\tau) = \phi_a S_a exp\left\{\left(-\mu_a - \sum_{k=1}^{a_{max}} \gamma_{ak} S_k\right)\tau\right\} \tag{2.6}$$

Consider the special case of two age-classes, Class 1 juveniles (n_1) from "young" mothers and Class 2 juveniles (n_2) from "old" mothers. The two age-class Ricker model is

$$n_1(\tau) = \phi_1 S_1 exp\left\{(-\mu_1 - \gamma_{11} S_1 - \gamma_{12} S_2)\,\tau\right\} \tag{2.7}$$

$$n_2(\tau) = \phi_2 S_2 exp\left\{(-\mu_2 - \gamma_{21} S_1 - \gamma_{22} S_2)\,\tau\right\}$$

Productivity (R) in the two age-class system is

$$R = n_1(T) + n_2(T) \tag{2.8}$$

where T is the length of time of the juvenile period. The total stock size is $\hat{S} = S_1 + S_2$ and the proportion p of $\hat{S}$ from "old" fish is

$$p = \frac{S_2}{S_1 + S_2} = \frac{S_2}{\hat{S}} \tag{2.9}$$

Finally, I reparameterize so that $\alpha_a = \phi_a e^{-\mu_a T}$ and $\beta_{ak} = \gamma_{ak} T$. This yields the following equation for productivity in the two age-class Ricker model

$$R = \alpha_1 (1-p)\hat{S} e^{-((1-p)\beta_{11} + p\beta_{12})\hat{S}} + \alpha_2 p \hat{S} e^{-((1-p)\beta_{21} + p\beta_{22})\hat{S}} \tag{2.10}$$

I can now manipulate the parameters α_a and β_{ak} to give an advantage to Class 2 offspring over Class 1 offspring—simulating the age-dependent maternal effect—and then look at productivity (R) as a function of the population age-structure (p) and the spawning

stock biomass ($\hat{S}$). One of the advantages of this parameterization is that we are able to reduce the two density-independent parameters, ϕ and μ, to one parameter, α.

In the next sections, we examine two cases of the two age-class Ricker model with a maternal effect: in Case 1 the maternal effect only impacts the density-independent factors, in Case 2 the maternal effect only impacts the density-dependent factors.

2.2.1 Case 1: Maternal effect in density-independent factors

The first case I consider is $\alpha_2 > \alpha_1$ and $\beta_{11} = \beta_{12} = \beta_{21} = \beta_{22} = \beta$. Here, the maternal effect impacts the density-independent survival, but has no impact on the density-dependent interactions. Recall that $\alpha_a = \phi_a e^{-\mu_a T}$. Therefore this case would arise if the greater growth and starvation resistance of Class 2 larvae in the pelagic phase led them to be more robust. Alternatively, this case would result if fecundity increased with maternal age, a phenomenon ubiquitous in fishes and observed in rockfish (Bobko and Berkeley 2004). We find

$$R = \alpha_1 \hat{S} e^{-\beta \hat{S}} + \hat{S} e^{-\beta \hat{S}} (\alpha_2 - \alpha_1) p \tag{2.11}$$

For a given $\hat{S}$, R is a linear function of p, with slope $\hat{S} e^{-\beta \hat{S}} (\alpha_2 - \alpha_1)$. In Figure 2.1(b), the slope of the lines $R(p)$ depend on the difference $\alpha_2 - \alpha_1$; the strength of the maternal effect depends on the difference $\alpha_2 - \alpha_1$ and not the ratio α_2/α_1, as we might have initially guessed.

If $\beta \hat{S}$ is very large, or $\hat{S}$ is very small, then the difference in α is no longer

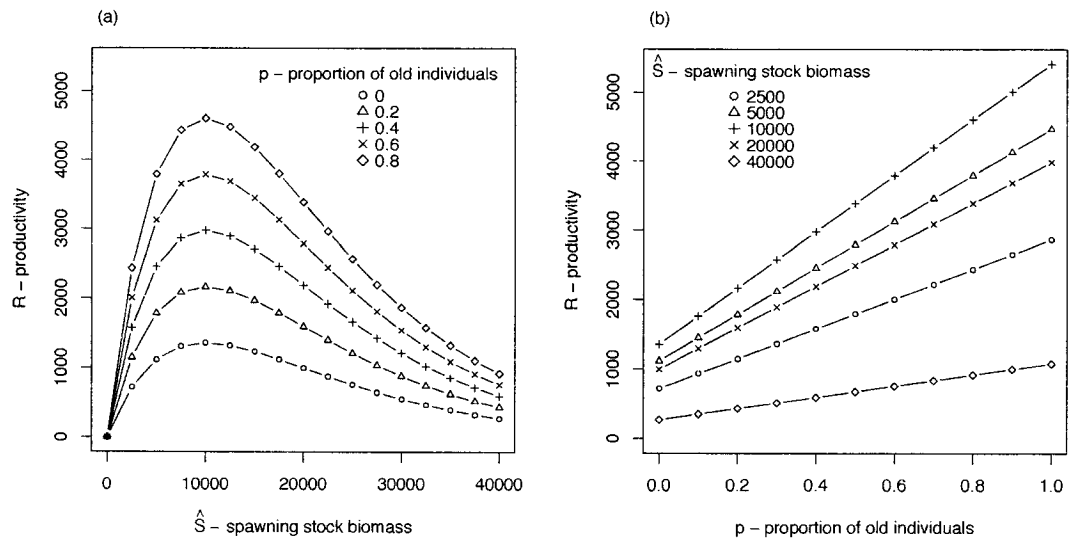

Figure 2.1: Two plots of Equation (2.11) from Case 1, the Ricker model with the maternal effect in the density-independent factors only. Panel (a) shows recruitment as a function of spawning stock biomass and panel (b) shows recruitment as a function of the proportion of old fish in the population. $\alpha_1 = 0.37$ ($\mu_1 = 0.01$, $\phi = 1$), $\alpha_2 = 1.47$ ($\mu_1 = 0.01$, $\phi = 4$), $\alpha_2 - \alpha_1 = 1.1$, and $\beta = 1e-4$ ($\gamma = 1e-6$, $T = 100$). Note: in a standard Ricker model, maximum productivity occurs when spawning stock biomass is $1/\beta$.

important (i.e., the maternal effect is no longer important). This observation is borne out in Figure 2.1(a). When $\hat{S}$ is very large or very small, there is very little difference in R for various values of p. But, at intermediate population sizes, changes in p result in a large spread in R. The implication is that when population size is high, density-dependent pressure severely limits the total number of individuals who survive. This property, which is a standard feature of a Ricker model, obscures the impact of even a strong maternal effect when either $\hat{S}$ or β is large.

Also, Figure 2.1(b) shows that, for any given population size, productivity increases as p increases. This result suggests that management for age-structure could

be effective.

2.2.2 Case 2: Maternal effect in density-dependent factors

The second case is that of a maternal effect that impacts the density-dependent factors but has no impact on the density-independent factors. There are many ways to manipulate the values of β_{ak} to model a maternal effect; I chose to model the case where Class 1 and Class 2 juveniles attract predators in equal numbers, but Class 1 juveniles are more vulnerable to predation (i.e., Class 1 individuals are harder hit by density-dependent mortality). We can represent this scenario by allowing inter-class rates to be affected by the maternal effect, $\beta_{21} < \beta_{12}$, but leaving intra-class rates unaffected, $\beta_{22} = \beta_{11}$. Here, I consider a limiting case of this condition: $\beta_{21} = 0$ while $\beta_{22} = \beta_{11} = \beta_{12} = \beta$ and $\alpha_1 = \alpha_2 = \alpha$.

Applying this condition to Equation (2.10) yields

$$R = \alpha\hat{S}\left[(1-p)e^{-\beta\hat{S}} + pe^{-p\beta\hat{S}}\right] \tag{2.12}$$

This result is not as easy to interpret as Equation (2.11); as a result we look to Figure 2.2 for interpretation. Figure 2.2(a) shows a pattern opposite to the pattern in Figure 2.1(a). Here when $\hat{S}$ is large, the maternal effect changes recruitment, but when $\hat{S}$ is small, the maternal effects matters very little. In this case, increasing the proportion of old adults in the population initially increases productivity, but as the proportion of old adults in the population increases further, productivity declines. Class 2 juveniles

do survive better, but as their numbers increase, their success comes at the expense of Class 1 juveniles. We see that the lowest productivity occurs when $p = 0$, but the highest productivity occurs at intermediate values of p. Also, the larger population size is, the more extreme the concavity of the function is. Productivity is most significantly affected by changes in p at the largest population sizes.

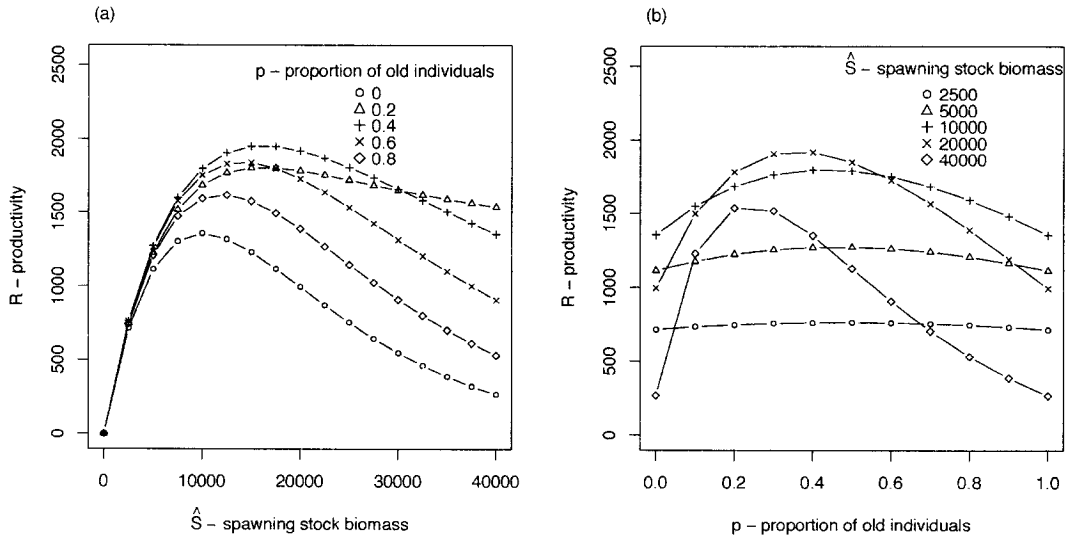

Figure 2.2: Two plots of Equation (2.12) from Case 2, the Ricker model with the maternal effect in the density-independent factors only. $\alpha = 0.37$ ($\mu = 0.01$, $\phi = 1$), $\beta = 1e-4$ ($\gamma = 1e-6$, $T = 100$). Note: in a standard Ricker model, maximum productivity occurs when spawning stock biomass is $1/\beta$.

In Figure 2.2(a) when $p = 0.2$, this Ricker stock-recruitment relationship looks remarkably similar to a traditional Beverton-Holt stock-recruitment relationship.

2.2.3 Case 3: Maternal effect in no predation model

Rather than solve a new differential equation we simply treat the case where $\Delta(n) = 0$ as a special case of the Ricker model, where $\gamma_{ak} = 0$. To get productivity for the two age-class no predation model, we substitute $\gamma_{ak} = 0$ into Equation (2.10) (recall that $\beta_{ak} = \gamma_{ak}T$)

$$R = [(1-p)\alpha_1 + p\alpha_2]\hat{S} = \alpha_1\hat{S} + p\hat{S}(\alpha_2 - \alpha_1) \tag{2.13}$$

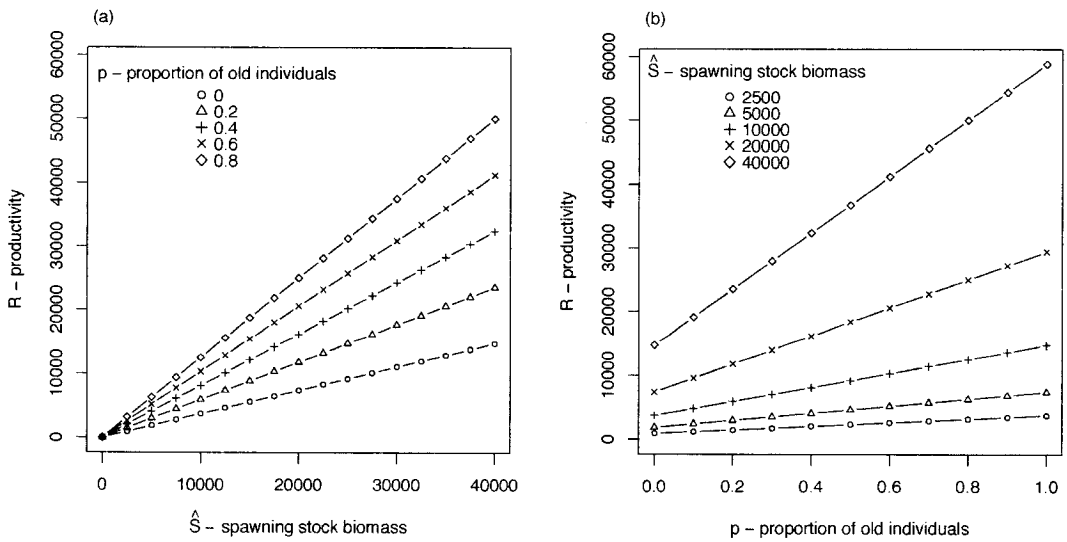

Figure 2.3: Two plots of Equation (2.13) from Case 3, the no predation model with a maternal effect. $\alpha_1 = 0.37$ ($\mu_1 = 0.01$, $\phi = 1$), $\alpha_2 = 1.47$ ($\mu_1 = 0.01$, $\phi = 4$), $\alpha_2 - \alpha_1 = 1.1$.

To model a maternal effect we use the same condition as Case 1, $\alpha_2 > \alpha_1$, with the same interpretation. The stock-recruitment relationship, $R(\hat{S})$, is linear and

has a slope that is the weighted average $(1-p)\alpha_1 + p\alpha_2$. $R(p)$ is also linear, with slope $\hat{S}(\alpha_2 - \alpha_1)$. Once again the parameter $\alpha_2 - \alpha_1$ affects the strength of the maternal effect. We can see in Figure 2.3 that increasing p leads to straightforward increases in productivity.

2.3 The Beverton-Holt Model

In the Beverton-Holt model density-dependent mortality is proportionate to juvenile density, $\Delta(n) = \gamma n$. The multi-class differential equation for the Beverton-Holt model is

$$\frac{1}{n_a}\frac{dn_a}{d\tau} = -\mu_a - \sum_{k=1}^{a_{max}} \gamma_{ak} n_k \tag{2.14}$$

In vector form this is

$$\text{diag}(\boldsymbol{n})^{-1}\frac{d\boldsymbol{n}}{d\tau} = -\boldsymbol{\mu} - \boldsymbol{\gamma}\boldsymbol{n} \tag{2.15}$$

where $\boldsymbol{n}$ and $\boldsymbol{\mu}$ are vectors of length a_{max}, and $\boldsymbol{\gamma}$ is a matrix of dimension $a_{max} \times a_{max}$. In general this equation cannot be solved analytically and must be solved numerically. The numerical integration is described in Section B.3.6. Here, to build intuition we examine a special case that *can* be solved analytically.

2.3.1 Case 4: A special case with a maternal effect in density-dependent mortality

Again, we reduce the problem to the two age-class model

$$\begin{aligned} \frac{dn_1}{d\tau} &= -\mu_1 n_1 - \gamma_{11} n_1^2 - \gamma_{12} n_1 n_2 \\ \frac{dn_2}{d\tau} &= -\mu_2 n_2 - \gamma_{21} n_1 n_2 - \gamma_{22} n_2^2 \end{aligned} \tag{2.16}$$

For the special case, we let $\gamma_{11} = \gamma_{21} = 0$ to obtain

$$\begin{aligned} \frac{dn_1}{d\tau} &= -\mu_1 n_1 - \gamma_{12} n_1 n_2 \\ \frac{dn_2}{d\tau} &= -\mu_2 n_2 - \gamma_{22} n_2^2 \end{aligned} \tag{2.17}$$

Equation 2.17 is the case where Class 1 individuals affect no density-dependent mortality. This can be thought of as interference competition, where Class 1 juveniles do not interfere with Class 2 juveniles or with other Class 1 juveniles, but Class 2 juveniles do interfere with Class 1 juveniles and with other Class 2 juveniles. Alternatively, this scenario can be explained with a predation attraction mechanism: it is the larger Class 2 individuals that attract predators, impacting both Class 1 and Class 2 juveniles. In either case, the maternal effect has a strong impact on the density-dependent factors.

The solution of Equation (2.17) is

$$R = \frac{n_1(0)e^{-\mu_1 T}}{\left[1 + \frac{\gamma_{22}}{\mu_2} n_2(0)\left(1 - e^{-\mu_2 T}\right)\right]^{\frac{\gamma_{12}}{\gamma_{22}}}} + \frac{n_2(0)e^{-\mu_2 T}}{1 + \frac{\gamma_{22}}{\mu_2} n_2(0)\left(1 - e^{-\mu_2 T}\right)} \tag{2.18}$$

The numerators, $n_1^0 e^{-\mu_1 T}$ and $n_2^0 e^{-\mu_2 T}$, give the number of juveniles which survive to time T in the absence of any density-dependent effects for Class 1 and Class 2 juveniles, respectively. These numbers are scaled by a denominator that accounts for density-dependent interactions. In the case where $\gamma_{12} = \gamma_{22}$, Class 1 and Class 2 numbers are scaled equally by density-dependence. Typically, we anticipate $\gamma_{12} \geq \gamma_{22}$, and that more Class 1 juveniles are lost to density-dependent factors than Class 2 juveniles. In this special case of the Beverton-Holt model, juveniles from "young" mothers are more vulnerable than juveniles from "old" mothers.

The denominators of Equation (2.18) feature the non-dimensional parameter $\frac{\gamma_{22}}{\mu_2} n_2(0)$. This parameter measures the importance of density-dependent factors relative to density-independent factors. When density-dependent factors are relatively important, $\gamma_{22} n_2(0) >> \mu_2$, productivity is relatively low.

If we further restrict the special case so that $\gamma_{12} = \gamma_{22}$ and also reintroduce p and the initial condition from Equation (2.5) ($n_a(0) = \phi_a S_a$), Equation (2.18) reduces to

$$R = \frac{\phi_1(1-p)\hat{S}e^{-\mu_1 T} + \phi_2 p\hat{S}e^{-\mu_2 T}}{1 + \frac{\gamma_{22}}{\mu_2}\phi_2 p\hat{S}\left(1 - e^{-\mu_2 T}\right)} \tag{2.19}$$

Now we define the density-independent parameter $\alpha_a = \phi_a e^{-\mu_a T}$, as we did in the Ricker

model, and define a new parameter

$$\tilde{\beta}_2 = \frac{\gamma_{22}}{\mu_2}\phi_2\left(1 - e^{-\mu_2 T}\right) \tag{2.20}$$

Equation 2.20 is the same reparameterization that is used in a traditional, single age-class Beverton-Holt model (Quinn and Deriso 1999). Recall that ϕ_2 is the per-capita number of juveniles at the start of the benthic stage; $\left(1 - e^{-\mu_2 T}\right)$ is the proportion of Class 2 settlers that do not survive to time T for density-independent reasons. The ratio γ_{22}/μ_2 is the relative importance of density-dependent mortality to density-independent mortality in the benthic stage. Put these together, and $\tilde{\beta}_2$ is approximately the per-capita rate of mortality to time T of Class 2 individuals due to density-dependent mortality. If we substitute these parameters into Equation (2.19) we obtain

$$R = \frac{\alpha_1\hat{S} + (\alpha_2 - \alpha_1)\hat{S}p}{1 + \tilde{\beta}_2 p\hat{S}} \tag{2.21}$$

First, notice the limits $p \to 0$ (no old fish) and $p \to 1$ (no young fish)

$$\lim_{p\to 0} R = \alpha_1\hat{S} \qquad \lim_{p\to 1} R = \frac{\alpha_2\hat{S}}{1 + \tilde{\beta}_2\hat{S}} \tag{2.22}$$

In these special cases the Class 1 fish effect no density-dependent mortality; in the absence of Class 2 fish, recruitment approaches a density-independent function. When there are only Class 2 fish, then recruitment reduces to a traditional Beverton-Holt stock-recruitment function (Quinn and Deriso 1999).

Notice that the parameter $\alpha_2 - \alpha_1$ appears again. In the Ricker model this difference determined the slope of the function $R(p)$ (i.e., the strength of the maternal effect). Here its role is difficult to isolate from p.

Finally, if $\hat{S} >> 1$ then Equation (2.21) is approximately

$$\lim_{\hat{S}\to\infty} R = \frac{(1-p)\alpha_1 + p\alpha_2}{p\tilde{\beta}_2} \tag{2.23}$$

For a given p, the stock-recruitment curve asymptotes to a constant value, as in a traditional Beverton-Holt model. But, if p changes as $\hat{S}$ changes, this disrupts the asymptotic property of this Beverton-Holt model.

2.3.2 Case 5: Maternal effect in ϕ_a

Figure 2.4 shows the numerical solution of the two age-class Beverton-Holt model when the maternal effect only impacts the survival of the pelagic phase. We can see that productivity generally increases as a function of p, but the magnitude of the increase is smaller when $\hat{S}$ is high.

Raising p from a low value to an intermediate value (0 to 0.2) has a much larger impact on productivity than raising p from an intermediate value to a high value (0.4 to 0.6).

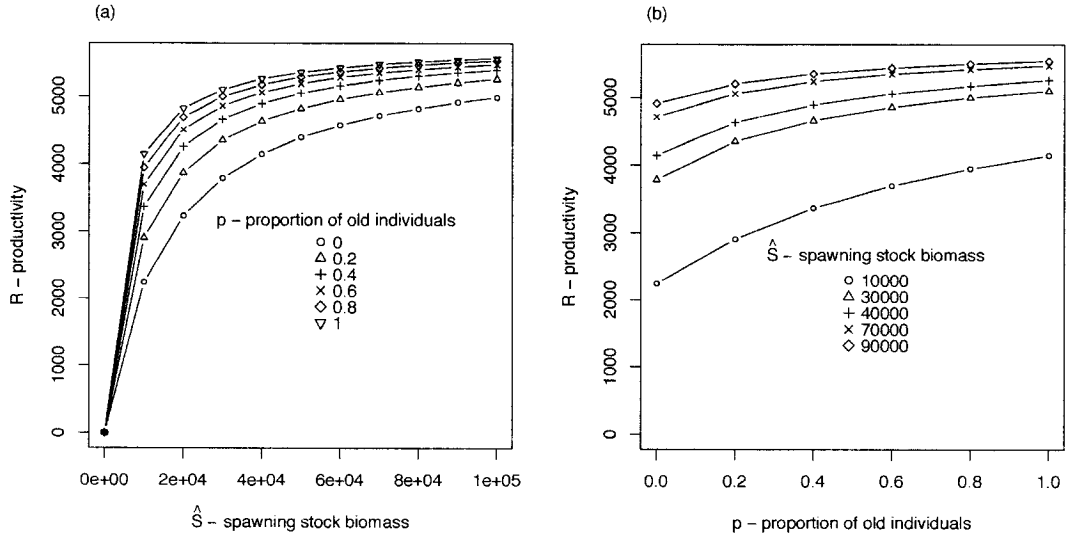

Figure 2.4: Two plots of the numerical solution to Equation (2.16); this plot is from Case 4, the Beverton-Holt model with the maternal effect in the density-independent pelagic stage. $\phi_1 = 1$, $\phi_2 = 4$, $\mu_1 = \mu_2 = 0.01$, $\gamma_{11} = \gamma_{12} = \gamma_{21} = \gamma_{22} = 1e-6$.

2.3.3 Case 6: Maternal effect in μ_a

Figure 2.5 shows the numerical solution of the two age-class Beverton-Holt model when the maternal effect only impacts the density-independent mortality rate of the benthic phase. In this case the maternal effect causes juveniles to be more robust in the benthic stage but does not effect survival of the pelagic stage or their ability to avoid predators. This situation may occur if larger size is helpful in the benthic phase, but survival of the pelagic stage is determined by luck rather than quality of the individual.

Here, productivity also consistently increases with p, but the pattern contrasts with the previous case; the magnitude of the difference increases with population size. We do see the same phenomenon as in Case 5, where increasing from a low to intermediate value of p effects productivity more than increasing from an intermediate to high

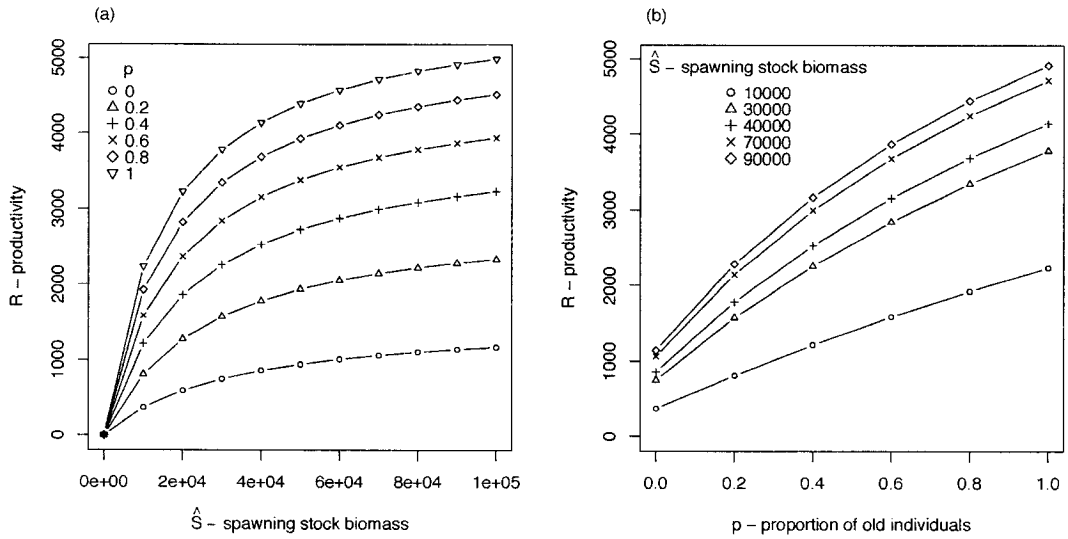

Figure 2.5: Two plots of the numerical solution to Equation (2.16); this plot is Case 5, the Beverton-Holt model with the maternal effect in the density-independent component of the benthic stage. $\phi_1 = \phi_2 = 1$, $\mu_1 = .03$, $\mu_2 = 0.01$, $\gamma_{11} = \gamma_{12} = \gamma_{21} = \gamma_{22} = 1e-6$.

value of p. Though, here the effect is less pronounced.

2.3.4 Case 7: Maternal effect in γ_{ak}

Figure 2.6 shows the numerical solution of the two age-class Beverton-Holt model when the maternal effect only impacts the density-dependent mortality rate of the benthic phase, γ. This is the same limit as in Case 2 of the Ricker model, $\gamma_{11} = \gamma_{12} = \gamma_{22}$ while $\gamma_{21} = 0$. Once again, when the maternal effect impacts the density-dependent mortality rates, the function becomes much more complex. Productivity does not necessarily increase with p; it is concave with respect to p. As in the case when the maternal effect impacts μ, the magnitude of the productivity differences are largest when population density is high.

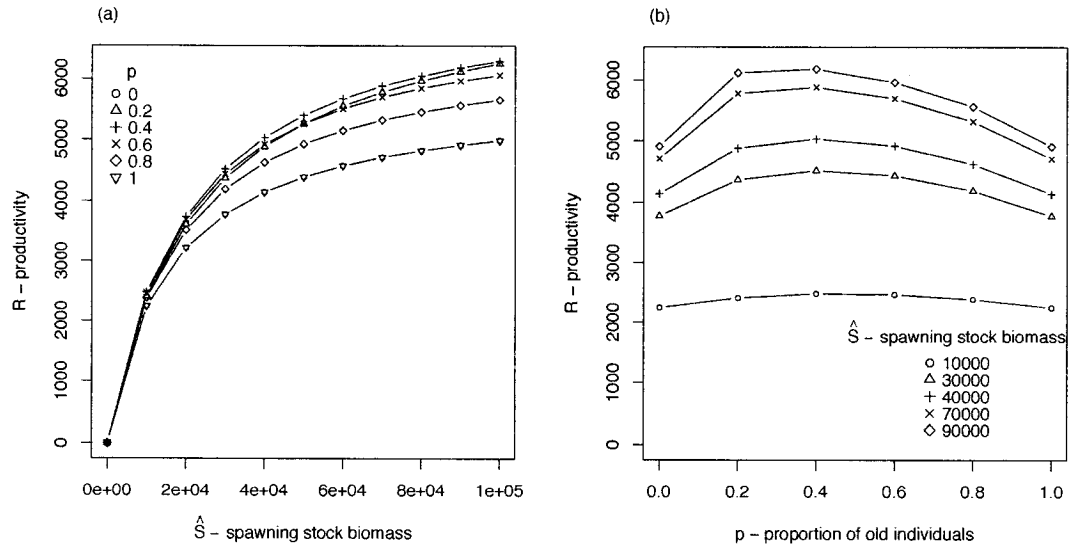

Figure 2.6: Two plots of the numerical solution to Equation (2.16); this plot is Case 6, the Beverton-Holt model with the maternal effect in the density-dependent component of the benthic stage. $\phi_1 = \phi_2 = 1$, $\mu_1 = \mu_2 = 0.01$, $\gamma_{11} = \gamma_{12} = \gamma_{22} = 1e-6$, $\gamma_{21} = 0$.

2.4 Discussion

Our motivating question is: How will productivity respond to an age-dependent maternal effect? We want the best possible answer given substantial uncertainty about the impact of maternal effects on survival and the form of density-dependent mortality.

Productivity is positively correlated with p (the proportion of old fish) when the maternal effect only impacts the pelagic phase, because then it only impacts density-independent factors. However, the larger the population size, the less the maternal effect matters, unless there is almost no compensation in the benthic phase.

In cases where the maternal effect impacts density-dependent mortality rates in the benthic stage, the story is significantly more complex. Here, the maternal effect

confers an advantage to some individuals in the population, but also changes the competitive environment for other individuals. As a result, whole population consequences are not easy to predict. When part of the advantage conferred by the maternal effect is an escape from density-dependent mortality, a potential trade-off arises between the success of the offspring from older mothers and overall productivity. We discover the possibility that more old fish may fail to increase productivity, and may even decrease productivity.

In cases where a Beverton-Holt mechanism dominates, larger populations are *generally* as or more productive than smaller populations; however in some cases a younger population is more productive than an older population of the same size. When a Ricker mechanism prevails, it seem that there is a broad range of circumstances in which a smaller population is more productive than a larger population. This outcome is a feature of a traditional Ricker model with no maternal effects, but the maternal effect exacerbates the phenomenon.

When there is no predation, the story is very simple: more old fish lead to higher productivity. This case is ecologically unrealistic but should not be immediately dismissed. Rockfish have highly variable recruitment, and it is probable that the adult population is sustained by rare and very large recruitment classes (Love et al. 2002). Very large recruitment classes are the classes most likely to overwhelm predation pressure and resemble a no predation model (recall the low predation case in Figure 1.5a).

It appears there is a relatively narrow set of circumstances where managing for

age-structure would be harmful to productivity. The circumstances that cause concern are when juveniles densities are very high and there is a large number of juveniles with a strong competitive advantage due to a superior ability to avoid predation. In all other cases, we expect that increasing the proportion of old fish in a population with an age-dependent maternal effect will yield higher productivity. We do not have the information we need to quantify how much higher productivity could be, but these models suggest that very large (50–500%) increases are possible.

In the two age-class population, p is a natural metric for age-structure. It is natural to think of p as a very small proportion; however, its value is a function of the threshold age (a_t) between "young" and "old." If we assume a steady-state age distribution then

$$p(a_t) = \frac{\int_{a_t}^{a_{max}} e^{-Ms} ds}{\int_{a_{mat}}^{a_{max}} e^{-Ms} ds} = \frac{e^{-Ma_t} - e^{-Ma_{max}}}{e^{-Ma_{mat}} - e^{-Ma_{max}}} \tag{2.24}$$

where a_{max} is maximum age, a_{mat} is age of maturity and M is the rate of natural mortality. For Black rockfish, maximum age is about fifty years, age of maturity is about six years (Love et al. 2002), $M = 0.115\ yr^{-1}$ (Ralston and Dick 2003), and based on the observed maternal effect, we can guess $a_t = 10$ (Berkeley et al. 2004a). In this example, a fully protected Black rockfish population with a steady-state age-distribution has $p = 0.63$ (i.e., 63% of the population is older than ten years). In contrast, current Black rockfish populations are heavily harvested, and only about 16% of the reproductive population is older than ten years (Ralston and Dick 2003).

If the maternal effect simultaneously impacts both the density-independent factors and the density-dependent factors, productivity gains from the advantage in the density-independent factors could swamp productivity losses from harmful compensation in the density-dependent factors. I do not show this situation here because to address it fully would require better information than I have about the relative magnitudes of density-independent and density-dependent mortality rates, and the relative impact of the maternal effect on these rates. I revisit this subject in the following chapter.

Finally, I note that in several cases here, the intensity of the maternal effect depends on the difference $\alpha_2 - \alpha_1$ rather than the ratio α_2/α_1—it seems the ability to survive the environment is more important than the ability relative to conspecifics. This result may be useful for the design of empirical studies of maternal effect's impact on survival.

Chapter 3

The Simulation Model

We now have a productivity model that allows us to connect differential larval quality to maternal age. While productivity has inherent ecological interest, age-dependent maternal effects have attracted attention in the context of over-fished populations facing long recovery times. For this reason I will now present a simulation of the recovery of an overfished population. The population dynamics are age-structured and the recruitment function is the multivariate Beverton-Holt productivity function developed in the previous chapter.

This population simulation is a powerful tool for addressing the uncertainty we have about (1) the magnitude of pre-recruitment survival and mortality rates (2) the persistence of the maternal effect and (3) the magnitude of the maternal effect. I calculate how time to recovery depends on each of these unknown variables, and seek robust patterns.

Wherever possible I have used data to parameterize the simulation. However,

in the maternal effects productivity model, the base parameters $\hat{\phi}$, $\hat{\mu}$ and $\hat{\gamma}$ present a special problem because there are no data to meaningfully inform what these values should be. Each simulation run takes time, and there are many runs for each combination of base parameters, so I must find a representative subset of the reasonable values for each base parameter. I describe here how I parameterized the model.

3.1 Stock-Recruitment Model

The number of individuals of age a in year t is $N(a,t)$, while the number of juveniles in year t is $n(a,\tau,t)$ or simply $n_a(\tau)$ when t is constant. For juveniles, a indicates their maternal age. Here τ is the time index for the pre-recruitment period; $\tau = 0$ at the time of settlement to the benthic habitat, thus,

$$n(a,0,t) = \phi(a)P_m(a)W(a)N(a,t) \tag{3.1}$$

where W is weight at age a (defined below in Equation 3.10), P_m is the probability a fish is mature at age a, and ϕ is the number of juveniles that settle per unit of mature adult biomass of age a. P_m is modeled with a sigmoidal curve

$$P_m(a) = \frac{1}{1 + e^{-c_m(L(a)-L_{50})}} \tag{3.2}$$

where L is length at age a and is defined in Equation 3.9, half of fish length L_{50} are mature and c_m is a constant that determines the steepness of the maturity curve.

Survival through the benthic phase is modeled with the modified Beverton-Holt function given by Equation 2.14. The model is introduced in Section 2.3. Equation 3.1 serves as the initial condition needed to solve Equation 2.14.

To calculate number of recruits in year t, I evaluate the solution of Equation 2.14 at time T, the time of recruitment, and sum across maternal ages,

$$N(1,t) = \sum_a n(a,T,t) \tag{3.3}$$

3.2 Maternal Effects Model

To model an age-dependent maternal effect, I allow the survival and mortality rates—ϕ, μ and γ—to depend on maternal age. In the case of the pelagic survival rate, ϕ, I use a sigmoidal curve with an inflection point at a_{ME}, the age at which the rate is half of the maximum possible rate. Thus,

$$\phi(a) = \hat{\phi}\left(1 + \frac{p_\phi}{1 + e^{-c_\phi(a - a_{ME})}}\right) \tag{3.4}$$

where $\hat{\phi}$ is the base settlement rate and p_ϕ is the maximum proportionate increase above $\hat{\phi}$ due to the maternal effect. Offspring of the youngest mothers have a settlement rate of approximately $\hat{\phi}$, and offspring of the oldest mothers ($a >> a_{ME}$) have a settlement rate of approximately $(1 + p_\phi)\hat{\phi}$. The parameter c_ϕ controls the steepness of the transition from a settlement rate of $\hat{\phi}$ to a settlement rate of $(1 + p_\phi)\hat{\phi}$. When c_ϕ is large there is a very sudden transition in settlement when maternal age reaches a_{ME}, when c_ϕ is small

the transition is gradual. The relationship between ϕ and maternal age is illustrated in Figure B.5a.

Density-independent mortality in the benthic stage is also modeled with a sigmoidal curve, except in this case mortality is a declining function of maternal age.

$$\mu(a) = \hat{\mu}\left(1 - \frac{p_\mu}{1 + e^{-c_\mu(a - a_{ME})}}\right) \tag{3.5}$$

where $\hat{\mu}$ is the base density-independent mortality rate for the benthic stage and p_μ is the minimum proportionate decrease of $\hat{\mu}$ due to the maternal effect. Offspring of the youngest mothers have a density-independent mortality rate of approximately $\hat{\mu}$ and offspring of the oldest mothers ($a >> a_{ME}$) have a density-independent mortality rate of approximately $(1-p_\mu)\hat{\mu}$. The parameter c_μ controls the steepness of the transition from a rate of $\hat{\mu}$ to a rate of $(1 - p_\mu)\hat{\mu}$. When c_μ is large there is a very sudden transition in mortality when maternal age reaches a_{ME}, and when c_μ is small the transition is gradual. The relationship between μ and maternal age is illustrated in Figure B.5b.

Modeling density-dependent mortality in the benthic stage is slightly more complex than either ϕ or μ; density-dependent mortality will depend both on an individual's maternal age and on its competitors' maternal ages. Thus, γ is a square matrix of dimension $a_{max} \times a_{max}$. I model this in two steps. First I model the intra-class mortality rates with a sigmoidal curve

$$\gamma(a, a) = \hat{\gamma}\left(1 - \frac{p_\gamma}{1 + e^{-c_\gamma(a - a_{ME})}}\right) \tag{3.6}$$

where $\hat{\gamma}$ is the base density-dependent mortality rate for the benthic stage and p_γ is the minimum proportionate decrease of $\hat{\gamma}$ due to the maternal effect. Offspring of the youngest mothers have a density-dependent mortality rate of $\hat{\gamma}$ and offspring of the oldest mothers have a density-dependent mortality rate of $(1-p_\gamma)\hat{\gamma}$. The parameter c_γ controls the steepness of the transition from a rate of $\hat{\gamma}$ to a rate of $(1-p_\gamma)\hat{\gamma}$. When c_γ is large there is a very sudden transition in mortality when maternal age reaches a_{ME}, when c_γ is small the transition is gradual.

Second, I model inter-class density-dependent mortality rates as a function of the difference between an individual's maternal age, and their competitor's maternal age, $a-k$

$$\gamma(a,k) = \gamma(a,a)e^{-v_\gamma(a-k)} \tag{3.7}$$

Here, v_γ controls the rate at which the mortality rate changes with respect to the difference in maternal age between two juveniles: when v_γ is small it matters very little if there is a difference in maternal age; when v_γ is large γ is very sensitive to differences in age between conspecifics. The relationship between γ and maternal age is illustrated in Figure B.5c for cases where $k = 10$.

3.3 Adult Population Model

$N(a,t)$ is the number of adults of age a at time t. It is calculated as the number of adults at age $a-1$ at time $t-1$ less the number that have died due to natural causes

or fishing; this is written

$$N(a+1,t+1) = N(a,t)e^{-M(a)-F(a)} \tag{3.8}$$

where $M(a)$ is the rate of natural mortality experienced by adults of age a and $F(a)$ is the rate of fishing mortality experienced by adults of age a. Both natural and fishing mortality are functions of length, and length is a calculated with the von Bertalanffy growth equation

$$L(a) = L_\infty \left(1 - e^{-\kappa(a-a_0)}\right) \tag{3.9}$$

Here L_∞ is the asymptotic length, κ is the growth rate, and a_0 is the theoretical age of a fish of length zero centimeters. The von Bertalanffy growth function is illustrated in Figure B.3.

Individual weight is a standard allometry of length

$$W(a) = w_1 L(a)^{w_2} \tag{3.10}$$

where $W(a)$ is weight, and w_1 and w_2 are constants. The appropriate values for the constants can usually be found in the literature, and in the case of rockfish, estimates for these constants can be found in *Rockfishes of Northeast Pacific* (Love et al. 2002).

Adults are removed from the population by natural mortality. The rate of natural mortality, $M(a)$, experienced by an individual of age a is a function of its length. There is a component to the natural mortality based on the length of the individual, m_1,

and a component that is independent of the individual's length, m_0 (Lorenzen 2000),

$$M(a) = m_0 + \frac{m_1}{L(a)} \tag{3.11}$$

This simulation is age-structured, rather than length structured, and therefore natural mortality is made into a function of age via Equation 3.9. The natural mortality function is shown as a function of both length and age in Figure B.4.

The simulation has a finite number of age classes. The greatest age class must accommodate individuals older than the maximum age in the simulation a_{max}, where $a_{max} >> a_{ME}$:

$$N(a_{max}, t+1) = [N(a_{max}, t) + N(a_{max} - 1, t)]\, e^{-M(a_{max})-F(a_{max})} \tag{3.12}$$

Fishing mortality as a function of age is given by

$$F(a) = \hat{F}S(L(a)) \tag{3.13}$$

where $\hat{F}$ is the rate of fishing mortality and S is the selectivity function. To emulate data for nearshore rockfish, this simulated fishery has a double-sided selectivity curve: very young individuals are not selected by this fishery, and very old individuals are selected at a reduced rate (Ralston and Dick 2003). The selectivity function is

$$S(a) = \frac{s_y}{1 + e^{-c_y(L(a)-L_y)}} - \frac{s_y - s_o}{1 + e^{-c_o(L(a)-L_o)}} \tag{3.14}$$

where s_y is the maximum selectivity for young fish, c_y is the steepness of the gain in selectivity, and L_y is the inflection point of the ascent and the length at which selectivity is half of s_y. The minimum selectivity for old fish is s_o, c_o is the steepness of the descent in selectivity, and L_o is inflection point of the descent and the length at which selectivity is halfway between s_y and s_o. In Appendix B.3.5 I describe how the selectivity function is parameters are chosen based on the stock-assessment and includes an illustration of the double-sided selectivity function used for the the results presented throughout this thesis.

3.4 Parameterization

I selected twenty-seven sets of pre-recruitment rates, shown in Table 3.2, eighteen cases of the maternal effect, shown in Table 3.3, and six harvest levels, for a total of 2,916 parameter combinations. Each set of parameter was run for three values of σ_ϕ, and the two nonzero values were iterated ten times. This sums to a total 61,236 attempted simulation runs. In some cases, the simulation failed because the simulated population fell to zero biomass (i.e., the simulated population went extinct). Simulation failures occurred more often when there was high environmental variability (Table 3.1). Failures were well distributed across the parameter space, so that no parameter bias was introduced. The final data set includes 53,022 measurements of TTR.

Table 3.1: Numbers of attempted and successful simulation runs.

σ_ϕ	Runs Attempted	Runs Successful	Success Rate
0	2,916	2,910	99.8%
1	29,160	28,446	97.6%
2	29,160	21,666	74.3%
Total	61,236	53,022	86.6%

3.4.1 Stock-Recruitment Model

We would like to compare the simulated data to *S. melanops* data to confirm that the simulated population is analogous to a natural population. In particular, we want to choose values for $\hat{\phi}$, $\hat{\mu}$ and $\hat{\gamma}$ that produce values of recruitment and population biomass that are comparable to values for a natural population. The most recent stock assessment of *S. melanops* provides us estimates of current recruitment, equilibrium biomass and steepness. In the case of no maternal effect, the stock recruitment model (Equation 2.14) reduces to a standard Beverton-Holt model so that

$$R = \frac{\alpha S}{1 + \beta S} \tag{3.15}$$

where R is the number of recruits, S is the spawning stock biomass and α and β are defined in terms of the base parameters

$$\alpha = \hat{\phi} e^{-\hat{\mu} T} \qquad \beta = \hat{\phi} \frac{\hat{\gamma}}{\hat{\mu}} \left(1 - e^{-\hat{\mu} T}\right) \tag{3.16}$$

Here T is the length of juvenile period (see Figure 1.4). In all of the simulation cases the mortality rates are parameterized so that $T = 100$. Here, asymptotic recruitment is α/β. If we assume that recruitment at equilibrium biomass (R_0) is equal to the asymptotic recruitment, then

$$R_0 = \frac{\alpha}{\beta} \tag{3.17}$$

This gives us the means to calculate equilibrium recruitment as a function of the base parameters in the absence of a maternal effect. If we assume a steady-state age-distribution, then we can estimate equilibrium biomass to be

$$B_0 = R_0 \sum_{a=1}^{a_{max}} e^{-Za} \tag{3.18}$$

where a indexes age and Z is the rate of total mortality. We can also calculate steepness (h), defined as

$$h = \frac{R(0.2B_0)}{R(B_0)} \tag{3.19}$$

In the most recent stock-assessment for Black rockfish, recruitment is estimated at 2,000–4,000 individuals, equilibrium biomass is estimated around 20,000 metric tons, steepness is estimated at about 0.65 and natural mortality is about 0.115 yr^{-1} (Ralston and Dick 2003). In Table A.1 I show calculations of R_0, B_0 and h for these base parameters in the case of no maternal effect. In Figure 3.1 I show estimates of recruitment given $\hat{\mu}$ and $\hat{\gamma}$.

Table 3.2 shows the range of base parameter values used to create the simulated

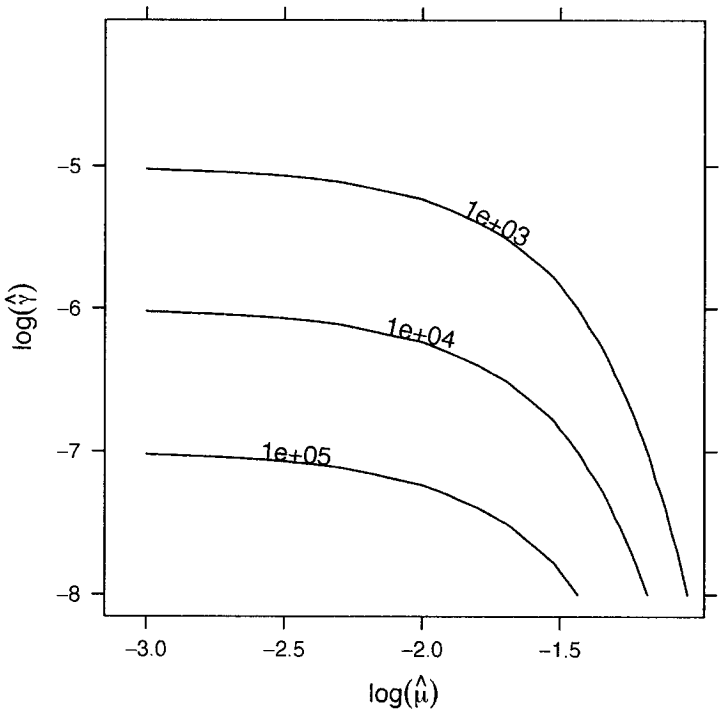

Figure 3.1: Contours give an estimates of asymptotic recruitment as a function of $\hat{\mu}$ and $\hat{\gamma}$ in the absence of maternal effects. Recruitment is estimated using Equation 3.17. This is for large spawning stock biomass (when $S \rightarrow \infty$ in Equation 3.15) where recruitment depends only on $\hat{\mu}$ and $\hat{\gamma}$ and is independent of $\hat{\phi}$.

data shown here. I chose parameter values that spanned the range of appropriate values. Also, I chose parameters values that produced robust simulated populations. Parameters values too close to the edge of the parameter space created simulation runs with populations that would go extinct even in the absence of fishing. This was the basis of my choice for values of $\hat{\phi}$. Simulations with $\hat{\phi} < 0.5$ would not persist under most circumstance. Simulations with $\hat{\phi} > 2$ would quickly grow to unreasonably large sizes of adult biomass and produce steepness values much larger than appropriate for

rockfish (see Table A.1).

Table 3.2: All twenty-seven sets of pre-recruit mortality rates used in the simulation results.

$\hat{\phi}$	$\hat{\mu}$	$\hat{\gamma}$	$\hat{\phi}$	$\hat{\mu}$	$\hat{\gamma}$	$\hat{\phi}$	$\hat{\mu}$	$\hat{\gamma}$
0.5	0.001	5e-7	0.5	0.01	5e-7	0.5	0.03	5e-7
1	0.001	5e-7	1	0.01	5e-7	1	0.03	5e-7
2	0.001	5e-7	2	0.01	5e-7	2	0.03	5e-7
0.5	0.001	1e-6	0.5	0.01	1e-6	0.5	0.03	1e-6
1	0.001	1e-6	1	0.01	1e-6	1	0.03	1e-6
2	0.001	1e-6	2	0.01	1e-6	2	0.03	1e-6
0.5	0.001	5e-6	0.5	0.01	5e-6	0.5	0.03	5e-6
1	0.001	5e-6	1	0.01	5e-6	1	0.03	5e-6
2	0.001	5e-6	2	0.01	5e-6	2	0.03	5e-6

3.4.2 Maternal Effects Model

To address the range of uncertainty in the persistence of the maternal effect I simulated eighteen versions of a maternal effect. The parameter values for each of these cases are shown in Table 3.3. These cases include scenarios where there is no maternal effect (none), scenarios where the maternal effect has dissipated by the time of settlement (pelagic only), cases where the maternal effect impacts both pre- and post-settlement processes (pelagic and benthic), and scenarios where the maternal effect impacts only post-settlement processes (benthic only).

For each productivity parameter that can be impacted by a maternal effect, there is a curvature parameter that controls the steepness of the effect (c_ϕ, c_μ, and c_γ). This parameter can be tuned, but is instead held constant for all of the results shown

Table 3.3: Parameter values for the eighteen cases of the maternal effect. Case 1 is the case of no maternal effect. Cases 2–5 the maternal effect is only in the pre-settlement stage (it only effects ϕ). Cases 6–14 the maternal effect impacts both pre- and post-settlement processes. In Cases 6–10 the pre-settlement effect is constant ($p_\phi = 1$) while the post-settlement effect on the density-dependent parameter (p_γ) varies. In Cases 11–14 the post-settlement effect is constant ($p_\mu = 0.4$, $p_\gamma = 0.4$, $v_\gamma = 0.01$), while the pre-settlement effect (p_ϕ) varies. Cases 15–18 the maternal effect is only in the density-dependent part of the post-settlement stage (it only effects γ).

Case	Effect	p_ϕ	p_μ	p_γ	c_ϕ	c_μ	c_γ	v_γ
1	none	0.0	0.0	0.0	0.8	0.8	0.8	0.00
2		0.5	0.0	0.0	0.8	0.8	0.8	0.00
3	pelagic	1.0	0.0	0.0	0.8	0.8	0.8	0.00
4	only	1.5	0.0	0.0	0.8	0.8	0.8	0.00
5		2.0	0.0	0.0	0.8	0.8	0.8	0.00
6		1.0	0.4	0.8	0.8	0.8	0.8	0.01
7		1.0	0.4	0.6	0.8	0.8	0.8	0.01
8		1.0	0.4	0.4	0.8	0.8	0.8	0.01
9		1.0	0.4	0.2	0.8	0.8	0.8	0.01
10	pelagic and	1.0	0.4	0	0.8	0.8	0.8	0.01
11	benthic	0.5	0.4	0.4	0.8	0.8	0.8	0.01
12		1.0	0.4	0.4	0.8	0.8	0.8	0.01
13		1.5	0.4	0.4	0.8	0.8	0.8	0.01
14		2.0	0.4	0.4	0.8	0.8	0.8	0.01
15		0.0	0.0	0.8	0.8	0.8	0.8	0.00
16	benthic	0.0	0.0	0.6	0.8	0.8	0.8	0.00
17	only	0.0	0.0	0.4	0.8	0.8	0.8	0.00
18		0.0	0.0	0.2	0.8	0.8	0.8	0.00

in this thesis ($c_\phi = c_\mu = c_\gamma = 0.8$). I experimented with varying this parameter, but found that the qualitative patterns in the results were not strongly impacted by changes in the curvature. Therefore, I chose to hold the curvature constant at an intermediate value that approximates the steepness of the observed maternal effect (shown in Figure 1.1).

The parameters that control the magnitude of the maternal effect are p_ϕ, p_μ, p_γ and v_γ. The ranges for p_μ and p_γ are straightforward to select. They define the maximum proportion of decrease in mortality rate attainable for the offspring of the oldest mothers. As proportions, p_μ, p_γ are bound between zero and one. The cases listed in Table 3.3 use values for these parameters that are greater than or equal to zero and less than one.

The parameter p_ϕ is more difficult to bound; it is a proportionate increase in settlement rate. It must be greater than or equal to zero, but in theory it can be infinitely large. This parameter changes the average productivity of the population, and thus the maximum appropriate value is roughly related to the maximum value for $\hat{\phi}$. The $max(p_\phi\hat{\phi})$ should not be much greater than $max(\hat{\phi})$. In this case, $max(\hat{\phi}) = 2$ therefore I selected the $max(p_\phi) = 2$.

There is one last parameter in the maternal effect model, v_γ. This parameter controls the strength of inter-class age differences on the density-dependent interaction rate (Equation 3.7). In sensitivity analysis, I found that increases in this parameter behaved qualitatively like increases in p_γ. Since there was little difference between these parameters, I chose to minimize variation in this parameter to reduce the number

of tuning variables. This parameter is set to zero in all but the cases where the maternal effect impacts both pelagic and benthic processes. In these cases, I set v_γ to a level that produced similar quantitative changes as an 0.2 increase of p_γ.

3.4.3 Adult Population Model

The adult population simulation is based on the model species black rockfish (*S. melanops*). Many of the important biological parameters for this species are directly available in the scientific literature (e.g., the von Bertalanffy growth parameters and the weight allometry). Several other parameters are not directly available, but can be easily derived from data in the literature (e.g., the length-based and length-independent rates of natural mortality could be derived from estimates of total average mortality and the population length distribution). The sources of data-based parameters are summarized in Table 3.4.

3.4.4 Harvest Rate

Black rockfish is not an overfished species and is moderately productive for a rockfish. The most recent stock assessment estimates that black rockfish biomass is at 55% of unfished biomass. The current harvest rate for the Black rockfish fishery is equivalent to $\hat{F} = 0.075$ (Ralston and Dick 2003).

There are seven species of rockfish in rebuilding plans today. For these species, the harvest rules range from the equivalent of $\hat{F} = 0.0082$ (for Pacific Ocean Perch, *S. alutus*) to $\hat{F} = 0.049$ (for Bocaccio, *S. paucispinis*) (PFMC 2006).

Table 3.4: Data based parameter values used in simulation.

Parameter	Value	Equation	Source
L_∞	53.25 cm		
κ	0.15 cm/day	3.9	Love et al. 2002
t_0	-2.84 $days$		
w_1	0.0043 g	3.10	Love et al. 2002
w_2	3.362		
M	0.115 yr^{-1}		
m_0	0.8	3.11	see Section B.3.2
m_1	0.03		
s_y	1		
c_y	0.5		
L_y	33 cm	3.14	see Section B.3.5
s_o	0.3		
c_o	0.5		
L_o	45 cm		
c_m	0.4103	3.2	Love et al. 2002
L_{50}	39.53 cm		

In Chapters 4 and 5 I show time to recovery (TTR) as a function of harvest rate ($\hat{F}$). I present values of $\hat{F}$ that range from 0–0.1. This range includes the harvest rates in the current rockfish rebuilding plans. It also covers the realistic range for harvest rates under rebuilding: in most cases the simulated populations do not recover at $\hat{F} > 0.08$.

3.5 Measuring Time To Recovery

In Figure 3.2 I show a time series of spawning stock biomass from an example simulation run. In each case, I run the simulation until the population reaches an equilibrium biomass, B_0. Then fishing begins and continues until the population reaches an overfishing threshold at 15% of initial biomass (B_{15}). I then allow the population to rebuild, under various levels of fishing pressure, and measure how long it takes to reach a rebuilding target at 40% of initial biomass (B_{40}). Time To Recovery (TTR) is the number of years the population takes to recover from B_{15} to B_{40}. In the simulation, TTR is capped so it is never greater than 100 years.

The threshold targets B_{15} and B_{40} were chosen to reflect common management reference points. Amendment 1 of the Magnuson-Stevens Act requires that overfished stocks be rebuilt (PFMC 2006). However, the law gives considerable discretion to the fishery management councils to define when a stock is "overfished" and when it is "rebuilt." The reference point B_{40} is a common rebuilding target because it is a proxy for B_{msy}, the population biomass at maximum sustainable yield. The overfishing threshold

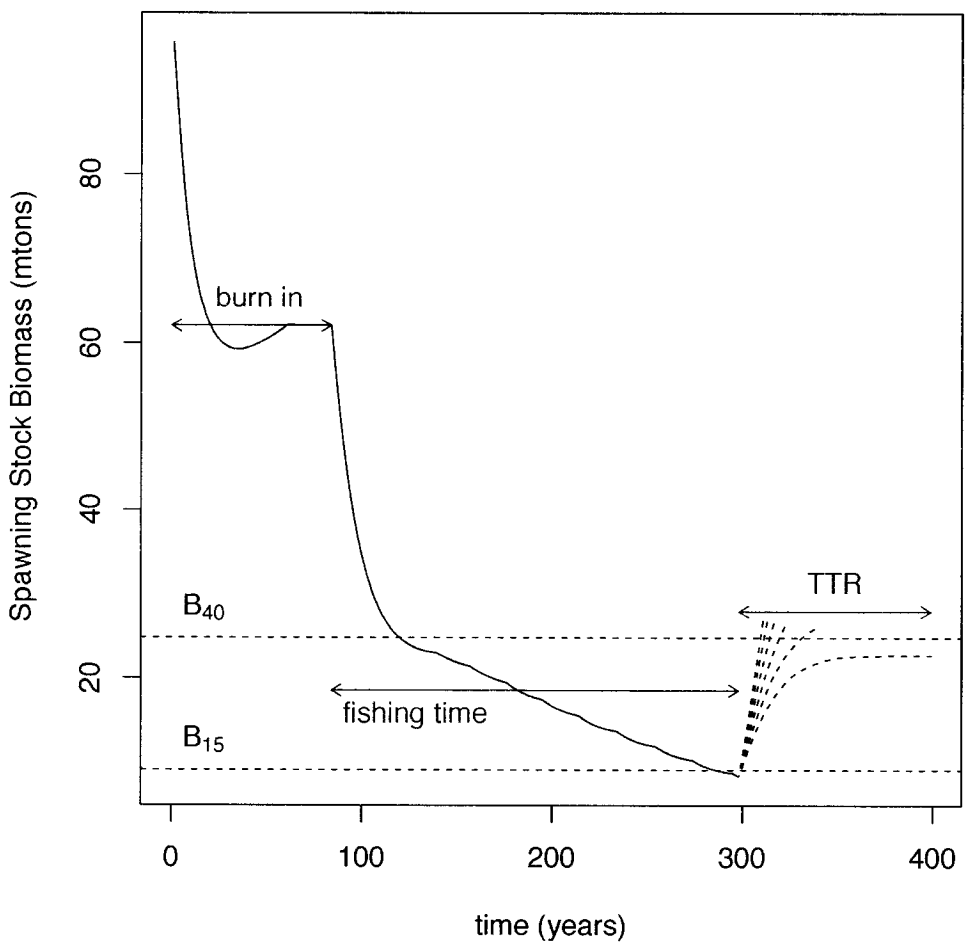

Figure 3.2: Example of a time series from the simulation. The simulation starts at an arbitrary initial condition and runs until it reaches a steady-state, the steady-state population is harvested at a high level until the population falls below the overfishing threshold, B_{15}. Fishing pressure is reduced to recover the population to the rebuilding target, B_{40}. The dashed lines show recovery trajectories under various fishing levels. $\hat{\phi} = 2$, $\hat{\mu} = 0.001$, $\hat{\gamma} = 5e-6$, $p_\phi = p_\mu = p_\gamma = v_\gamma = 0$.

is set on a stock by stock basis and the selection usually reflects the stock's productivity: more productive stocks can tolerate lower thresholds. The overfishing threshold is usually between B_{10}–B_{35}; the Pacific Fisheries Management Council uses a rebuilding threshold of B_{25} for rockfish. I chose to use a slightly lower overfishing threshold of B_{15} because most of the seven west coast rockfish stocks that are currently designated overfished have biomass estimates well below the B_{25} threshold: *S. ruberrimus* (7%), *S. entomelas* (23.6%), *S. levis* (7%), *S. paucispinis* (2%), *S. pinniger* (9.4%), *S. alutus* (13%), and *S. crameri* (14–31%) (PFMC 2006).

Chapter 4

Time To Recovery in a Static Environment

I now present the measurements of time to recovery obtained through deterministic runs of the simulation model presented in the previous chapter. In a complex system, such as this one, it is helpful to limit the amount of uncertainty considered at any one time. In this chapter, I present outcome distributions with large variance. However, none of this variance is due to external environmental variability. All of the variance in outcomes presented here is due to uncertainty in the magnitude of recruitment rates and uncertainty in the magnitude and persistence of the maternal effect. In the next chapter I will present stochastic outcomes of the simulation and examine how to interpret the conclusions of this chapter in the context of environmental variabililty.

4.1 Magnitude of the maternal effect

4.1.1 Averaging across all parameters

The final data set includes 2,910 deterministic measurements of TTR. To gain initial understanding of the results I performed a series of linear regressions on TTR. I show the results of two of these regressions in Table 4.1. Regression Model 1 includes all of the significant variables in the model, and regression Model 2 includes only the single most influential variable, the harvest rate. We can see that the harvest rate alone explains nearly half of the variability in TTR. But we can account for an additional 32% of the variability by including the maternal effect and the pre-recruitment survival and mortality rates.

In regression Model 1, TTR is negatively correlated with the density-independent maternal effects p_ϕ and p_μ, but it is positively correlated with density-dependent maternal effect p_γ. In Figure 4.1 I show boxplots of time to recovery versus the density-independent maternal effect in p_ϕ and the density-dependent maternal effect in p_γ. We can see that the linear regression accurately characterizes the relationship between time to recovery and a maternal effect that impacts the settlement rate; Increasing the strength of the maternal effect in the pelagic stage leads to faster recovery. The relationship between time to recovery and a maternal effect that impacts the density-dependent processes is more complex. A small effect is helpful, but a large effect is hurtful.

To approximate effect size, I multiplied the estimated coefficient values shown in Table 4.1 by the range of parameter values used in the simulation. It appears that

Table 4.1: Estimated coefficients and diagnostic statistics from two linear regression on TTR. Model 1 is the best fit linear model and Model 2 is a reduced model that explains much of the variability in TTR. Also shown is an approximation of the change in TTR attributable to changes in this parameter; to calculate this I multiplied the estimated coefficient by the range of the parameter value.

Parameter	Model 1 coefficients	Model 2 coefficients	Approximate ΔTTR	Parameter description
intercept	26.8	25.5		
$\hat{F}$	723.9	723.9	+14–72 yrs.	harvest rate
$\hat{\phi}$	-12.5		− 6–25 yrs.	settlement rate
$\hat{\mu}$	1,450.0		+ 1–43 yrs.	density-indep. juv. mortality
$\hat{\gamma}$	79,170.0		+ 0–1 yrs.	density-dep. juv. mortality
p_ϕ	-6.7		− 3–13 yrs.	maternal effect in ϕ
p_μ	-22.5		− 3–15 yrs.	maternal effect in μ
p_γ	9.4		+ 1–4 yrs.	maternal effect in γ
F-statistic	1,354	2,382		
p-value	<1e-15	< 1e-15		
R^2	0.77	0.45		
AIC	25,047	27,515		

there is a similar magnitude of impact when a maternal effect influences the density-independent processes whether it occurs in the pre- or post-settlement stages. A 40% decrease in the benthic rate of density-independent mortality has a similar impact on TTR as a 40% increase in the settlement rate. The impact of a maternal effect in the density-dependent processes is negative, but has a lower magnitude than the effect on the density-independent processes. Even a very strong maternal effect tends to have a smaller impact on TTR than changes in harvest rate.

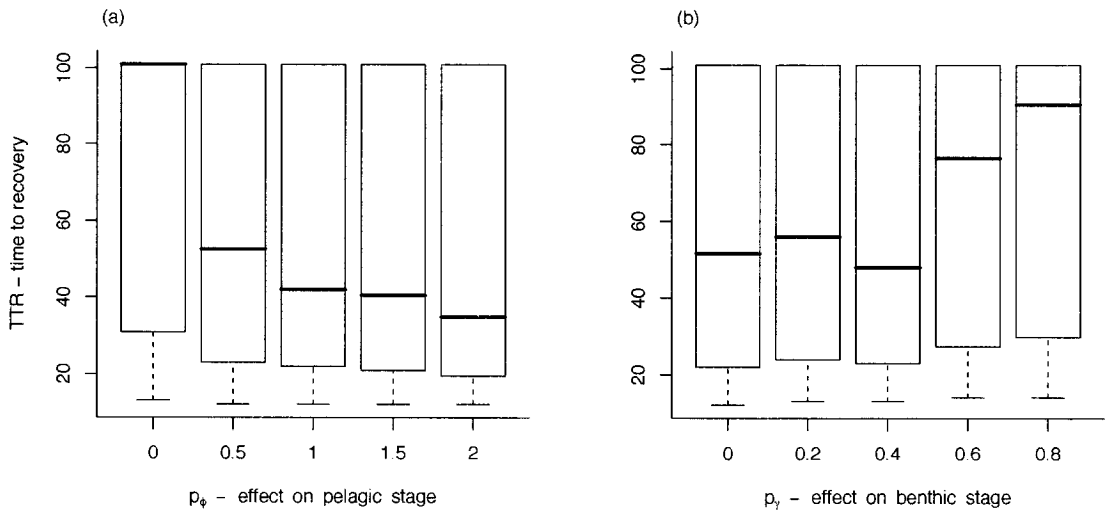

Figure 4.1: TTR versus the strength of the maternal effect in the pelagic factors p_ϕ and the density-dependent factors p_γ.

4.1.2 A specific case

In Figure 4.2 I show $TTR(\hat{F}, p_\phi|\hat{\phi}, \hat{\mu}, \hat{\gamma})$, time to recovery as a function of harvest rate and the maternal effect given a specific set of pre-recruitment survival and mortality rates. In this figure, the maternal effect only impacts the pre-settlement stage. In this case, we see that the maternal effect p_ϕ shortens time to recovery, and the stronger the effect the bigger the improvement in recovery times. We also see that when the harvest rate is very high, the maternal effect does not improve recovery times, because in all cases the population fails to recover. But also, when the harvest rate is very low the maternal effect has little impact. This result occurs because the population is recovering so quickly that the boost provided by the maternal effect is unimportant.

In Figure 4.3 I show something similar, $TTR(\hat{F}, p_\gamma|\hat{\phi}, \hat{\mu}, \hat{\gamma})$, but here the ma-

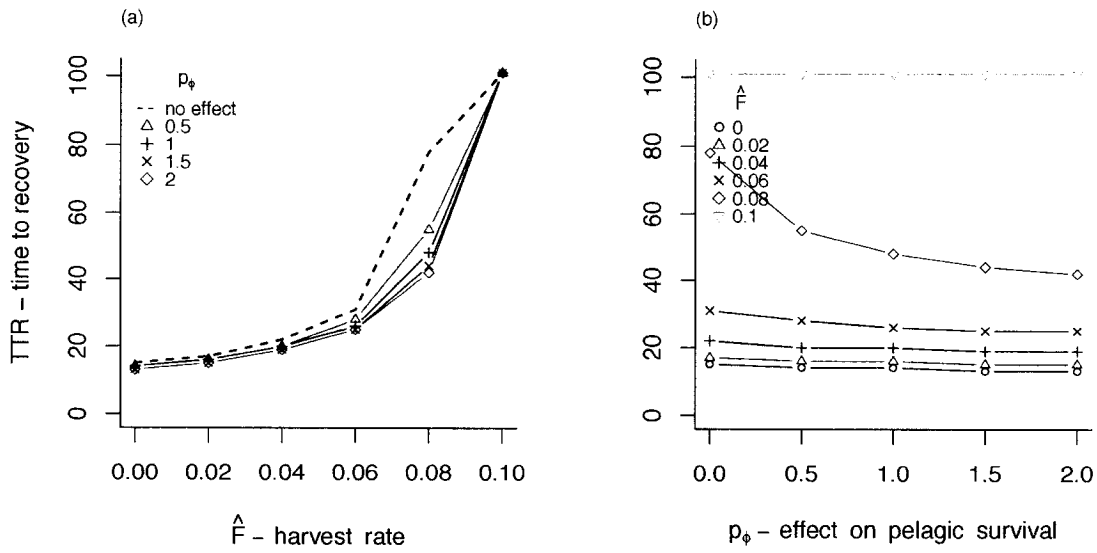

Figure 4.2: Two views of the case where the maternal effect only impacts the pelagic stage ($p_\mu = p_\gamma = 0$). The black dashed line gives the case with no maternal effect. Here, the base rates are $\hat{\phi} = 1$, $\hat{\mu} = 0.001$, $\hat{\gamma} = 5e - 6$.

ternal effect impacts both pre- and post-settlement processes. In this case time to recovery is usually shortened by the addition of a maternal effect that is impacting both density-independent and density-dependent processes. However, the stronger the effect on the density-dependent processes, the less improvement we see in recovery times.

These two figures illustrate the pattern that holds throughout the parameter set: if the maternal effect only impacts the density-independent processes, then TTR always improves; but, when the maternal effect influences the density-dependent processes, then TTR generally improves less and may even get worse.

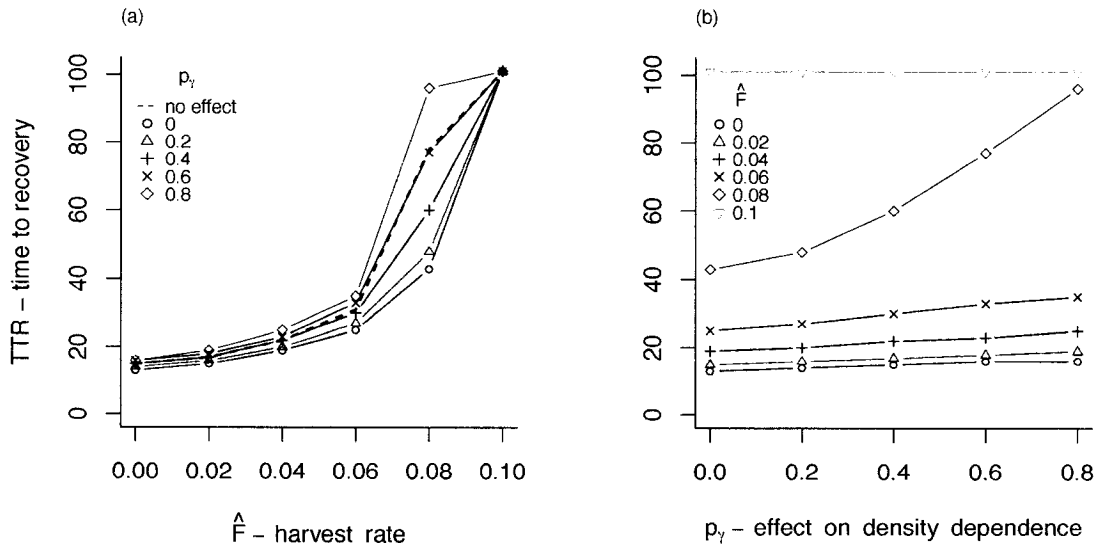

Figure 4.3: Two views of the case where the maternal effect impacts both the pelagic and benthic stages ($p_\phi = 1$ and $p_\mu = 0.4$). The black dashed line gives the case with no maternal effect. Here, the base rates are $\hat{\phi} = 1$, $\hat{\mu} = 0.001$, $\hat{\gamma} = 5e - 6$

4.2 Change in time to recovery

In Figure 4.4 I show a histogram of the change in TTR due to a maternal effect as a function of the strength of the maternal effect, defined as

$$\Delta TTR = TTR(\hat{\phi}, \hat{\mu}, \hat{\gamma}, p_\phi, p_\mu, p_\gamma) - TTR(\hat{\phi}, \hat{\mu}, \hat{\gamma} | p_\phi = p_\mu = p_\gamma = 0) \qquad (4.1)$$

We see that the distribution of ΔTTR is left skewed. Most cases lead to reductions in TTR, but a handful of cases do cause an increase in TTR. These cases arise when settlement rates are relatively low and p_γ is high (a strong impact on the density-dependent factors).

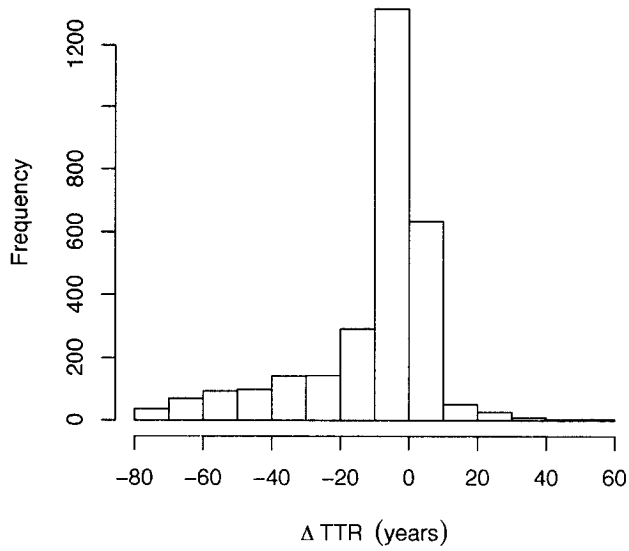

Figure 4.4: Histogram of ΔTTR values shows left skew, indicating that a maternal effect is more likely to accelerate recovery than to decelerate recovery.

In Figure 4.5 I show TTR as a function of the maternal effect. We can see that there is a clear trend in panel (a): bigger changes in lead to p_ϕ the shorter recovery times. However, the effect in panel (b) is less coherent, and there is no obvious trend. Also, decreases of TTR tend to be of larger magnitude than increases of TTR. It appears that increasing the intensity of the maternal effect in γ mitigates any improvements we would otherwise see; this reduced effect causes the negative correlation between TTR and p_γ found in Table 4.1.

In a full third of the cases, $|\Delta TTR|$ is no more than one year; i.e. the impact of the maternal effect is trivial. Most of these occur for one of three reasons: the

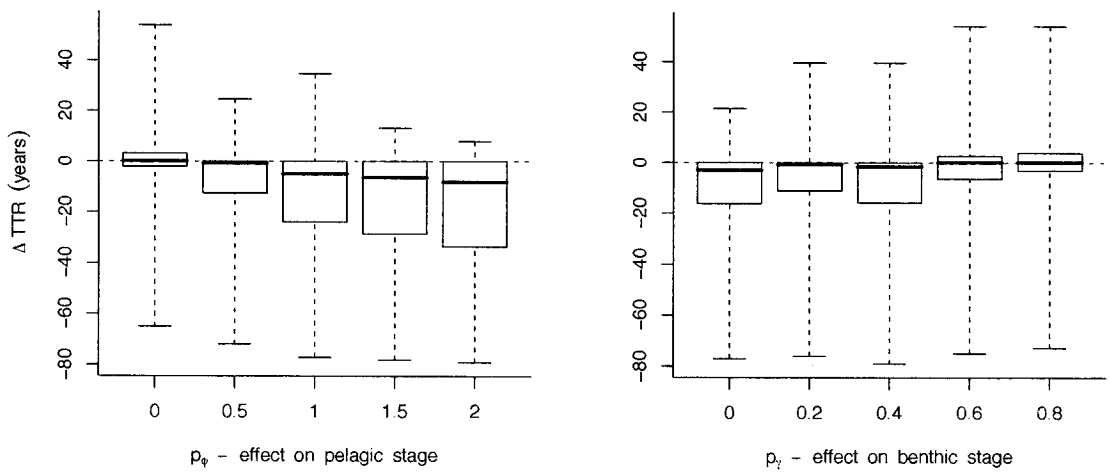

Figure 4.5: ΔTTR is defined in Equation 4.1. Here we show boxplots of ΔTTR with respect to the strength of the maternal effect. The edges of the box (called hinges) occur at the upper and lower quartiles (so that 75% of the data is within the range of the box hinges), the median is indicated with a black horizontal line, and the whiskers extend to the maximum and minimum values. A dashed red line zero.

population fails to recover with or without a maternal effect, harvest fraction is very small, or the settlement rate is high but the benthic mortality is low. This last scenario is illustrated in Figure 4.6. The basic pattern illustrated in Figures 4.2–4.3 continues to hold, but the magnitude of the effect is trivial.

4.3 Magnitude of early life survival and mortality rates

It turns out that an important determinant of the impact of the maternal effect is the relative survival and mortality rates pre- and post-settlement. In Figure 4.7, I show several outcomes of the stock-recruitment function. I have labeled the four types

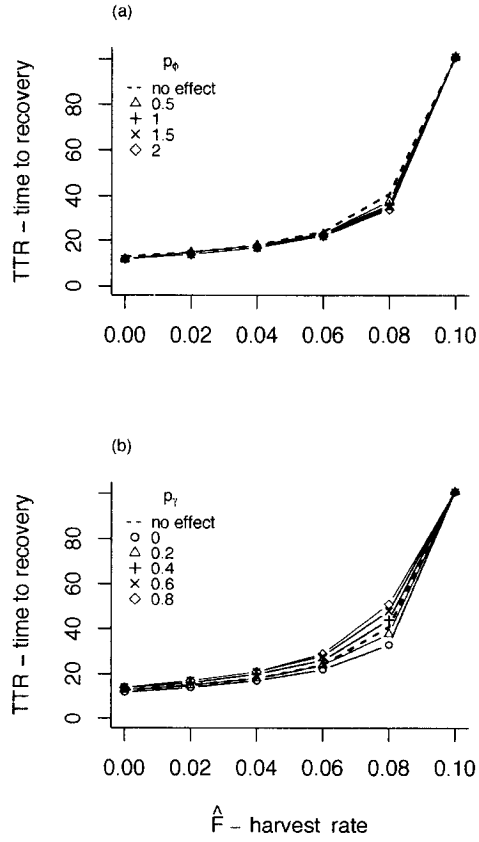

Figure 4.6: Panel (a) shows the case where the maternal effect only impacts the pelagic stage ($p_\mu = p_\gamma = 0$) and panel (b) shows the case where the maternal effect impacts both the pelagic and benthic stages ($p_\phi = 1$ and $p_\mu = 0.4$). The black dashed line gives the case with no maternal effect. Here, the base rates are $\hat{\phi} = 2$, $\hat{\mu} = 0.001$, $\hat{\gamma} = 5e - 7$

of populations according to their relative settlement and benthic mortality rates. The highest recruitment is from the populations with a high settlement rate followed by low post-settlement mortality (HL). The lowest recruitment is from the populations with a low settlement rate followed by high post-settlement mortality (LH). The addition of a maternal effect in the benthic stage has a substantially different impact on the four types of populations.

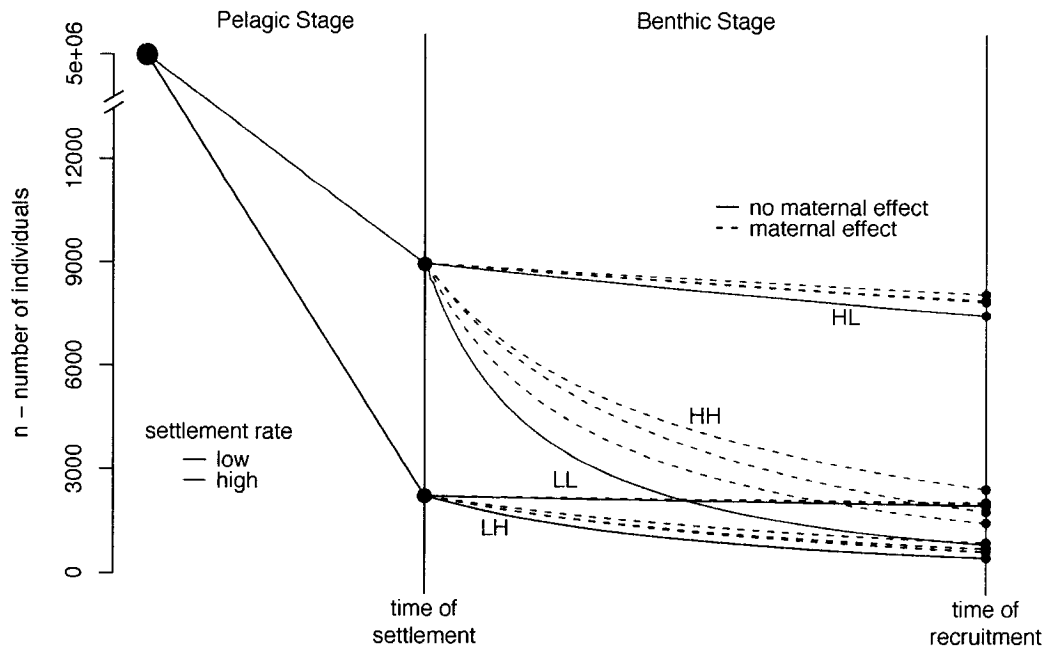

Figure 4.7: The stock-recruitment function with high and low settlement rates, and high and low juvenile mortality rates. The labels HL, HH, LL and LH correspond to the cases shown in Figures 4.8 and 4.9. A high settlement rate is defined as $\hat{\phi} = 2$ and a low settlement rate is $\hat{\phi} = 0.5$. High juvenile mortality is $\hat{\mu} = 0.01$ and $\hat{\gamma} = 5e - 6$, and low juvenile mortality is $\hat{\mu} = 0.001$ and $\hat{\gamma} = 1e - 7$. The dashed lines show three versions of a maternal effect in the benthic stage, these are (i) $p_\mu = 0.4$, $p_\gamma = 0.4$ and $v_\gamma = 0$, (ii) $p_\mu = 0$, $p_\gamma = 0.8$ and $v_\gamma = 0$, and (iii) $p_\mu = 0.4$, $p_\gamma = 0.2$ and $v_\gamma = 0.01$.

In Figure 4.8, I show time to recovery for high and low settlement rates versus high and low juvenile mortality rates. Just as in Figure 4.7, populations with low

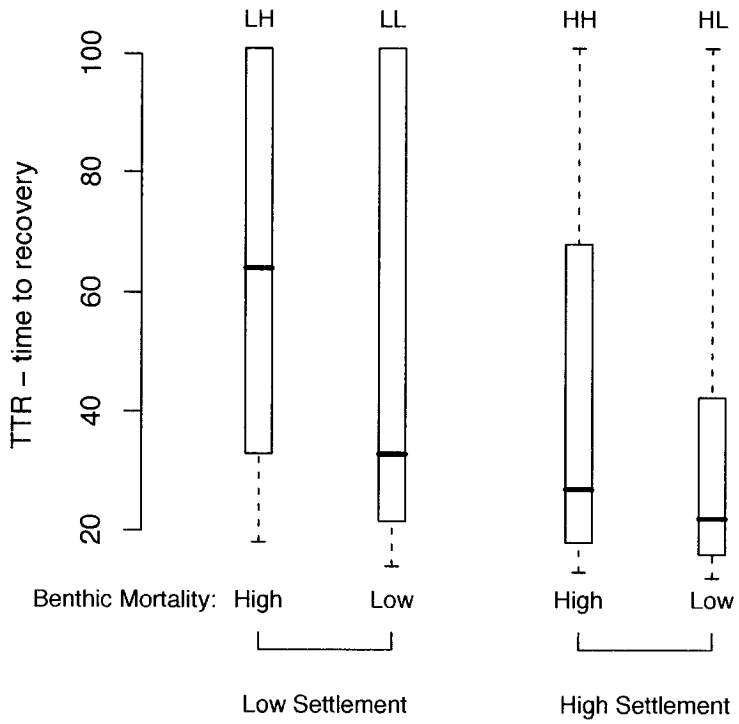

Figure 4.8: Time to recovery as a function of relative mortality and survival rates. Here, low settlement is defined as $\hat{\phi} = 0.5$ and high settlement is $\hat{\phi} = 2$. Low juvenile mortality is $\hat{\mu} = 0.001, \hat{\gamma} = 5e-7$ and high juvenile mortality is $\hat{\mu} = 0.01, \hat{\gamma} = 5e-6$.

settlement and high post-settlement mortality (LH) are the least productive and recover the slowest. Populations with a high settlement and low post-settlement mortality (HL) are the most productive and recover the fastest. The boxplots in Figure 4.8 include all eighteen cases of the maternal effect. We can compare the recovery times shown in Figure 4.8 to the change in recovery times shown in Figure 4.9. The maternal effects

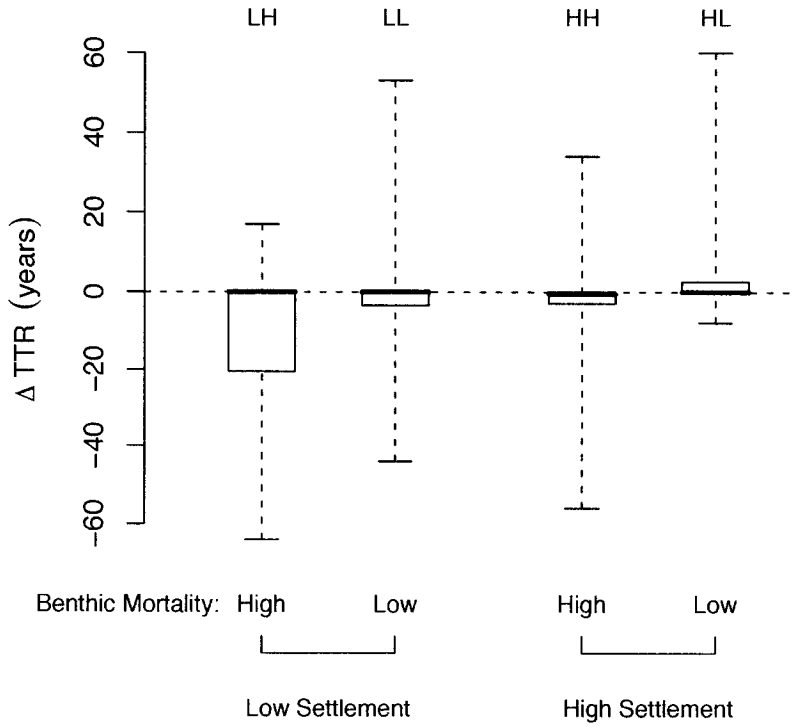

Figure 4.9: Change in time to recovery as a function of relative mortality and survival rates. Here, low settlement is defined as $\hat{\phi} = 0.5$ and high settlement is $\hat{\phi} = 2$. Low juvenile mortality is $\hat{\mu} = 0.001, \hat{\gamma} = 5e - 7$ and high juvenile mortality is $\hat{\mu} = 0.01, \hat{\gamma} = 5e - 6$.

have the largest impact on those same populations that are slowest to recover. The biggest change in TTR occurs in the least productive populations and the smallest changes in TTR occurs in the most productive populations. Also, importantly, in the most productive population ΔTTR is often positive. The most productive populations are the most likely to be negatively impacted by the addition of a maternal effect.

The expression of the maternal effect follows a slightly different pattern in

Figures 4.9 and 4.7. These outcomes are not directly comparable because the outcomes shown in Figure 4.9 include all eighteen kinds of maternal effect while the maternal effects shown in Figure 4.7 only impact the benthic processes. The benthic only maternal effects shown in Figure 4.7 are most strongly expressed in cases where the benthic mortality rate is high (HH and LH). When the benthic mortality rate is low (HL and LL), the benthic only maternal effect has little impact.

4.4 Discussion

I have shown time to recovery as a function of the strength of a hypothetical maternal effect. I have varied the intensity of the maternal effect and I have varied how the effect impacts the different life history stages. Despite the large number of scenarios examined, a few robust patterns consistently emerge. In most cases the presence of a maternal effect either improves recoverability of an overfished population or has no impact. Life-history influences the results: the change in TTR depends on whether or not the early life advantage ultimately leads to improved competitveness in the juvenile stage. And there is a large set of circumstances where even a very strong maternal effect has little to no impact on TTR.

The linear regressions shown in Table 4.1 allows us to draw out a key point: TTR is negatively correlated with a maternal effect in the density-independent factors ϕ and μ, but is positively correlated with the maternal effect in the density-dependent mortality rate, γ. In general, a maternal effect that improves the ability of fish to survive

the pelagic stage reduces TTR. However, if the maternal effect impacts the ability of some juveniles to compete at the expense of others, then the maternal effect increases TTR. This linear analysis is very limited; it only allows us to consider the effect in one parameter at a time, but these basic observations are held up by closer inspection of the simulated data.

When the harvest rate is too high, the maternal effect has no impact on TTR because the population never recovers. This result can be seen in Figure 4.6; there is no relationship between TTR and p_ϕ or p_γ when $\hat{F} = 0.1$. It is also interesting that the maternal effect has little influence when $\hat{F}$ is low. In these cases the population recovers relatively quickly and benefits little from the old fish advantage.

There is an additional circumstance in which the maternal effect has little influence: when settlement rates are high and benthic mortality rates are low.

Still, in this simulated population, harvest rate is the overwhelmingly most important tool for lowering TTR. This conclusion is reinforced by Table 4.1 where the $\hat{F}$'s effect on TTR is far larger than the effect of the maternal effect parameters. The maternal effect has a noticeable impact on TTR, but is small compared to harvest reductions.

Chapter 5

Time To Recovery in a Variable Environment

Fisheries biologists have long known that recruitment of marine fishes is highly variable (Sissenwine 1984). Environmental variability is usually identified as a primary source of recruitment variability. There are many reasons that survival of young fish depends on the environment. Some of the most notable include the unpredictable timing of phytoplankton blooms (the nutrition source for many larval fishes), the intensity and timing of current regimes that can aid or hamper larval and juvenile migrations and the impact of water temperature on basal metabolic rates (Bakun 1996).

Rockfish, like most marine animals, have a bipartite early life history comprised of a pelagic stage followed by a benthic stage. Survival of the pelagic larval stage is strongly influenced by environmental factors, but characterizing the relationship has proven to be a challenge: juvenile rockfish are dependent on upwelling fronts for nutrition

(Bjorkstedt et al. 2002), but excessive upwelling currents can harm pelagic larvae by carrying them away from suitable habitat (Ainley et al. 1993). Variation in year class strength (i.e., rankings) can be largely explained by changes in sea surface temperature. However actual abundances fail to correlate with common climate indices (Ralston and Howard 1995). Similarly, recruitment from disparate locations are strongly correlated to each other, suggesting an important role played by large-scale physical factors. However no predictive physical mechanism is evident (Field and Ralston 2005).

Consider the example of variability in settlement rates. The best index of settlement comes from the annual pelagic juvenile rockfish survey conducted by the Southwest Fisheries Science Center of NOAA-Fisheries. Times series from the cruise are shown in Figure 5.1. The pelagic juvenile rockfish survey collects rockfish during the brief window of time after they have undergone the physiological transition to become a juvenile (flexion), but before they have settled to the benthic habitat. The survey data are an index of settlement rather than a measurement of settlement. The observations are collected at standard stations in the core of the survey area (36.5-38.5 N latitude). They are standardized to the unit "number of 100 day old fish" and fitted to a generalized linear model with year, station, and calendar date as main effects only. In some years, an estimate is not possible due to very sparse positive tows these are set to a value equal to one-half the minimum positive observation, a decision rule that has been used in applying these data in stock assessments (Steve Ralston, personal communication).

The first thing to note in Figure 5.1 is the extremely high rate of correlation between time series. In Figure 5.2, I show a histogram of the pairwise correlation

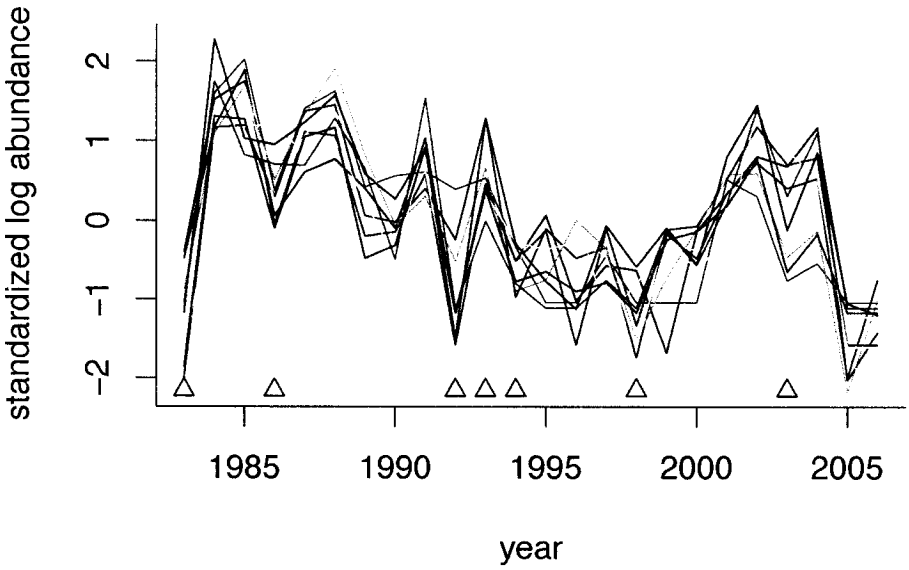

Figure 5.1: Standardized log of abundance from the annual pelagic juvenile rockfish survey, conducted by the SWFSC. These data are collected shortly before the transition from pelagic to benthic habitat, and are an index of the number of juveniles to settle. The ten time series shown are for *Sebastes entomelas, flavidus, goodei, hopkinsi, jordani, melanops, mystinus, paucispinis, pinniger,* and *saxicola.* The triangles mark El Niño years.

coefficients of the ten time series. The mean correlation coefficient is 0.76. This high level of inter-species correlation is a strong argument that external factors drive variability in this system. External factors could include large scale physical conditions or variation in predation pressure.

The second notable feature of the time series in Figure 5.1 is the appearance of serial autocorrelation in the time series. This is immediately promising, because in the northeast Pacific ocean physical conditions are often driven by the El Niño Southern

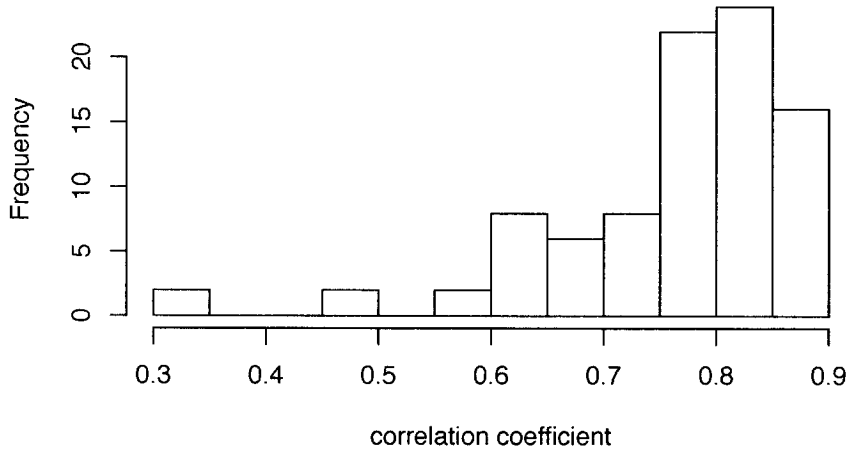

Figure 5.2: The distribution of correlation coefficients for pairwise comparisons of the ten time series shown in Figure 5.1. The histogram summarizes 100 coefficients, the mean correlation is 0.76. The high level of correlation between settlement indices for ten species is used to argue that survival to settlement is strongly influenced by environmental factors.

Oscillation (ENSO). ENSO is a short term climate cycle that varies on the time scale of 3–7 years. Strong ENSO events are often correlated with poor settlement classes (see the triangles in Figure 5.1). Therefore, we might expect the serial autocorrelation in settlement time series to be connected to ENSO.

Physical conditions in the northeast Pacific ocean are also influenced by the long term climate cycle of the Pacific Decadal Oscillation (PDO). However, the PDO varies on time scales of 20–50 years. The time series shown in Figure 5.1 are far too short to detect autocorrelation on the PDO time scale.

To compare the settlement time series with ENSO, we can estimate the scales

Table 5.1: Coeffcients and variances for best fit AR(p) models, defined in Equation 5.1

Species	ψ_1	ψ_2	σ
S. hopkinsi	0.5530		0.7256
S. jordani	0.4504		0.8332
S. mystinus	0.3244		0.9353
S. paucispinis	0.2219	0.3287	0.8703

of autocorrelation in the settlement time series by fitting an autoregressive model, such as

$$X_t = \psi_1 X_{t-1} + \psi_2 X_{t-2} ... \psi_i X_{t-i} + \epsilon_t \tag{5.1}$$

$$\epsilon \sim Norm(0, \sigma_\phi)$$

where X_t is the settlement index at time t and ψ_i is the i-th order correlation coefficient. Unfortunately when we do this, we find that there is no detectable autocorrelation in most of the time series. In Table 5.1, I show the correlation coefficients for those time series that do exhibit serial autocorrelation, and even in these cases the scale of correlation is only one or two years, not the three to seven years of ENSO.

This presents us with a dillemma. Clearly, recruitment is tied to environmental variability, but the nature of the relationship is not clear. Fogarty (1993) found that variability in recruitment is generally well described by a lognormal distribution; this gives us a default initial model. However, serial autocorrelation has been observed in long-term population time series in the Northeast Pacific Ocean (Hollowed et al. 2001).

We know that environmental conditions are important in this system, and we know that some environmental conditions exhibit serial autocorrelation over annual time-scales. For the purposes of simulation, is it better to model recruitment variability with or without serial autocorrelation? And will it matter?

I model environmental variability in two ways: (1) as a lognormal process and (2) as a lognormal, autocorrelated process where autocorrelation is due to ENSO-like time scales. I do not include long term autocorrelation due to the PDO, although certainly this variation is significant. I chose to exclude consideration of long term environmental variation because the time scale of PDO variability (decades) is similar to the time scale of time to recovery. This makes it difficult to summarize across PDO conditions. Therefore, all results presented here are to be interpreted as occuring within a given PDO regime.

5.1 The Climate Model

In the model, environmental noise impacts the rate of settlement, the life stage most vulnerable to physical conditions. I define a new rate of settlement $\Phi(a,t)$ that is a function of time as well as maternal age

$$\Phi(a,t) = z(t)\phi(a) \tag{5.2}$$

Where $\phi(a)$ is the rate of settlement defined in Equation 3.4 and $z(t)$ is our simulated climate index,

$$z(t) = \psi_0\xi(t) + \psi_1 z(t-1) + \psi_2 z(t-2) + \psi_3 z(t-3) + ... \tag{5.3}$$

where ξ is a bias corrected lognormally distributed random variable

$$\xi(t) = exp\left(-x(t) + \frac{1}{2}\sigma_\phi^2\right) \tag{5.4}$$
$$x \sim Norm(0, \sigma_\phi)$$

I define two versions of the climate index, with and without autocorrelation, these coefficients are given in Table 5.2. The serially autocorrelated climate index came from the best fit of an autoregressive model to the SOI (a measure of ENSO) done by Chu and Katz (1985). They also measured the variability, $\sigma = 1.43$. However here the environmental variability, σ_ϕ, is left as a tunable parameter, assuming values between zero and two. The settlement time series shown in Figure 5.1 have standard deviations that range from 1.6 (for *S. melanops*) to 2.8 (for *S. entomelas*) (personal communication, Ralston 2007). However, in the simulation model I found that $\sigma_\phi > 2$ caused a very high failure rate (see Table 3.1). The simulation population parameters are based on *S. melanops* biology.

Table 5.2: Coefficients for simulated climate index, z, defined in Equation 5.3. Index 1 is a lognormally distributed process with no autocorrelation. Index 2 is a lognormally distributed process with serial autocorrelation. Coefficients for Index 2 come from Chu and Katz (1985).

	ψ_0	ψ_1	ψ_2	ψ_3
Index 1	1	0	0	0
Index 2	0.63	0.43	0.16	-0.22

5.2 Comparison of Environmental Indices

In Figure 5.3, I show a comparison between Index 1 and Index 2 for time to recovery given harvest rate. For a comparison, it is best to include simulation runs that differ in the form of the climate index, but are otherwise similar. However, we do not want to examine comparisons of all 2,916 sets of parameters. Instead, I selected the parameters most sensitive to changes in the settlement rate. Recruitment tracks the settlement rate most closely when juvenile mortality is low. Therefore I chose low juvenile mortality rates ($\hat{\mu} = 0.001$ and $\hat{\gamma} = 5e-7$), coupled with a moderately high value for the settlement rate ($\hat{\phi} = 1$), and environmental variability ($\sigma_\phi = 1$). High values of these parameters increase impact of changes to the settlement rate, but the highest values produce too many failed runs (see Table 3.1). I ran this set of parameters for all eighteen cases of the maternal effect and iterated each set twenty times.

It appears from Figure 5.3 that Index 2 produces consistenly faster recoveries than Index 1. We can test the difference in means with a t-test and the difference in variances with an F-test. In Table 5.3, I present the results of these tests for the averaged set shown in Figure 5.3; additionally I show a few individual cases of the maternal effect

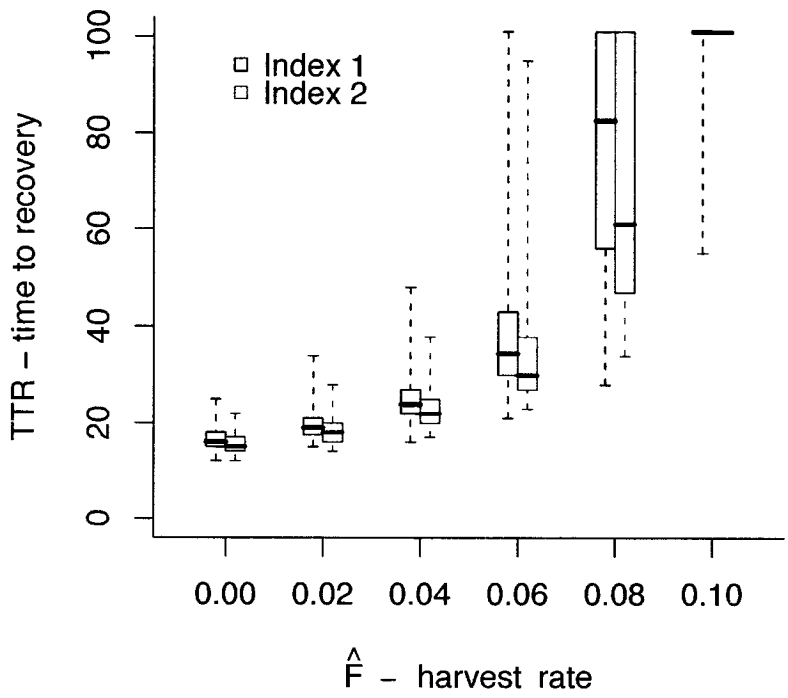

Figure 5.3: Comparison of Index 1 and Index 2 given harvest rate. Here, $\hat{\phi} = 1$, $\hat{\mu} = 0.001$, $\hat{\gamma} = 5e-7$, $\sigma_\phi = 1$, and each parameter combination is iterated twenty times. Results averaged across all eighteen cases of the maternal effect.

to demonstrate that there is no apparent interaction between the maternal effect and the index type. We see that there is a statistically significant difference between the means of the recovery times produced by the two indices. Index 2 does consistently produce recovery times a few years faster, and, as harvest rates increase, the difference grows larger. There appears to be no difference in the variance of recovery times produced by the two indices.

Table 5.3: Comparison of Index 1 and Index 2 (defined in Table 5.2. I test for the differences in TTR mean (t-test) and variance (F-test) using two forms of the climate index z. Here, $\hat{\phi} = 1$, $\hat{\mu} = 0.001$, $\hat{\gamma} = 5e-7$, $\sigma_\phi = 1$, and each parameter combination is iterated twenty times. Some cases of the maternal effect are shown separately: "all" cases is the average across Cases 1–18, in Case 1 there is no maternal effect, in Case 3 the effect is only in the pelagic stage and in Case 6 the effect is in both the pelagic and the benthic stages—parameters for the Cases are given in Table 3.3. In the columns for the p-value, $**$ represents $p < 0.001$ and $*$ represents $p < 0.05$. And 95% C.I. stands for 95% confidence interval.

$\hat{F}$	Case	t -statistic	p-value	95% C.I.	F-statistic	p-value	95% C.I.
0	all	5.96	**	0.8 – 1.6	1.14	0.32	0.9 – 1.5
	1	5.00	**	1.7 – 4.1	2.18	0.23	0.6 – 6.3
	3	3.25	*	0.5 – 2.2	5.03	*	1.4 – 15.0
	6	2.12	*	0.0 – 2.2	2.34	0.23	0.6 – 7.9
0.04	all	4.69	**	1.2 – 2.8	1.31	*	1.0 – 1.7
	1	5.25	**	3.0 – 7.0	1.15	0.86	0.3 – 3.3
	3	3.21	*	0.7 – 3.2	4.55	*	1.2 – 13.6
	6	1.50	0.15	– 0.6 – 3.3	2.71	0.16	0.7 – 9.2
0.08	all	4.01	**	4.6 – 13.4	0.88	0.32	0.7 – 1.1
	1	2.12	*	0.1 – 36.0	0.93	0.85	0.3 – 2.7
	3	3.24	*	5.6 – 25.5	14.7	**	3.9 – 43.7
	6	0.41	0.69	−10.2 – 15.2	1.14	0.88	0.3 – 3.9

5.3 Time To Recovery with Environmental Variability

In Table 5.4, I show the results of two linear regressions on TTR, similar to the regression Models 1 and 2, shown in Table 4.1. Regression Model 3 includes all of the significant variables in the model, and regression Model 4 includes only the single most influential variable, the harvest rate. For brevity, I show only the results that using Index 2. We can see that in the stochastic case, the harvest rate alone accounts for 38% of the variability, less than the 45% accounted for by the harvest rate in the deterministic Model 2. Adding the additional variables in Model 3 is consistent with an additional 31% of the variability, very similar to the deterministic case. However, the overall best fit Model 3 only explains 69% of the variance, even with the variate σ_ϕ included. In contrast, in the deterministic case Model 1 accounted for 77% of the variance. Otherwise, the coefficient estimates are fairly similar between Model 1 and Model 3, in both cases we observe the positive correlation between TTR and the density-independent parameters p_ϕ and p_μ and the negative correlation between TTR and the density-dependent parameter p_γ. Additionally, we estimate that environmental variability alone adds to TTR approximately 3.4 years per unit of σ_ϕ.

In Figure 5.4, I show TTR as a function of harvest rate for each value of σ_ϕ. We see that populations with environmental variability in the settlement rates ($\sigma_\phi > 0$) recover slower than those with no environmental variability in the settlement rates ($\sigma_\phi = 0$). The difference in recovery times is larger under greater fishing pressure.

Table 5.4: Estimated coefficients and diagnostic statistics from two linear regression on TTR. Model 3 is the best fit linear model and Model 4 is a reduced model that explains much of the variability in TTR. Also shown is an approximation of the change in TTR attributable to changes in this parameter, to calculate this I multiplied the estimated coefficient by the range of the parameter value.

Parameter	Model 3 coefficients	Model 4 coefficients	Approximate ΔTTR	Parameter description
intercept	28.1	33.7		
$\hat{F}$	643.6	643.6	+13–64 yrs.	harvest rate
$\hat{\phi}$	-12.5		− 6–25 yrs.	settlement rate
$\hat{\mu}$	1,427.0		+ 1–43 yrs.	density-indep. juv. mortality
$\hat{\gamma}$	886,900.0		+ 0–5 yrs.	density-dep. juv. mortality
p_ϕ	-6.7		− 3–13 yrs.	maternal effect in ϕ
p_μ	-18.7		− 3–15 yrs.	maternal effect in μ
p_γ	4.6		+ 1–4 yrs.	maternal effect in γ
σ_ϕ	3.4		+ 3–7 yrs.	environmental variability
F-statistic	15,060	32,350		
p-value	<1e-15	< 1e-15		
R^2	0.69	0.38		
AIC	466,773	504,363		

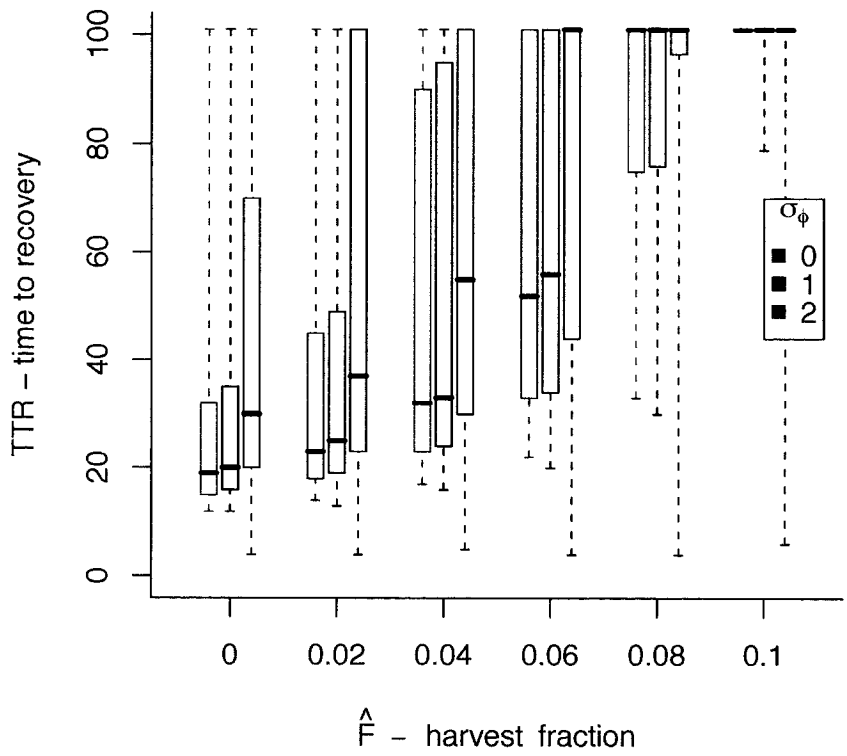

Figure 5.4: Time to recovery as a function of harvest rate, broken down by values of the environmental variance, σ_ϕ. This result uses the serially autocorrelated climate index, Index 2.

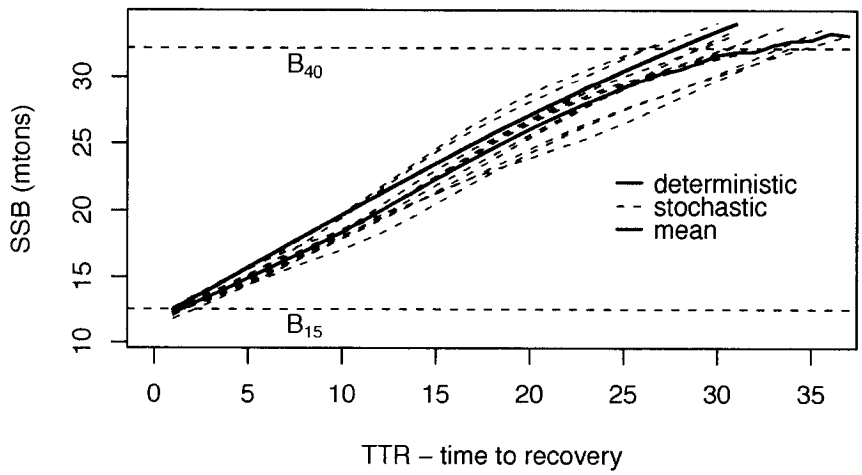

Figure 5.5: Example of recovery trajectories: SSB (spawning stock biomass) as a function of time spent rebuilding. The deterministic trajectory ($\sigma_\phi = 0$) is shown along with ten stochastic trajectories ($\sigma_\phi = 1$). The thick red line shows the annual means of the stochastic trajectories. In all cases, $\hat{F} = 0.04$, $\hat{\phi} = 0.5$, $\hat{\mu} = 0.01$, $\hat{\gamma} = 5e-6$, $p_\phi = 0.5$, $p_\mu = 0.4$, $p_\gamma = 0.4$, and $v_\gamma = 0.01$.

The results presented in Table 5.4 and Figure 5.4 show that on average across a wide range of circumstances there is a positive correlation between the amount of environmental variability and the time required to recover. To understand this result, we can examine a single recovery case and compare the deterministic recovery time series ($\sigma_\phi = 0$) to the stochastic recovery time series ($\sigma_\phi = 1$). I show this in Figure 5.5. For the stochastic case, there are ten iterations and I have included the mean of these ten trajectories. We can see that on average the stochastic trajectories are slower to recover than the deterministic trajectory. However, there are two stochastic outcomes that recover more quickly than the deterministic case.

5.4 Maternal Effects and Environmental Variability

In Figure 5.4 there is an interaction between σ_ϕ and $\hat{F}$. Populations that are fished at high levels are more vulnerable to environmental variability. This is because highly fished population have a lower standing biomass and are thus less productive. However, fished populations also have truncated age-structure, and to some extent their loss of productivity is attributable to lost age-structure. Recall that many of the cases included in these results have age-dependent maternal effects. We can isolate the impact of the age-dependent maternal effect by considering the interaction between σ_ϕ and $\hat{F}$ in the absence of a maternal effect. In Figure 5.6 I show the same result as Figure 5.4 for only those cases where there is no maternal effect.

The populations with no maternal effect recover more slowly on average than the populations with a maternal effect. However, the pattern in Figure 5.6 is very similar to the pattern in Figure 5.4. Populations recover more slowly when there is environmental variability. Populations fished at high levels are more vulnerable to environmental variability than populations with little or no fishing.

A comparison of the two outcomes reveals that the interaction between σ_ϕ and $\hat{F}$ is more pronounced in the presence of maternal effects. At high fishing levels, there is little difference between the two cases. But at low fishing levels, the case that includes maternal effects is more tolerant of environmental variability.

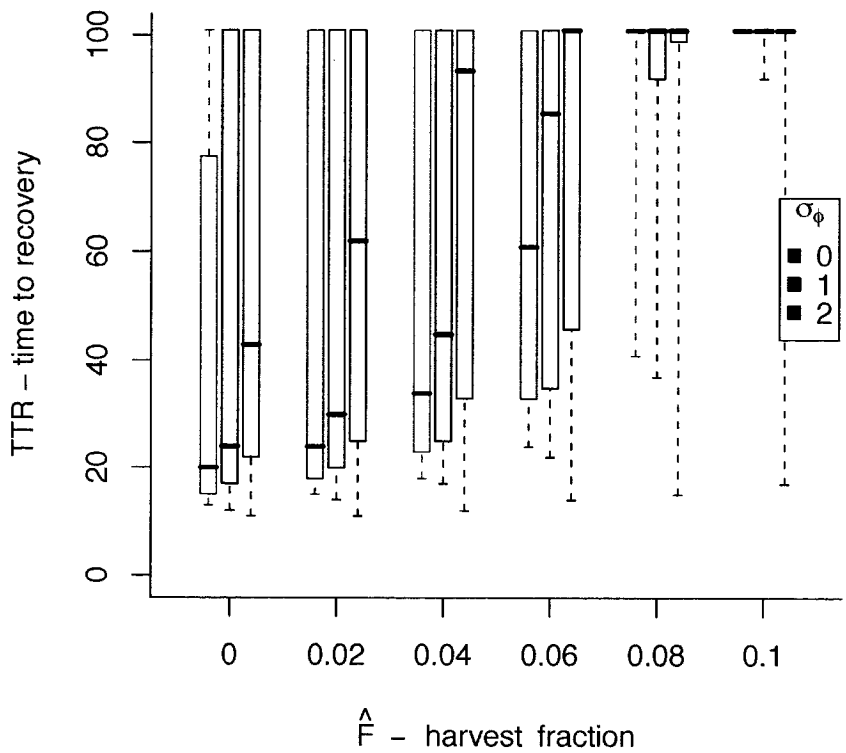

Figure 5.6: Time to recovery in the absence of a maternal effect as a function of harvest rate, broken down by values of the environmental variance, σ_ϕ. This result uses the serially autocorrelated climate index, Index 2.

5.5 Discussion

We found that increasing environmental noise decreases rates of recovery. This statement means that all of the observations made in a deterministic simulation should be interpreted conservatively with respect to harvest rate—natural populations subject to environmental variability are less resilient to fishing pressure than deterministic model populations.

This result may be counterintuitive because the stochastic process has the same mean settlement rate as the deterministic process and includes many above average settlement events, as can be seen in Figure 5.1. The post-settlement stage acts to dampen variability, and does so in a biased way. Large settlement classes are more significantly culled more than small settlement classes are favored. The net result is that a stochastic settlement rate will have a lower mean recruitment rate than a deterministic settlement rate of the same mean.

We could have predicted this by recalling Jensen's inequality (Hogg and Craig 1959), which states if f is a concave function and X is a random variable then

$$E[f(X)] \leq f(E[X]) \tag{5.5}$$

Our recruitment function is not truly concave. However numerical solutions suggest that it is concave throughout most of the important parameter space (see Figures 2.4–2.6 for a visual example). Jensen's inequality does not apply perfectly here. However it does assure us that it is not surprising to find that the stochastic process has a lower

mean than the deterministic process.

Neither of the two climate models I use are entirely satisfactory: Index 1 ignores temporal structure in the data that I believe are a factor, on the other hand, Index 2 is a much cleaner autocorrelation effect than is actually observed. Furthermore, the two indices produce different results. The differences are usually only a few years, but when harvest rates are high, the exact same population parameters can yield more than twelve years difference in average recovery time.

In Figure 5.3 we are presented with an interaction between harvest rate and the form of climate influence, the difference in mean TTR is larger when harvest rate is high. When $\hat{F} \geq 0.08$, the difference in means is strongly influenced by failure to recover. Non-recovery drives the largest differences in mean.

The two indices produce the same number of good years and bad years. Using Index 2 those good years tend to come in clumps, as do the bad years, whereas using Index 1 the good years and bad years are thoroughly interspersed. This fact suggests that clumps of good years are more helpful for speeding recovery than clumps of bad years are hurtful.

Mature biomass grows over the course of the recovery period. Generally, each year the population produces more larvae than the previous year. Also, with each advancing year, the proportion of settlers culled by density-dependent processes grows. Early in the time series, a string of good years would maximize production from populations with severely compromised reproductive capacity, but facing little density-dependent pressure. Later in the time series, the population produces large recruit

classes nearly regardless of climate, because larval production is so high. Thus, a string of good years early on can give a larger boost to recovery than the same number of good years spread evenly throughout the time series.

Just as often as a string of good years, the early years of the recovery period will bring a string of bad years. Compromised reproductive potential coupled with bad conditions leads to recruitment failures, while adult biomass continues to build. The results presented here suggest that the boost provided from a string of bad years is more helpful than the harm done by a string of recruitment failures.

Finally, an age-dependent maternal effect buffers populations against environmental variability. However, populations fished at high levels lose this buffer when they lose the older age classes of mothers. Highly fished populations with a maternal effect behave much like populations without a maternal effect.

Chapter 6

Conclusion

We would like to know whether age-dependent maternal effects should be a consideration when rebuilding overfished populations. We have several uncertainties that inhibit our ability to predict the population consequences of the effect:

1. Persistence of the maternal effect The population consequences of an age-dependent maternal effect depend a great deal on the persistence of the effect. Our initial evidence that persistence is important came in Chapter 2, where we considered versions of the maternal effect that influence one parameter at a time. Each of the cases was distinct.

More thorough investigations in Chapter 3 uncovered three types of outcomes for the age-dependent effect. The first type of outcome is the case where the maternal effect observed in a laboratory fails to translate to ocean conditions, or its influence dissipates quickly. In either case, the effect has little impact on the quantity or quality

of individuals to settle, and there are no population consequences of the effect.

The second type of outcome is the "pelagic only" effect. Here, the maternal effect is a significant aid to larvae and substantially improves their survival of the long pelagic period. However, the additional aid has ended by the time of settlement. In this case, if one were to examine the cohort of settlers, there would be no relationship between maternal age and individual quality.

In this case, an older population produces larger settlement classes than a younger population of the same mature biomass. In many cases, the older population will be much more productive than the younger population. Here, any management action that increases the number of older mothers will improve population productivity and recoverability.

The third type of outcome is the "pelagic and benthic" effect. Here, the maternal effect interacts with density-dependent processes. In this case, a relationship between maternal age and individual quality exists within a cohort of settlers. The most likely relationship will be juveniles from older mothers being larger than others. Larger juveniles are better at avoiding predators (either directly or by interference competition for shelter space). However, predation is density-cued. The presence of these juveniles will continue to attract predators to the region, while their superior ability to avoid predators causes this additional predation pressure to be displaced onto less able conspecifics.

In this case, the maternal effect may or may not have a positive impact on settlement rates and the ability of individuals to survive adverse physical condition.

Primarily, the maternal effect improves the success of a subpopulation, and thereby improves overall recruitment success. However, the displacement of density-dependent mortality onto less able individuals mitigates the positive impacts. If the displacement is large enough, or if population density is sufficiently high, the negative impacts can outweigh the positive impacts.

Here, there remains strong potential to improve population productivity and recoverability by increasing the mean age of the reproductive population. However, more careful consideration must be given to the details. For example, marine reserves have been suggested as a tool to raise the mean age of a population. But the older subpopulation within a reserve is also more densely distributed. It is not clear whether this increased density causes higher density-dependent pressures on juveniles, but it is a factor to be considered before implementing marine reserves.

2. Magnitude of maternal effect advantage We examined a large range of magnitudes of the maternal effect and found the patterns to be intuitive. In Table 5.4 we see that the addition of a maternal effect in the density-independent processes (p_ϕ and p_μ) improves recovery time 3–15 years on average. The maternal effect in the density-dependent processes (p_γ) may have a negative impact on average, but the magnitude of the change is smaller than the advantages above, only 1–4 years change on average.

When we considered an individual example, Figures 4.2 and 4.3, we found that the stronger the effect, the larger the change in recovery time. When we summarized across many cases, Figure 4.5, the pattern was maintained, although barely so in panel

(b).

We found that the expression of the maternal effect depends significantly on the ecological context in which it occurs. The context appears to be more significant than the magnitude of the effect itself. In Figure 4.5(b) the range of contexts are so important they nearly destroy our ability to detect the signal of the effect's magnitude at all.

For example, in Figure 4.3(b) we see that when harvest is high ($\hat{F} = 0.08$) a change in the maternal effect magnitude from a small effect to a moderate effect (p_γ changes from 0.2 to 0.4) leads to a twelve year difference in recovery time. Whereas in the same figure, when harvest is low ($\hat{F} = 0.02$) the same change in the maternal effect causes almost no change in recovery time. We saw something similar in Figure 4.7. The same maternal effect applied to four different sets of early life survival rates led to very different changes in recruitment.

3. Magnitude of early life survival rates I do not show any figures with these rates as the independent variables. Instead I summarize results for all twenty-seven sets of rates. There is an effect of the magnitude of these rates on recovery times. This effect is summarized in Tables 4.1 and 5.4. We find that the important patterns are robust to magnitudes of the basic rates.

Our key concern is not the magnitudes of the rates themselves, but rather their relative magnitudes. A system with a high settlement rate followed by a low juvenile mortality rate (HL) is ecologically distinct from a system with a low settlement rate

and a high juvenile mortality rate (LH). The HL population is very productive, but the addition of a maternal effect either has no impact at all or has a negative impact on recovery time. The LH population is less productive, but the addition of a maternal effect can have a very large and positive impact on recovery.

4. Functional form of density-dependence In Chapter 2 we saw that the functional form of the density-dependence matters primarily when juvenile density is very high. Our uncertainty about the functional form of density-dependence, coupled with our uncertainty about juvenile mortality rates and maternal effects, leaves us with fairly poor ability to predict the recruitment that results from a large settlement class. We can see an example of this in Figure 4.7. The high settlement rate produces a much wider range of possible recruitment outcomes than the lower settlement rate.

Large settlement classes occur because we have (1) high reproductive biomass, (2) a high per-mother settlement rate, (3) a maternal effect that impacts the settlement rate *and* a maternal population sufficiently old to express it, or (4) an exceptionally good set of climate conditions leading to exceptionally high survival of the pelagic stage. In short, we require good production, good success and/or good luck.

The years that have these positive factors in place are not our greatest source of concern. Managers should avoid relying on large settlement classes to support high harvest rates. We should recognize our decreased predictive ability when juvenile densities are high and respond with conservative harvest levels.

5. Environmental variability Natural populations contend with tremendous environmental variability and this lowers their capacity to cope with fishing pressure. The addition of a maternal effect may buffer populations to the environment, but even populations with a maternal effect will not exhibit this buffering if they are fished at high levels. An age-dependent maternal effect may create more productive populations, but managers should be extremely hesitant to allocate the higher productivity for harvest. It is important to set harvest rates conservatively.

In general, quality guidance for management requires more information. We could greatly improve our predictive ability with empirical study and I suggest two areas of study that I would prioritize to improve our understanding of the population consequences of age-dependent maternal effects.

First, we should seek evidence for an age-dependent maternal effect in the settlement cohort. For example, in black rockfish timing of settlement appears to correlate with timing of parturition (i.e., the first to be released are the first to settle) (Miller and Shanks 2004). Also, older mother's tend to parturate earlier in the season (Bobko and Berkeley 2004). If we observe a trend in individual quality with respect to timing of settlement—for example the earlier settlers tend to be larger—it would be suggestive of an age-dependent maternal effect that persists to the benthic stage.

Second, a great deal of predictive ability is lost because of our limited ability to quantify juvenile mortality. We require better measurements of the magnitude of juvenile mortality (i.e., daily measurements of juvenile survival) such as those collected by Johnson (2006 ab). We would also benefit from better characterization of the preda-

tion pressure faced by juvenile rockfish, such as the study by Hobson et al. (2001) that found opportunistic and density-cued predation by blue rockfish, *S. mystinus*.

The results presented in this thesis suggest that past fishing may have had a greater impact than previously believed, because changes in age-structure have reduced the recoverability of populations with age-dependent maternal effects. The failure to predict the consequences of lost age-structure have had very negative consequences for rockfish populations. I have not offered a specific prescription for incorporating age-dependent maternal effects into stock assessments. However, I believe the qualitative understanding gained by this analysis does offer helpful guidance for when to be concerned about age-structure and an additional argument for conservative harvest rates.

Appendix A

Productivity Parameters

Table A.1: Calculations of R_0, B_0 and h assuming $Z = 0.115\ yr^{-1}$ and no maternal effect.

$\hat{\phi}$	$\hat{\mu}$	$\hat{\gamma}$	$\alpha(\hat{\phi},\hat{\mu})$	$\beta(\hat{\phi},\hat{\mu},\hat{\gamma})$	$R_0(\alpha,\beta)$	$B_0(R_0,Z)$	$h(\alpha,\beta,B_0)$
0.5	0.001	5.0E-07	0.45	2.38E-05	19017	155879	0.54
0.5	0.001	1.0E-06	0.45	4.76E-05	9508	77939	0.54
0.5	0.001	5.0E-06	0.45	2.38E-04	1902	15588	0.54
0.5	0.01	5.0E-07	0.18	1.58E-05	11640	95409	0.39
0.5	0.01	1.0E-06	0.18	3.16E-05	5820	47704	0.39
0.5	0.01	5.0E-06	0.18	1.58E-04	1164	9541	0.39
0.5	0.03	5.0E-07	0.02	7.92E-06	3144	25769	0.23
0.5	0.03	1.0E-06	0.02	1.58E-05	1572	12885	0.23
0.5	0.03	5.0E-06	0.02	7.92E-05	314	2577	0.23

Table A.1: Calculations of R_0, B_0 and h assuming $Z = 0.115\ yr^{-1}$ and no maternal effect.

$\hat{\phi}$	$\hat{\mu}$	$\hat{\gamma}$	$\alpha(\hat{\phi},\hat{\mu})$	$\beta(\hat{\phi},\hat{\mu},\hat{\gamma})$	$R_0(\alpha,\beta)$	$B_0(R_0,Z)$	$h(\alpha,\beta,B_0)$
1	0.001	5.0E-07	0.90	4.76E-05	19017	155879	0.68
1	0.001	1.0E-06	0.90	9.52E-05	9508	77939	0.68
1	0.001	5.0E-06	0.90	4.76E-04	1902	15588	0.68
1	0.01	5.0E-07	0.37	3.16E-05	11640	95409	0.50
1	0.01	1.0E-06	0.37	6.32E-05	5820	47704	0.50
1	0.01	5.0E-06	0.37	3.16E-04	1164	9541	0.50
1	0.03	5.0E-07	0.05	1.58E-05	3144	25769	0.26
1	0.03	1.0E-06	0.05	3.17E-05	1572	12885	0.26
1	0.03	5.0E-06	0.05	1.58E-04	314	2577	0.26
2	0.001	5.0E-07	1.81	9.52E-05	19017	155879	0.80
2	0.001	1.0E-06	1.81	1.90E-04	9508	77939	0.80
2	0.001	5.0E-06	1.81	9.52E-04	1902	15588	0.80
2	0.01	5.0E-07	0.74	6.32E-05	11640	95409	0.64
2	0.01	1.0E-06	0.74	1.26E-04	5820	47704	0.64
2	0.01	5.0E-06	0.74	6.32E-04	1164	9541	0.64
2	0.03	5.0E-07	0.10	3.17E-05	3144	25769	0.31
2	0.03	1.0E-06	0.10	6.33E-05	1572	12885	0.31

Table A.1: Calculations of R_0, B_0 and h assuming $Z = 0.115\ yr^{-1}$ and no maternal effect.

$\hat{\phi}$	$\hat{\mu}$	$\hat{\gamma}$	$\alpha(\hat{\phi},\hat{\mu})$	$\beta(\hat{\phi},\hat{\mu},\hat{\gamma})$	$R_0(\alpha,\beta)$	$B_0(R_0,Z)$	$h(\alpha,\beta,B_0)$
2	0.03	5.0E-06	0.10	3.17E-04	314	2577	0.31
5	0.001	5.0E-07	4.52	2.38E-04	19017	155879	0.90
5	0.001	1.0E-06	4.52	4.76E-04	9508	77939	0.90
5	0.001	5.0E-06	4.52	2.38E-03	1902	15588	0.90
5	0.01	5.0E-07	1.84	1.58E-04	11640	95409	0.80
5	0.01	1.0E-06	1.84	3.16E-04	5820	47704	0.80
5	0.01	5.0E-06	1.84	1.58E-03	1164	9541	0.80
5	0.03	5.0E-07	0.25	7.92E-05	3144	25769	0.43
5	0.03	1.0E-06	0.25	1.58E-04	1572	12885	0.43
5	0.03	5.0E-06	0.25	7.92E-04	314	2577	0.43
10	0.001	5.0E-07	9.05	4.76E-04	19017	155879	0.95
10	0.001	1.0E-06	9.05	9.52E-04	9508	77939	0.95
10	0.001	5.0E-06	9.05	4.76E-03	1902	15588	0.95
10	0.01	5.0E-07	3.68	3.16E-04	11640	95409	0.89
10	0.01	1.0E-06	3.68	6.32E-04	5820	47704	0.89
10	0.01	5.0E-06	3.68	3.16E-03	1164	9541	0.89
10	0.03	5.0E-07	0.50	1.58E-04	3144	25769	0.56

Table A.1: Calculations of R_0, B_0 and h assuming $Z = 0.115\ yr^{-1}$ and no maternal effect.

$\hat{\phi}$	$\hat{\mu}$	$\hat{\gamma}$	$\alpha(\hat{\phi},\hat{\mu})$	$\beta(\hat{\phi},\hat{\mu},\hat{\gamma})$	$R_0(\alpha,\beta)$	$B_0(R_0,Z)$	$h(\alpha,\beta,B_0)$
10	0.03	1.0E-06	0.50	3.17E-04	1572	12885	0.56
10	0.03	5.0E-06	0.50	1.58E-03	314	2577	0.56

Appendix B

Methods

This appendix contains the methods of the thesis at a level of detail that should allow an interested person to reproduce the results exactly. Much of the document is devoted to explaining the *R* code used to generate the results (*R* Development Core Team 2005). Throughout the document *R* code is presented in boxes such as

Box 0.0a filename.R

```
filename = function(parameters){
    Rfunction(parameters)
    }
```

The box title gives the file name. In many cases, each *R* file is divided into several boxes, and each box is accompanied by an explanation of the purpose of this section of code. In many cases, the code is presented with relevant equations.

I begin by describing the basic simulation model used for calculating time to recovery (see Chapter 3). Next, I present an example code for processing the output of

many runs of the simulation to generate a single, useful matrix of simulated data. I then show an example of a plotting code. Finally, I describe called functions that support the simulation. See Figure 1.6 for a schematic of the computational approach.

B.1 The Simulation Model

Objective: I describe how to input the parameter list and output age-structured population data along with some calculations.

B.1.1 Header

As in all *R* functions, the function name and the file name must be the same. I pass a list of parameters to the the function. The elements of this list are given in Table B.1. The first task of the simulation is to record the start time so that later we can calculate how long the run took. We also need to generate a unique name for the output file. I do this by using the start time combined with the basic parameter values. The start time is a sufficiently unique name if the runs are only performed on one machine at a time. However, if one simultaneously runs simulations on multiple computers that save to the same directory, it is possible for runs on different machines to have the same start time. To prevent overwriting of data when this happens, I used a combination of the start time and parameter values for the run name. This produces run names that are not intuitive, but are unique. I found it to be unimportant that the file names were not intuitive.

We set the working directory so that output files will be saved to the cor-

Table B.1: Elements of the list of input parameters for Simulation function

Parameter	*R* Name	Equation	Brief Description	*R* Class
$\hat{F}$	harvest.fraction	3.13	harvest rate	vector
a_{max}	a.max	3.12	maximum age	numeric
$\hat{\phi}$	phi.hat	3.4	settlement rate	numeric
$\hat{\mu}$	mu.hat	3.5	d.i. juv. mortality rate	numeric
$\hat{\gamma}$	gamma.hat	3.6	d.d. juv. mortality rate	numeric
				numeric
p_ϕ	p.phi	3.4		numeric
p_μ	p.mu	3.5		numeric
p_γ	p.gamma	3.6		numeric
c_ϕ	c.phi	3.4	maternal effects model	numeric
c_μ	c.mu	3.5		numeric
c_γ	c.gamma	3.6		numeric
v_γ	v.gamma	3.6		numeric
a_{ME}	a.ME	3.4		numeric
T	j.days	2.8	length of juvenile period	vector
Δh	h	B.7	step size of numerical solution	numeric
σ_ϕ	sigma.p	5.5	environmental variability	numeric
ν	rf	B.2	proportion in reserve	numeric

rect place. And we source a script (simulation_environment.R) that loads all of the subroutines needed to complete the simulation. These are described in the Section B.3.

Box 1.1a Simulation.R

```
Simulation = function(parms){
    start.time = Sys.time()
    runname = format(Sys.time(),"%b%d_%H-%M") # create a unique run name
    runname = paste(runname, as.character(parms$phi.hat*10),
                as.character(parms$mu.hat*1000), as.character(parms$p.phi*100),
      as.character(parms$p.mu*100), as.character(parms$p.gamma*100), sep="")
    setwd("~ /Simulation ")
    source("simulation_environment.R")
```

B.1.2 Parameters

Here I list those parameters not included in the input list of parameters. These are either what I consider to be constant features of the population, or parameters that control the structure of the simulation. I set a maximum number of iterations (or years) for the burn in, the fishing down period and the rebuilding period.

Box 1.2a Simulation.R (cont.)

```
# Time #
    age = c(1:parms$a.max)
    burn.max = 350
    hard.fish.max = 400
    rebuild.max = 100
    t.max = burn.max + hard.fish.max + rebuild.max
```

Box 1.2b Simulation.R (cont.)

```
# Length #
    L.inf = 53.25
    k = 0.15
    t.0 = -2.84
    L = VBFUN(L.inf,k,t.0,age)
# Weight #
    w.0 = 0.0043
    w.1 = 3.362 # taken from RF book in grams
    W = w.0*L ^ w.1
    W = W*1e-6 # convert to mtons
```

Individual weight is a standard allometry of length

$$W(a) = w_1 L(a)^{w_2} \tag{B.1}$$

where $L(a)$ is length at age a, $W(a)$ is weight at age a, and w_1 and w_2 are constants. The appropriate values for the constants can be found in the literature. In this case, estimates for these constants are found in *Rockfishes of Northeast Pacific* (Love et al. 2002).

The remaining functions are described in the section Called Functions.

Box 1.2c Simulation.R (cont.)

```
# Natural Mortality (adults) #
    m.0 = 0.8
    m.1 = 0.03
    M = NatMFUN(m.0,m.1,L)
# Maturity #
    Length.fifty.mat = 39.53
    curve.mat = 0.4103
    P.m = maturityFUN(Length.fifty.mat, curve.mat, L)
## Pelagic survival ##
    phi = phiFUN(parms$phi.hat, parms$p.phi, parms$a.ME, parms$c.phi, age)
```

Box 1.2d Simulation.R (cont.)

```
## Fishery ##
    F.hard = max(0.1,max(parms$harvest.fraction))
    f.max = length(parms$harvest.fraction)
    selectivity = selectivityFUN(1,0.5,33,0.3,0.5,45,L)
    rf = parms$rf
    harvest.fraction = parms$harvest.fraction
    a.max = parms$a.max
```

B.1.3 Initial Conditions

To initiate the simulation, I create several matrixes for storing calculations. I choose initial values for several. I set an initial value for the iteration counter "hard.fish," and for the variable "recruits."

Box 1.3a Simulation.R (cont.)

```
burnin.A = matrix(0,t.max,a.max)

burnin.B = matrix(0,t.max,a.max)

burnin.A[1,] = 1000*(1-parms$rf)*exp(-0.01*age)

burnin.B[1,] = 1000*parms$rf*exp(-0.01*age)

out.A = rep(0,(a.max+3))

out.B = out.A

rebuild.times = rep(999,f.max)

hard.fish = 0

recruits = 1000
```

B.1.4 Burn In

There are two populations in the simulation, A and B. Population B has the potential to have different fishing mortality from population A. This functionality is *not* used in the thesis. In all cases shown here, fishing mortality for population B is set to zero during rebuilding so that population B is a protected population. Harvest rate is set to zero for the duration of the burn-in. This allows the simulation to find a steady-state for population biomass in the absence of fishing.

Box 1.4a Simulation.R (cont.)

```
print(" begin burn")
    for(t in 2:burn.max){
        F = 0 * selectivity
        P = 0 * selectivity
```

Figure B.1 illustrates the mixing of the populations. The juvenile stage includes density-dependent mortality. The two pools of juveniles are mixed so that all individuals in both populations experiences the same population density. The juveniles then settle to population A at the rate $(1-\nu)$ and to population B at the rate ν. This is a very simple way to model a marine reserve.

$$N(1,t) = \begin{cases} (1-\nu)n(T,t) & if\ pop.\ A \\ \nu n(T,t) & if\ pop.\ B \end{cases} \tag{B.2}$$

where $n(T,t)$ is the number of recruits in year t. We also have the option of making the rate of settlement a random variable. We set the environmental variance σ_ϕ in the input parameter list. When $\sigma_\phi = 0$, the model is deterministic, but when $\sigma_\phi > 0$

$$\phi \sim lognormal(\hat{\phi}, \sigma_\phi) \tag{B.3}$$

$N(a,t)$ is the number of adults of age a at time t, it is calculated as the number of adults at age $a-1$ at time $t-1$ reduced by the fraction that have died due to natural

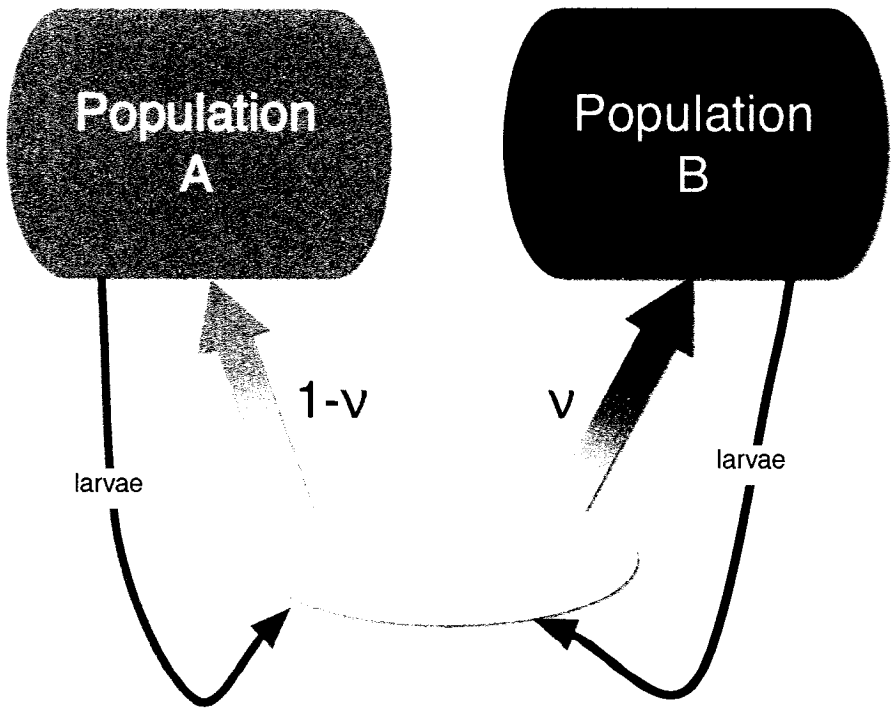

Figure B.1: In the model, the adult population is divided into two sub-populations; this functionality is *not* used in the thesis. Population B is a harvest refuge, or marine reserve population. The two adult populations contribute to the same pool of juveniles. Because the juveniles are pooled, the rate of density-dependent mortality depends on the combined density of both populations.

causes or fishing; this is written

$$N(a+1,t+1) = N(a,t)e^{-M(a)-F(a)} \tag{B.4}$$

where $M(a)$ is the rate of natural mortality experienced by adults of age a, and $F(a)$ the rate of fishing mortality experienced by adults of age a. Both natural and fishing mortality are functions of length, and length is a calculated with the von Bertalanffy growth equation (Equation 3.9).

The simulation has a finite number of age classes; therefore, the greatest age class must accommodate individuals older than the maximum age in the simulation a_{max}, where $a_{max} >> a_{ME}$. The number at a_{max} is time-stopped as

$$N(a_{max},t+1) = \left[N(a_{max},t) + N(a_{max}-1,t)\right] e^{-M(a_{max})-F(a_{max})} \tag{B.5}$$

Box 1.4b Simulation.R (cont.)

```
# set variability in settlement for this year
        phi.t = phi * P.m * exp(rnorm(1,0,parms$sigma.p) - 0.5*parms$sigma.p ^ 2)
```

Box 1.4c Simulation.R (cont.)

```
## Population A ##
        burnin.A[t,1] = (1-rf)*recruits
        burnin.A[t,2:(a.max-1)] = burnin.A[t-1,1:(a.max-2)]*exp(-M[1:(a.max-2)]
                                                                -F[1:(a.max-2)])
        burnin.A[t,a.max] = burnin.A[(t-1),(a.max-1)] * exp(-M[a.max-1]
                -F[a.max-1]) + burnin.A[(t-1),a.max] * exp(-M[a.max]-F[a.max])
        settlers.A = phi.t* burnin.A[t,]
## Population B ##
        burnin.B[t,1] = rf*recruits
        burnin.B[t,2:(a.max-1)] = burnin.B[t-1,1:(a.max-2)]*exp(-M[1:(a.max-2)]
                                                                -P[1:(a.max-2)])
        burnin.B[t,a.max] = burnin.B[(t-1),(a.max-1)] * exp(-M[a.max-1]
                -P[a.max-1]) + burnin.B[(t-1),a.max] * exp(-M[a.max]-P[a.max])
        settlers.B = phi.t* burnin.B[t,]
        recruits = abmPECEFUN((settlers.A + settlers.B), parms)$recruits
```

Some sets of parameters reach a steady-state quickly, and others slowly. We must allow for a long burn-in to accommodate the slow populations. To save time, we end the burn-in as soon as possible. In every iteration we test for a steady-state, defined as less

than 0.1% change in total population biomass for at least ten consecutive iterations. The burn-in ends as soon as a steady-state is found.

We record the number of iterations (years) in the burn-in. Biomass at the steady-state is also called equilibrium biomass, B_0. Once we have equilibrium biomass, we calculate the overfishing threshold, fifteen percent of initial biomass, B_{15}, and the rebuilding target, forty percent of initial biomass, B_{40}. To conclude, I print a message to screen stating the end of the burn-in.

Box 1.4d Simulation.R (cont.)

```
## Tests ##
        N.test = rowSums(burnin.A + burnin.B)
        if(N.test[t]<10) break
        if(t>10) local.mean = mean(N.test[(t-10):t]) else next
        test = abs(N.test[t]-local.mean)/local.mean
        if(test < 0.001) break
        if(t > burn.max) break
        } ## end burn.in (first part of t loop)


    burn = t
    B.15 = 0.15*sum((burnin.A[burn,] + burnin.B[burn,])*W)
    B.40 = 0.4*sum((burnin.A[burn,] + burnin.B[burn,])*W)
print(paste("begin hard fishing, t = ", as.character(t)))
```

B.1.5 Fishing Down

For this portion of the simulation, we fish the population from equilibrium biomass down to the overfishing threshold, from B_0 to B_{15}. We set fishing of both populations A and B to the same high level. Fishing mortality as a function of age is given by

$$F(a) = \hat{F}S(L(a)) \tag{B.6}$$

where $\hat{F}$ is the rate of fishing mortality and S is the selectivity function (see Eq. ??).

Box 1.5a Simulation.R (cont.)

```
F = F.hard * selectivity

P = F.hard * selectivity

for(t in (burn+1):t.max){
```

At this time we repeat exactly the code shown in Box 1.4b.

We calculate the population biomass and stop once it falls below B_{15}. However, the population could equilibrate and fail to reach the overfished threshold. To avoid this outcome, we test for a steady-state in the same was as before, and look for less than 0.1% change in population biomass for ten consecutive iterations. If we find a steady-state before reaching B_{15}, we increase the fishing pressure by 10%.

We record the number of iterations in the fishing down period, and we print to screen a message indicating the end of this stage.

Box 1.5b Simulation.R (cont.)

```
# Tests #
        B.test = sum((burnin.A[t,]+burnin.B[t,])*W)
        if(B.test <= 0) break
        if(B.test <= B.15) break
        hard.fish = hard.fish + 1 # count how long we have been fishing hard
        if(hard.fish > hard.fish.max) break
        N.test = rowSums(burnin.A + burnin.B)
        if(t < (burn+10)) next
        local.mean = mean(N.test[(t-10):t])
        test = abs(N.test[t]-local.mean)/local.mean
        if(test < 0.01) F = F*1.1
        } # end hard fishing part of t loop
    fish.burn = t
print(paste("begin rebuild, t = ", as.character(t)))
```

B.1.6 Rebuilding

Now, we rebuild the population from the overfishing threshold to the rebuilding target, from B_{15} to B_{40}. We do this for several harvest rates, specified in the input list of parameters. For each element of harvest.fraction, we set the harvest level and create a new matrix.

Box 1.6a Simulation.R (cont.)

```
for(f in 1:f.max){

    N.A = matrix(0,t.max,a.max)

    N.B = matrix(0,t.max,a.max)

    N.A[1:fish.burn,] = burnin.A[1:fish.burn,]

    N.B[1:fish.burn,] = burnin.B[1:fish.burn,]

    for(t in (fish.burn+1):t.max){

        F = harvest.fraction[f] * selectivity

        P = 0 * selectivity
```

The population dynamics shown in Box 1.6c are identical to the code shown in Box 1.4b, except now we are filling different matrices.

Box 1.6b Simulation.R (cont.)

```
# set variability in settlement for this year

        phi.t = phi * P.m * exp(rnorm(1,0,parms$sigma.p)

                                                - 0.5*parms$sigma.p ^ 2)
```

Box 1.6c Simulation.R (cont.)

```
## Population A ##
        N.A[t,1] = (1-rf)*recruits
        N.A[t,2:(a.max-1)] = N.A[t-1,1:(a.max-2)]*
                                        exp(-M[1:(a.max-2)]-F[1:(a.max-2)])
        N.A[t,a.max] = N.A[(t-1),(a.max-1)] *
                                exp(-M[a.max-1]-F[a.max-1]) + N.A[(t-1),a.max] *
                                                        exp(-M[a.max]-F[a.max])
        settlers.A = phi.t*N.A[t,]
## Population B ##
        N.B[t,1] = rf*recruits
        N.B[t,2:(a.max-1)] = N.B[t-1,1:(a.max-2)]*
                                        exp(-M[1:(a.max-2)]-P[1:(a.max-2)])
        N.B[t,a.max] = N.B[(t-1),(a.max-1)] *
                                exp(-M[a.max-1]-P[a.max-1]) + N.B[(t-1),a.max] *
                                                        exp(-M[a.max]-P[a.max])
        settlers.B = phi.t*N.B[t,]
        recruits = abmPECEFUN((settlers.A + settlers.B), parms)$recruits
```

Now we test to see if the population has reached B_{40}. Once it has reached B_{40}, we stop the rebuilding and record how long the rebuild took.

Box 1.6d Simulation.R (cont.)

```
## Tests ##
    B.test = sum((N.A[t,]+N.B[t,])*W)
    if(B.test < 10) break
    if(B.test >= B.40) break
    if((t-fish.burn) > rebuild.max) break
    } ## end rebuilding part of t loop)
    rebuild.times[f] = t-fish.burn
```

B.1.7 Output

Before we move on to the next harvest level, we perform some calculations to include in the output file. We calculate total biomass and spawning stock biomass (SSB). We build two matrices with these time series, and we append the current rebuilding harvest rate to each row of data. We append these matrices to the similar matrices calculated for previous harvest levels. Now we move to the next harvest level.

Box 1.7a Simulation.R (cont.)

```
    biomass.A = rowSums(t(W*t(N.A)))

    biomass.B = rowSums(t(W*t(N.B)))

    SSB.A = rowSums(t(W*P.m*t(N.A)))

    SSB.B = rowSums(t(W*P.m*t(N.B)))

    harvest.rate = rep(harvest.fraction[f],t)

    tmp.A = cbind(harvest.rate,biomass.A[1:t],SSB.A[1:t],N.A[1:t,])

    tmp.B = cbind(harvest.rate,biomass.B[1:t],SSB.B[1:t],N.B[1:t,])

    out.A = rbind(out.A,tmp.A)

    out.B = rbind(out.B,tmp.B)

print(paste("end rebuild, f = ", as.character(f),", t = ",as.character(t)))

    } # end f loop
```

The objects named "out.A" and "out.B" include numbers of individuals by age and year, including all of the rebuilding trajectories. We trim the empty first rows. Then, we create a list object with the elements out.A, out.B, the input list of parameters. This object is a vector with rebuilding times and the number of iterations in the burn-in and in the fishing down period. We save this object to a file with name *out.Rdata, where * is the run name defined at the start.

Finally, we calculate the end time and print to screen the duration of simulation. The function outputs the text object "runname" and ends.

Box 1.7b Simulation.R (cont.)

```
## output file ##

end = dim(out.A)[1]

out.A = out.A[2:end,]

out.B = out.B[2:end,]


out = list(out.A=out.A,out.B=out.B,parms=parms,

                    rebuild.times=rebuild.times,burn=burn,fish.burn=fish.burn)

save(out,file=paste("Simulationout/",runname,"out.Rdata",sep=""))


## end ##

end.time = Sys.time()

print(start.time - end.time)

runname

} # end function
```

I store the output "runname" for several runs of the simulation, as shown in Box 1.7c. In this way, I create a list of run names to be used by a processing script for extracting data from many simulation output files.

Box 1.7c example run

```
for(i in 1:i.max){
    run.name.list[i] = Simulation(parameters[[i]])
    } # end i loop
```

B.2 Handling the Data

B.2.1 Processing

Objective: I describe how to input a list of individual run names output from Simulation.R, extract data from each output file, and create a single matrix of summarized data from many runs.

The processing function takes two inputs: a list of text objects that are names of output files from the simulation and a text object to be used for a filename for the processed ouput. We go to the directory where the output files are, determine the number of files to included, and iterate through the file names.

For each file name, we load the output file. We determine the number of rebuilding harvest levels included in this output file. We create an object $TTR.m$ with one row per harvest level and fifteen. The first column is used to store the run name.

Box 2.1a Processing.R

```
Processing = function(run.names, file.name){
    setwd("~/Simulation/Simulationout")
    r.max = length(run.names)
    for(r in 1:r.max){
        load(paste(run.names[r],"out.Rdata",sep=""))
        f.max = length(out[[3]]$harvest.fraction)
        TTR.m = matrix(0, nrow = f.max, ncol = 15)
        TTR.m[,1] = rep(run.names[r], f.max)
```

We attach the list from the output file—to allow easier referencing of its contents. The second column is for rebuilding times, the second column for harvest levels. The remaining columns are filled with the input parameters used to generate the rebuilding times.

We now detach the list from the environment to prevent the R workspace from being overburdened with assigned values. We save the object $TTR.m$ to a comma delimitted file and move to the next run name/output file. Each new $TTR.m$ is added to the same file. The command "append=TRUE" allows the data to be added to a current file without overwriting the data already present in the file.

Box 2.1b Processing.R cont.

```
attach(out)
    TTR.m[,2] = out[[4]]      # rebuilding times
    TTR.m[,3] = parms$harvest.fraction
    TTR.m[,4] = rep(parms$rf, f.max)
    TTR.m[,5] = rep(parms$p.phi, f.max)
    TTR.m[,6] = rep(parms$p.mu, f.max)
    TTR.m[,7] = rep(parms$p.gamma, f.max)
    TTR.m[,8] = rep(parms$phi.hat, f.max)
    TTR.m[,9] = rep(parms$mu.hat, f.max)
    TTR.m[,10] = rep(parms$gamma.hat, f.max)
    TTR.m[,11] = rep(parms$c.phi, f.max)
    TTR.m[,12] = rep(parms$c.mu, f.max)
    TTR.m[,13] = rep(parms$c.gamma, f.max)
    TTR.m[,14] = rep(parms$v.gamma, f.max)
    TTR.m[,15] = rep(parms$sigma.p, f.max)
detach(out)
```

Box 2.1c Simulation.R (cont.)

```
write.table(TTR.m, file = paste("~/Simulation/ttr", file.name,".txt", sep = ""),
            append = TRUE, sep = ",", row.names = FALSE, col.names = FALSE)
        } # end r loop
} # end function
```

B.2.2 Plotting

Objective: I describe how to input a summary matrix created by Processing.R and make plots.

To generate Figure B.2, we input a data matrix (TTR) generated by the processing script with column names added. We input the values for $\hat{\phi}$, $\hat{\mu}$, and $\hat{\gamma}$ we would like to plot.

We attach the object TTR, so that we can easily call on the column names. Next, we write conditions to select the cases of interest. We create conditions for the case of no maternal effect (cond.noME), the case of a maternal effect in only the pre-settlement stage (cond.A) and the case of a maternal effect in both pre- and post-settlement stages (cond.B and cond.C).

Since the condition of no maternal effect is the same for all these plots, we go ahead and create an object with the values of time to recovery versus harvest fraction in th case of no maternal effect. The vector is ordered to facilitate neat plotting.

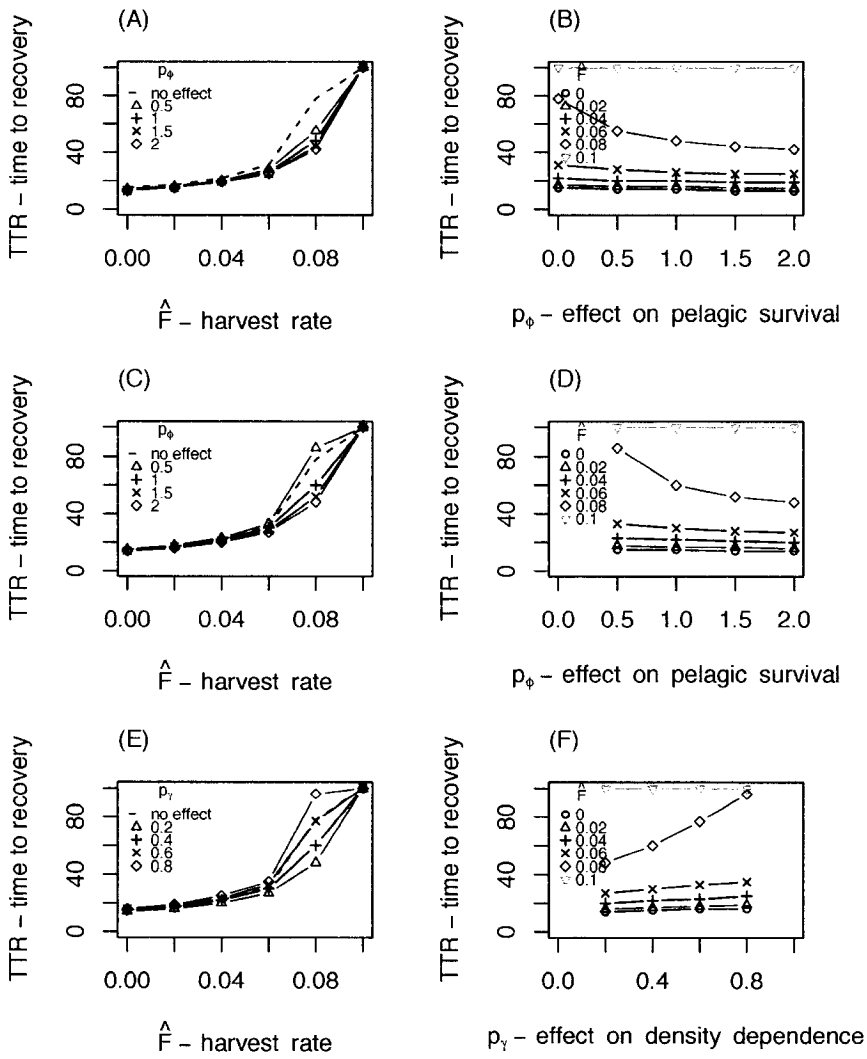

Figure B.2: Example of output from plotting script, where phi.cond=1, mu.cond=0.01, and gamma.cond=5e-6.

Box 2.2a Plotting.R

```
Plotting = function(TTR,phi.cond,mu.cond,gamma.cond){
    attach(TTR)
    cond.base = phi.hat==phi.cond & mu.hat==mu.cond &
                                                gamma.hat==gamma.cond
    cond.A = p.mu==0 & p.gamma==0 & v.gamma==0 & cond.base
    cond.B = p.phi==1 & p.mu==0.4 & v.gamma==0.01 & cond.base
    cond.C = p.mu==0.4 & p.gamma==0.4 & v.gamma==0.01 & cond.base
    cond.noME = cond.A & p.phi==0
    tmp.noME = cbind(harvest.fraction[cond.noME],ttr[cond.noME])
    tmp.noME = tmp.noME[order(tmp.noME[,1]),]
```

Next, we identify the levels of the other variables of interest. For each variable we create a vector of text elements to be used in the legend and a vector of numeric elements to be used in plotting, and then we determine the number of levels of the variable. In the case of ϕ and γ we rename the element zero to read "no effect."

We also find the length of the object TTR.

Box 2.2b Plotting.R cont.

```
F.hat.txt = levels(factor(harvest.fraction))
    F.hat = as.numeric(F.hat.txt)
    F.max = length(F.hat)
phi.txt = levels(factor(p.phi))
    phi.levels = as.numeric(phi.txt)
    p.max = length(phi.levels)
    phi.txt=c("no effect",phi.txt[2:p.max])
mu.txt = levels(factor(p.mu))
    mu.levels = as.numeric(mu.txt)
    m.max = length(mu.levels)
gamma.txt = levels(factor(p.gamma))
    gamma.levels = as.numeric(gamma.txt)
    g.max = length(gamma.levels)
    gamma.txt=c("no effect",gamma.txt[2:g.max])
ttr.max = max(ttr)
```

We open a quartz device and set it to accommodate six plots. Quartz devices are the graphical device used by Mac OSX, but other operating system rely on other types of graphical devices. We create a scaling factor "leg.cex" to help with the uniform sizing of the legends.

The first plot, Figure B.2(A), is time to recovery versus harvest fraction in the case that the maternal effect only impacts the pre-settlement stages. The initial plot

command creates the plotting frame, names the axes, etc., but it does plot any data. For each value of p_ϕ, the data are selected, ordered, and then plotted. The dashed line is added for the case of no maternal effect. Finally a legend is added and the label "(A)" is added.

Box 2.2c Plotting.R cont.

```
quartz(width=6,height=7.5)
    par(mfcol=c(3,2),cex.axis=1.5,cex.lab=1.5, mex=1.5,mar=c(5,4,2,2)+.1)
    leg.cex = 1

plot(F.hat,type="n",ylab="TTR - time to recovery",
                                xlab=expression(hat(F)~~-~~harvest~~rate),
                                    ylim=c(0,ttr.max),xlim=range(F.hat))
```

Box 2.2d Plotting.R cont.

```
    for(p in 2:p.max){
        tmp = cbind(harvest.fraction[cond.A & p.phi == phi.levels[p]],
                                        ttr[cond.A&p.phi == phi.levels[p]])
        tmp=tmp[order(tmp[,1]),]
        points(tmp,type="b",pch=p,col=p)
        } # end p loop
```

Box 2.2e Plotting.R cont.

```
lines(tmp.noME,lty="dashed")
legend(0,ttr.max,legend=phi.txt,pch=c(-1,2:p.max),
                                    lty=c(2,rep(-1,(p.max-1))),col=1:p.max,
                                title=expression(p[phi]),bty="n",cex=leg.cex)
mtext("(A)",side=3,line=1,adj=0)
```

We do the same to create panels (C) and (E), using the new condition and allowing p_ϕ or p_γ to vary.

Box 2.2f Plotting.R cont.

```
plot(F.hat,type="n",ylab="TTR - time to recovery",
                            xlab=expression(hat(F)~~-~~harvest~~rate),
                                ylim=c(0,ttr.max),xlim=range(F.hat))
```

Box 2.2g Plotting.R cont.

```
for(p in 1:p.max){
    tmp = cbind(harvest.fraction[cond.C & p.phi == phi.levels[p]],
                                    ttr[cond.C & p.phi == phi.levels[p]])
    tmp=tmp[order(tmp[,1]),]
    points(tmp,type="b",pch=p,col=p)
    } # end p loop
```

Box 2.2h Plotting.R cont.

```
lines(tmp.noME,lty="dashed")
legend(0,ttr.max,legend=phi.txt,pch=c(-1,2:p.max),
                                        lty=c(2,rep(-1,(p.max-1))),
        col=1:p.max, title=expression(p[phi]),bty="n",cex=leg.cex)
mtext("(C)",side=3,line=1,adj=0)
```

Box 2.2i Plotting.R cont.

```
plot(F.hat,type="n",ylab="TTR - time to recovery",
                        xlab=expression(hat(F) - harvest  rate),
                        ylim=c(0,ttr.max),xlim=range(F.hat))
```

Box 2.2j Plotting.R cont.

```
for(g in 1:g.max){
    tmp = cbind(harvest.fraction[cond.B&
p.gamma == gamma.levels[g]],ttr[cond.B & p.gamma == gamma.levels[g]])
    tmp=tmp[order(tmp[,1]),]
    points(tmp,type="b",pch=g,col=g)
    } # end g loop
```

Box 2.2k Plotting.R cont.

```
    lines(tmp.noME,lty="dashed")
    legend(0,ttr.max,legend=gamma.txt,pch=c(-1,2:g.max),
  lty=c(2,rep(-1,(g.max-1))),col=1:g.max,title=expression(p[gamma]), bty="n",
                                                        cex=leg.cex)
    mtext("(E)",side=3,line=1,adj=0)
```

Panel (B) is created with the same condition as panel (A). But here, p_ϕ is put on the x-axis and $\hat{F}$ is allowed to vary. Panels (D) and (F) have similar relationships to panels (C) and (E), respectively.

Box 2.2l Plotting.R cont.

```
  plot(c(0:5)*.5,type="n",ylab="TTR - time to recovery",
            xlab=expression(p[phi]~~-~~effect~~on~~pelagic~~survival),
                                              ylim=c(0,ttr.max),xlim=c(0,2))
```

Box 2.2m Plotting.R cont.

```
    for(f in 1:F.max){
      tmp = cbind(p.phi[cond.A&harvest.fraction==F.hat[f]],
                                    ttr[cond.A&harvest.fraction==F.hat[f]])
      tmp=tmp[order(tmp[,1]),]
      points(tmp,type="b",pch=f,col=f)
    } # end f loop
```

Box 2.2n Plotting.R cont.

```
legend(0,ttr.max,legend=F.hat.txt,pch=1:F.max,
                col=1:F.max,title=expression(hat(F)),bty="n",cex=leg.cex)
mtext("(B)",side=3,line=1,adj=0)
```

Box 2.2o Plotting.R cont.

```
plot(c(0:5)*.5,type="n",ylab="TTR - time to recovery",
        xlab=expression(p[phi]~~-~~effect~~on~~pelagic~~survival),
                                        ylim=c(0,ttr.max),xlim=c(0,2))
```

Box 2.2p Plotting.R cont.

```
for(f in 1:F.max){
    tmp = cbind(p.phi[cond.C&harvest.fraction==F.hat[f]],
                                    ttr[cond.C&harvest.fraction==F.hat[f]])
    tmp=tmp[order(tmp[,1]),]
    points(tmp,type="b",pch=f,col=f)
    } # end f loop
```

Box 2.2q Plotting.R cont.

```
legend(0,ttr.max,legend=F.hat.txt,pch=1:F.max,
                col=1:F.max,title=expression(hat(F)),bty="n",cex=leg.cex)
mtext("(D)",side=3,line=1,adj=0)
```

The plot is complete, we can now detach the object TTR and end the function.

Box 2.2r Plotting.R cont.

```
    plot(c(0:5)*.2,type="n",ylab="TTR - time to recovery",
         xlab=expression(p[gamma]~~-~~effect~~on~~density~~dependence),
                                                ylim=c(0,ttr.max),xlim=c(0,1))
```

Box 2.2s Plotting.R cont.

```
        for(f in 1:F.max){
            tmp = cbind(p.gamma[cond.B&harvest.fraction==F.hat[f]],
                                              ttr[cond.B&harvest.fraction==F.hat[f]])
            tmp=tmp[order(tmp[,1]),]
            points(tmp,type="b",pch=f,col=f)
            } # end f loop
```

Box 2.2t Plotting.R cont.

```
        legend(0,ttr.max,legend=F.hat.txt,pch=1:F.max,
                        col=1:F.max,title=expression(hat(F)),bty="n",cex=leg.cex)
        mtext("(F)",side=3,line=1,adj=0)


    detach(TTR)
} # end function
```

B.3 Functions Called

This section describes all of the original subroutines called by Simulation.R.

B.3.1 Individual Growth

Length is a calculated with the von Bertalanffy growth function described in Equation 3.9. The code for executing this calculation is given in Box 3.1a and the outcome is illustrated in Figure B.3.

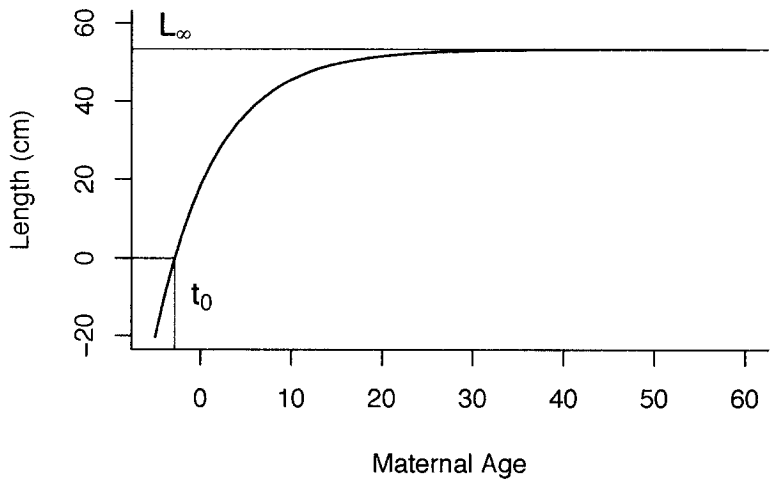

Figure B.3: The von Bertalanffy growth function connects length to age. Here, $L_\infty = 53.25$ cm, $\kappa = 0.15$ cm/day and $t_0 = -2.84$ days.

Box 3.1a VBFUN.R

```
VBFUN = function(L.inf,k,t.0,age){
    L.inf*(1-exp(-k*(age-t.0)))
    }
```

B.3.2 Natural Mortality

Adult natural mortality is described by Equation 3.11. The code to calculate this function is given in Box 3.2a and the outcome is illustrated in Figure B.4.

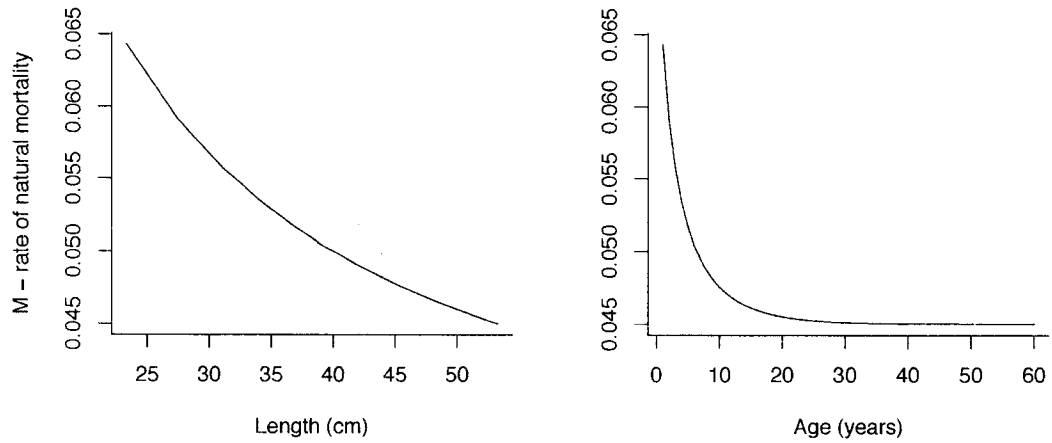

Figure B.4: The rate of natural mortality for adults, as a function of body length and as a function of age. Here, $m_0 = 0.03$ and $m_1 = 0.8$

Box 3.2a NatMFUN.R

```
NatMFUN = function(m.0,m.1,L){
    m.0 + m.1/L
    }
```

The parameters m_0 and m_1 are estimated. I used the population length distribution and natural mortality rate estimated in the stock assessment (Ralston and Dick 2003). I input the length distribution and solved for the values of m_0 and m_1 that yielded an average natural mortality rate equal to the stock assessment estimate of $M = 0.115\ yr^{-1}$.

B.3.3 Maturity

The probability of an adult being reproductively mature is described in Equation 3.2. The code to calculate this function is given in Box 3.3a.

Box 3.3a maturityFUN.R

```
maturityFUN = function(length.fiftymat, curvaturemat, length.vector){
    (1+exp(-curvaturemat*(length.vector - length.fiftymat))) ^ -1
    }
```

B.3.4 Maternal Effects Model

The maternal effects model is described in Section 3.2. There are several functions that contribute to the maternal effects model. The settlement rate is described in Equation 3.4 and the code to calculate this is given in Box 3.4a. The rate of density-independent juvenile mortality is described in Equation 3.5 and the code to calculate this is given in Box 3.4b. The rate of density-dependent juvenile mortality is described in Equations 3.6–3.7 and the code to calculate this is given in Box 3.4c. The outcomes for these functions are illustrated in Figure B.5.

Box 3.4a phiFUN.R

```
phiFUN = function(phi.min,phi.gain,a.ME,c.a,age){
    phi.hi = phi.gain*phi.min
    phi.min + phi.hi/(1+exp(-c.a*(age-a.ME)))
    }
```

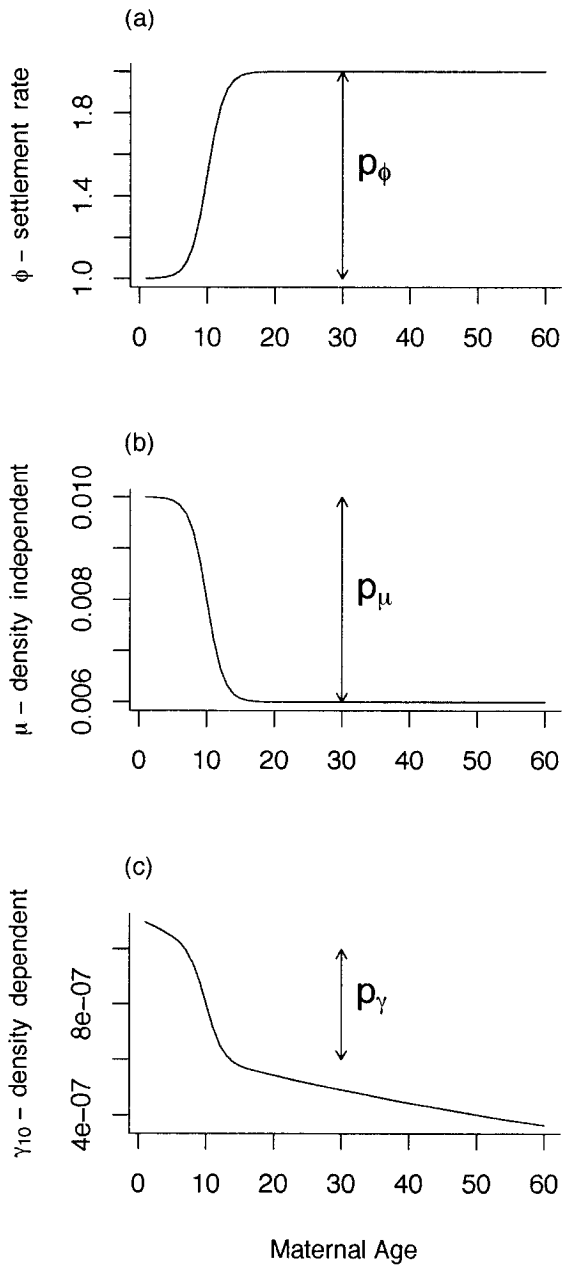

Figure B.5: Panel (a) shows the settlement rate with a maternal effect, $\hat{\phi} = 1$, $p_\phi = 1$, and $c_\phi = 0.8$. Panel (b) shows rate of density-independent mortality for juveniles with a maternal effect, $\hat{\mu} = 0.01$, $p_\mu = 0.4$, and $c_\mu = 0.8$. Panel (c) shows the rate of density-dependent mortality for juveniles with a maternal effect. Panel (c) shows only the rates experienced by juveniles with ten year old mothers, as a function of the maternal age of their conspecifics, $\hat{\gamma} = 1e-6$, $p_\gamma = 0.4$, $c_\gamma = 0.8$ and $v_\gamma = 0.01$. Throughout, the inflection point of the maternal effect occurs at age ten, $a_{ME} = 10$.

Box 3.4b muFUN.R

```
muFUN = function(mu.max,mu.loss,a.ME,c.mu,age){
    mu.low = mu.loss*mu.max
    mu.max - mu.low/(1+exp(-c.mu*(age-a.ME)))
    }
```

Box 3.4c gammaFUN.R

```
gammaFUN = function(gamma.max,gamma.loss,a.ME,c1.g,c2.g,age){
    a.max = length(age)
    gamma.low = gamma.loss*gamma.max
    gamma.base = gamma.max - gamma.low/(1+exp(-c1.g*(age-a.ME)))
    gamma = matrix(0,a.max,a.max)
    for(i in 1:a.max){
        for(j in 1:a.max){
            gamma[i,j] = gamma.base[i]*exp(-c2.g*(i-j))
        } # end i loop
    } # end j loop
    gamma
    }
```

B.3.5 Fishery Selectivity

The selectivity function is described in Equation 3.14. The code to calculate this is given in Box 3.5a and the outcome is illustrated in Figure B.3.5.

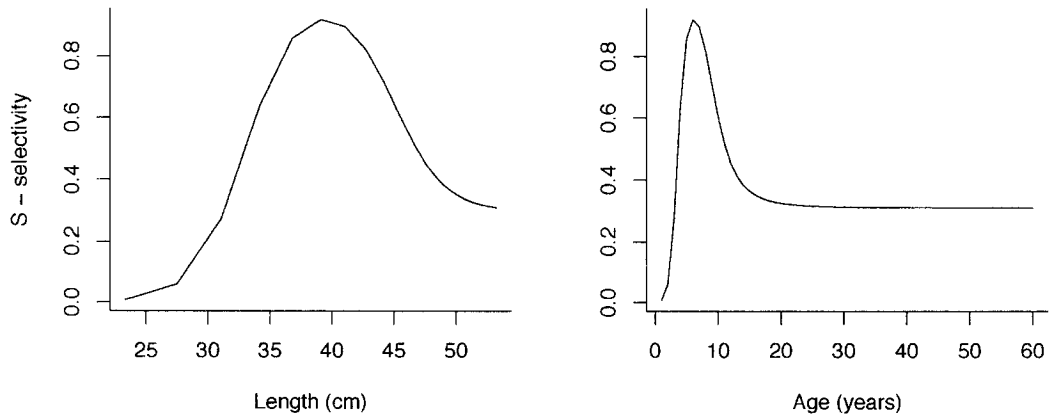

Figure B.6: The simulated fishery uses a two sided selectivity curve, based on the selectivity function used in the most recent stock assessment of Black rockfish (Ralston and Dick 2003). The Black rockfish fishery is dominated by recreational hook and line fishing, leading to the upper size limit in selectivity. I normalize S by setting $s_y = 1$. Also, $s_y = 1$, $c_y = 0.5$, $L_y = 33$ cm, $s_o = 0.3$, $c_o = 0.5$, $L_o = 45$ cm.

Box 3.5a selectivityFUN.R

```
selectivityFUN = function(s1,s2,s3,s4,s5,s6,L){
    s1*(1+exp(-s2*(L-s3)))  ^  -1 - s4*(1+exp(-s5*(L-s6)))  ^  -1
    }
```

The parameters used in the selectivity function are estimated. The stock assessment includes selectivity functions for six different fisheries (Ralston and Dick 2003) as well as the proportion of yield from each fishery. I fit the function in Equation 3.14 to the weighted average of the six selectivity functions.

B.3.6 Numerical ODE solver

In Section 2.3 I introduce the multi-variate Beverton-Holt stock-recruitment function given in Equation 2.15. For the many age class case, the solution of this function requires the initial condition given in Equation 3.1.

Equation 2.14 cannot be solved analytically and must be solved numerically. I found the most standard numerical method (a Runge-Kutta algorithm) to be ineffective. The difficulty is due to the stiffness of the differential equations (stiffness is usually defined to occur when there are multiple and very disparate time scales of variability; these time scales easily confound algorithms that are classified as explicit, such as the Runge-Kutta algorithm (Burden and Faires 2001)).

Instead, I used a semi-implicit method: a predictor-corrector method with a second order Adams-Bashforth algorithm as a predictor step and a second order Adams-Moulton algorithm as a corrector step (Burden and Faires 2001). This second order method is initialized with a fourth order Runge-Kutta with a very small step size.

In the special case of no maternal effect the problem reduces to a traditional Beverton-Holt model with a known analytical solution (Quinn and Deriso 1999). I used this special case to quantify the numerical error of the predictor-corrector method. I found that the algorithm converges quickly, but the initial Runge-Kutta steps introduce error to the final solution. However, there is never greater than one percent relative error, an acceptable amount of error for our purpose.

The initial steps are found with a fourth order Runge-Kutte numerical algo-

rithm: We would like to integrate a function $f(t, w)$, we choose a step size Δh and an initial condition, t_0, w_0. We use the algorithm in Equation B.7 to calculate the constants k_1--k_4. And we use these to calculate the next step with Equation B.8. We iterate for i as needed.

$$k_1 = \Delta h f(t_i, w_i) \tag{B.7}$$

$$k_2 = \Delta h f\left(t_i + \frac{\Delta h}{2}, w_i + \frac{k_1}{2}\right)$$

$$k_3 = \Delta h f\left(t_i + \frac{\Delta h}{2}, w_i + \frac{k_2}{2}\right)$$

$$k_4 = \Delta h f\left(t_{i+1}, w_i + k_3\right)$$

$$w_{i+1} = w_i + \frac{1}{6}[k_1 + 2k_2 + 2k_3 + k_4] \tag{B.8}$$

Box 3.6a abmPECEFUN.R

```
abmPECEFUN = function(n.init,parms){
## Part 1: parameters ##
    a.max = length(n.init)
    T = length(parms$j.days)
    h.rk = 0.001 # step size for RK4 method
    h.pece = parms$h # step size for ABM pece method
    abm.max = T/h.pece
    T.rk = 2 # days estimated by RK4 method

## Part 2: initialize ##
    n = matrix(0,nrow = abm.max, ncol=a.max)
    dn = matrix(0,nrow = abm.max, ncol=a.max)
    n[1,] = n.init
    mu = muFUN(parms$mu.hat, parms$p.mu,
                                        parms$a.ME, parms$c.mu, c(1:a.max))
    gamma = gammaFUN(parms$gamma.hat, parms$p.gamma, parms$a.ME,
                                        parms$c.gamma, parms$v.gamma, c(1:a.max))
```

The Runge-Kutte step is used to calculate the initial two steps of the predictor-corrector method. The equation's stiffness means that an explicit method, such as this, introduces a great deal of error. To minimize this, I use a much smaller step size for the Runge-

Kutte step, than the predictor-corrector step, $\Delta h_{rk} = 0.001$. It takes two thousand iterations of the Runge-Kutte step to calculate the first two steps for the predictor-corrector step.

For the remaining solution, I use a semi-implicit predictor-corrector method: we would like to integrate a function $f(t, w)$, we choose a step size, Δh, and use our initial values to make a prediction for w with a second order Adams-Bashforth algorithm

$$w_{i+1} = w_i + \frac{\Delta h}{2} [3f(t_i, w_i) - f(t_{i-1}, w_{i-1})] \tag{B.9}$$

We next refine, or correct, our prediction using a third order Adams-Moulton algorithm

$$w_{i+1} = w_i + \frac{\Delta h}{24} [9f(t_{i+1}, w_{i+1}) + 19f(t, w) - 5f(t_{i-1}, w_{i-1}) + f(t_{i-2}, w_{i-2})] \tag{B.10}$$

We iterate in i until we have our solution.

Box 3.6b abmPECEFUN.R cont.

```
## Part 3: the RK4 initial steps ##

    rk.max = T.rk/h.rk

    w = matrix(0,ncol=a.max,nrow=rk.max)

    w[1,] = n[1,] # initialize

    for(i in 1:(rk.max-1)){

        K1 = h.rk * (-mu - gamma%*% w[i,]) * w[i,]

        K2 = h.rk * (-mu - gamma%*% (w[i,] + 0.5*K1)) * (w[i,] + 0.5*K1)

        K3 = h.rk * (-mu - gamma%*% (w[i,] + 0.5*K2)) * (w[i,] + 0.5*K2)

        K4 = h.rk * (-mu - gamma%*% (w[i,] + K3)) * (w[i,] + K3)

        w[i+1,] = w[i,] + (K1 + 2*K2 + 2*K3 + K4)/6

        } # end i loop


    for(r in 1:(T.rk-1)) {n[r+1,] = w[r/h.rk,]

        dn[r,] = h.pece * (-mu - gamma%*% n[r,]) * n[r,]

        } # end r loop
```

Box 3.6c abmPECEFUN.R cont.

```
## Part 4: the ABM predictor-corrector methods ##

    for(a in (T.rk+1):abm.max){

        # predict: AB2
        n.p = n[a-1,] + (h.pece/2) * (3*dn[a-1,] - dn[a-2,])
        dn.p = (-mu - gamma%*% n.p) * n.p

        # correct: AM2
        n[a,] = n[a-1,] + (h.pece/12)*(5*dn.p + 8*dn[a-1,] - dn[a-2,])
        dn[a,] = (-mu - gamma%*% n[a,]) * n[a,]

        } # end a loop

out = list(n = n,dn = dn, gamma = gamma, mu = mu, recruits =
sum(n[abm.max,]))
} # end function
```

References

Adams, P. B., and D. F. Howard. 1996. Natural mortality of blue rockfish, *Sebastes mystinus*, during their first year in nearshore benthic habitats. *Fishery Bulletin* **94**:156–162.

Ainley, D. G., W. J. Sydeman, R. H. Parrish, and W. H. Lenarz. 1993. Oceanic Factors Influencing Distribution Of Young Rockfish (*Sebastes*) In Central California - A Predators Perspective. *California Cooperative Oceanic Fisheries Investigations Reports* **34**:133–139.

Bakun, A. 1996. Patterns in the Ocean: Ocean Processes and Marine Population Dynamics. California Sea Grant College System, National Oceanic and Atmospheric Adminstration in cooperation with Centro de Investigaciones Biolgicas del Noroeste.

Beckerman, A., T. G. Benton, E. Ranta, V. Kaitala, and P. Lundberg. 2002. Population dynamic consequences of delayed life-history effects. *Trends In Ecology and Evolution* **17**:263–269.

Beckerman, A. P., T. G. Benton, C. T. Lapsley, and N. Koesters. 2006. How effective are maternal effects at having effects? *Proceedings of the Royal Society B-Biological Sciences* **273**:485–493.

Benton, T. G., E. Ranta, V. Kaitala, and A. P. Beckerman. 2001. Maternal effects and the stability of population dynamics in noisy environments. *Journal of Animal Ecology* **70**:590–599.

Berkeley, S. A., C. Chapman, and S. M. Sogard. 2004a. Maternal age as a determinant of larval growth and survival in a marine fish, *Sebastes melanops*. *Ecology* **85**:1258–1264.

Berkeley, S. A., M. Hixon, R. Larson, and M. Love. 2004b. Fisheries Sustainability via protection of age structure and spatial distribution of fish populations. *Fisheries* **29**:23–32.

Birkeland, C., and P. K. Dayton. 2005. The importance in fishery management of leaving the big ones. *Trends In Ecology and Evolution* **20**:356–358.

Bjorkstedt, E. P., L. K. Rosenfeld, B. A. Grantham, Y. Shkedy, and J. Roughgarden. 2002. Distributions of larval rockfishes Sebastes spp. across nearshore fronts in a coastal upwelling region. *Marine Ecology-Progress Series* **242**:215–228.

Bobko, S. J., and S. A. Berkeley. 2004. Maturity, ovarian cycle, fecundity, and

age-specific parturition of black rockfish (*Sebastes melanops*). *Fishery Bulletin* **102**:418–429.

Boehlert G.W. and M.M. Yoklavich. 1983. Effects of temperature, ration, and fish size on growth of juvenile black rockfish, *sebastes-melanops*. *Environmental Biology Of Fishes*. **8**(1):17–28.

Burden, R. L., and J. D. Faires. 2001. Numerical Analysis, seventh edition. Brooks/Cole Thomas Learning, Pacific Grove.

Chu, P. S., and R. W. Katz. 1985. Modeling and Forecasting the Southern Oscillation: A Time-Domain Approach. *Monthly Weather Review* **113**:1876–1888.

Dorn, M. 2002. Advice on West Coast rockfish harvest rates from Bayesian meta-analysis of stock-recruit relationships. *North American Journal Of Fisheries Management* **22**:280–300.

Fogarty, M. J. 1993. Recruitment in randomly varying environments. *ICES Journal Of Marine Science* **50**:247.

Field, J. C. and S. Ralston. 2005. Spatial variability in rockfish (*Sebastes spp.*) recruitment events in the California Current System. *Canadian Journal of Fisheries and Aquatic Sciences* **62**(10): 2199–2210

Ginzburg, L. R. 1998. Inertial Growth: Population Dynamics Based on Maternal Effects. Pages 42–53 in T. A. Mousseau and C. W. Fox, editors. Maternal Effects as Adaptations. Oxford University Press, New York.

Harvey, C. J., N. Tolimieri, and P. S. Levin. 2006. Changes in body size, abundance, and energy allocation in rockfish assemblages of the northeast Pacifc. *Ecological Applications* **16**:1502–1515.

Haddon, M. 2001. Modelling and Quantitative Methods in Fisheries, Revised Printing edition. Chapman and Hall, Boca Raton, FL.

Hilborn, R. and M.Mangel. 1997. The ecological detective : confronting models with data, vol.28. Princeton University Press, Princeton, New Jersey

Hislop, J. R. G. 1988. The influence of maternal length and age on the size and weight of the eggs and the relative fecundity of the haddock, *Melanogrammus aeglefinus*. British waters. *Journal of Fish Biology* **32**:923–930.

Hixon, M. A., and G. P. Jones. 2005. Competition, predation, and density-dependent mortality in demersal marine fishes. *Ecology* **86**:2847–2859.

Hixon, M. A., and M. S. Webster. 2002. Density Dependence in Reef Fish Populations. in P. F. Sale, editor. Coral Reef Fishes. Academic Press, San Diego.

Hobson, E. , J. Chess, and D. Howard. 2001. Interannual variation in predation on first-year *Sebastes spp.* by three northern California predators. *Fishery Bulletin* **99**:292–302.

Hogg, R. V., and A. T. Craig. 1959. Introduction to mathematical statistics. Macmillan New York.

Hollowed, A. B., S. R. Hare, and W. S. Wooster. 2001. Pacific Basin climate variability and patterns of Northeast Pacific marine fish production. *Progress In Oceanography* **49**:257–282.

Johnson, D. W. 2006a. Density dependence in marine fish populations revealed at small and large spatial scales. *Ecology* **87**:319–325.

Johnson, D. W. 2006b. Predation, habitat complexity and variation in density-dependent mortality of temperate reef fishes. *Ecology* **87**:1179–1188.

Lacey, E. P. 1998. What is and Adaptive Environmentally Induced Parental Effect? Pages 54–66 in T. A. Mousseau and C. W. Fox, editors. Maternal Effects as Adaptations. Oxford University Press, New York.

Lenarz,W., R.Larson, and S.Ralston. 1991. Depth distributions of late larvae and pelagic juveniles of some fishes of the California Current. *California Cooperative Oceanic Fisheries Investigatinos Reports.* **32**:41–46.

Lorenzen, K. 2000. Allometry of natural mortality as a basis for assessing optimal release size in fish-stocking programmes. *Canadian Journal Of Fisheries And Aquatic Sciences* **57**:2374–2381.

Love, M. S., M. H. Carr, and L. J. Haldorson. 1991. The Ecology Of Substrate-Associated Juveniles Of The Genus Sebastes. *Environmental Biology Of Fishes* **30**:225–243.

Love, M. S., M. Yoklavich, and L. Thorsteinson. 2002. The Rockfishes of the Northeast Pacific. University of California Press, Berkeley.

Ludwig, G. M., and E. L. Lange. 1975. The Relationship of Length, Age, and Age-Length Interaction to the Fecundity of the Northern Mottled Sculpin, *Cottus b. bairdi. Transactions Of The American Fisheries Society* **104**:64–67.

Mangel, M. S., H.K. Kindsvater, and M.B. Bonsall. 2007. Evolutionary analysis of life span, competition, and adaptive radiation, motivated by the Pacific rockfishes (*Sebastes*). *Evolution* **61**(5):12081224

Marteinsdottir, G., and G. A. Begg. 2002. Essential relationships incorporating the influence of age, size and condition on variables required for estimation of reproductive potential in Atlantic cod *Gadus morhua. Marine Ecology Progress Series* **235**:235–256.

Methot, R.D. 2005. Technical Description of the Stock Synthesis II Assessment Program Version 1.17 March 2005.

Miller, J. A., and A. L. Shanks. 2004. Evidence for limited larval dispersal in black rockfish (*Sebastes melanops*): implications for population structure and marine-reserve design. *Canadian Journal Of Fisheries And Aquatic Sciences* **61**:1723–1735.

Moser, H. and G.Boehlert. 1991. Ecology of pelagic larvae and juveniles of the genus *Sebastes. Environmental Biology of Fishes* **30**(1):203–224.

Munch, S., A.Kottas, and M.Mangel. 2005. Bayesian nonparametric analysis of stock-recruitment relationships. *Canadian Journal of Fisheries and Aquatic Sciences* **62**(8):1808–1821.

Munch, S.B. , M.L. Snover, G.M. Watters, and M.Mangel. 2005a. A unified treatment of top-down and bottom-up control of reproduction in populations. *Ecology Letters* **8**(7):691695.

OFarrell, M. R., and L. W. Botsford. 2005. Estimation of change in lifetime egg production from length frequency data. *Canadian Journal of Fisheries and Aquatic Sciences* **62**:1626.

O'Farrell, M. R., and L. W. Botsford. 2006. The fisheries management implications of maternal-age-dependent larval survival. *Canadian Journal of Fisheries and Aquatic Sciences* **63**:2249–2258.

Palumbi, S. R. 2004. Fisheries science - Why mothers matter. *Nature* **430**:621–622.

Paradis, A.R. P.Pepin, and J.A. Brown. 1996. Vulnerability of fish eggs and larvae to predation: Review of the influence of the relative size of prey and predator. *Canadian Journal of Fisheries and Aquatic Science***53**(6):1226–1235

Pechenik, J. A., D. E. Wendt, and J. N. Jarrett. 1998. Metamorphosis Is Not a New Beginning. *BioScience* **48**:901–910.

PFMC (Pacific Fisheries Management Council). 2006. Pacific Coast Groundfish Fishery Management Plan For the California, Oregon, and Washington Groundfish Fishery As Amended Through Amendment 17. [Internet]. Pacific Fishery Management Council, Portland, OR. December 2006. Available from www.pcouncil.org

Pikitch, E.K., C. Santora, E. A. Babcock, A. Bakun, R. Bonfil, D. O. Conover, P. Dayton, P. Doukakis, D. Fluharty, B. Heneman, E. D. Houde, J. Link, P. A. Livingston, M. Mangel, M. K. McAllister, J. Pope, K. J. Sainsbury. 2004. Ecosystem-Based Fishery Management. *Science* **305**(5682): 346–347

Plaistow, S. J., C. T. Lapsley, and T. G. Benton. 2006. Context-dependent intergenerational effects: The interaction between past and present environments and its effect on population dynamics. *American Naturalist* **167**:206–215.

Plaza, G., G. Claramunt, and G. Herrera. 2002. An intra-annual analysis of intermediate fecundity, batch fecundity and oocyte size of ripening ovaries of Pacific sardine *Sardinops sagax* in northern Chile. *Fisheries Science* **68**:95–103.

Quinn, T. J., II, and R. B. Deriso. 1999. Quantitative Fish Dynamcis. Oxford University Press, New York.

Ralston, S., and E. J. Dick. 2003. The Status of Black Rockfish (*Sebastes melanops*) Off Oregon and Northern California in 2003. Stock Assessment **655**. [Internet]. Pacific Fishery Management Council, Portland, OR. May 2007. Available from http://www.pcouncil.org/groundfish/gfsafe0803/gfsafe0803.html

Ralston, S., and D. F. Howard. 1995. On The Development Of Year-Class Strength And Cohort Variability In 2 Northern California Rockfishes. *Fishery Bulletin* **93**:710–720.

Sakuma, K., S.Ralston, and D.Roberts. 1991. Diel vertical distribution of postflexion larval *Citharichthys spp.* and *Sebastes spp.* off central California. *Fisheries Oceanography.* **8**(1):68–76.

Shima, J. S., and A. M. Findlay. 2002. Pelagic larval growth rate impacts benthic settlement and survival of a temperate reef fish. *Marine Ecology Progress Series* **235**:303–309.

Sissenwine, M. P. 1984. Why Do Fish Populations Vary? Pages 59–94 in Exploitation of Marine Communities. Springer-Verlag, Berlin, Heidelberg, New York, Tokyo.

Sogard, S. M. 1997. Size-selective mortality in the juvenile stage of teleost fishes: A review. *Bulletin Of Marine Science* **60**:1129–1157.

Spencer, P., D. H. Hanselman, and M. W. Dorn. 2005. The effect of maternal age of spawning on estimation of Fmsy for Alaska Pacific ocean perch. in Proceedings of 23rd Wakefield Symposium. Alaska Sea Grant, Anchorage, Alaska.

Walters, C. and S.Martell. 2004. Fisheries Ecology and Management. Princeton University Press, Princeton, New Jersey

Zwillinger, D. 1992. Handbook of Differential Equations, 2nd edition. Academic Press, San Diego.